The 11th International Workshop on

Optical Waveguide Theory and Numerical Modelling

April 4-5, 2003, Prague, Czech Republic

Proceedings

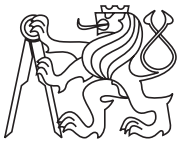

Czech Technical University in Prague
Prague, April 2003
100 copies

Volume Editors :

Ivan Richter
Petr Honsa

Contact :

Czech Technical University in Prague
Faculty of Nuclear Sciences and Physical Engineering
Břehová 7, 115 19 Prague 1, Czech Republic
Fax: (+420 2) 8468 4818
E-mail: richter@troja.fjfi.cvut.cz

ISBN 80-01-02720-1

Acknowledgements

We wish to thank to the

European Office of
Aerospace Research and Development

www.london.af.mil

who kindly supported the Workshop and thereby contributed to its success.

Preface

As a good tradition started two years ago in Paderborn, this year is again the traditional (11th in the series) Optical waveguide theory and numerical modelling workshop (April 4 - 5) organized jointly with the European conference on integrated optics (April 2 - 5), with two joint sessions, organized on Friday morning (April 4).

The OWTNM workshop is thus held in Prague, the beautiful capital of the Czech Republic. Therefore, together with OWTNM, you are also cordially invited to participate in the ECIO conference, both held under the auspices of the Czech Technical University in Prague, Faculty of Nuclear Sciences and Physical Engineering and Faculty of Electrical Engineering, and the Czech Academy of Sciences, Institute of Radio Engineering and Electronics, in cooperation with the Congress Department of the Czech Technical University. The OWTNM event is kindly supported by the European Office of Aerospace Research and Development. Due to the close connection to ECIO, the OWTNM meeting takes place in Masarykova kolej, Dejvice, Prague 6, Czech Republic, again after three years.

The aim is to promote personal contacts, to exchange ideas and to discuss current problems between scientists and experts for numerical modelling and theoretical description of optical waveguide structures. As mentioned, the event is organized as a Workshop with several structured interactive sessions and forums to allow for a wide interaction between participants. The emphasis is on invited and oral presentations although a good number of posters is also presented. Scientific topics for the workshop include both traditional and new topics within the field as (1) waveguide theory, (2) photonic bandgap structures, (3) photonic nanostructures, (4) waveguide gratings, (5) BPM improvements, (6) eigenmode solvers, (7) time domain methods, (8) laser modelling, (9) nonlinear media, (10) device-oriented modelling, and (11) others.

This year's workshop in Prague is already the 11th in the series of international workshops on Optical Waveguide Theory and Numerical Modelling held in the past in different places around Europe. Namely, the previous workshops took place in the following destinations: 2002 in Nottingham, UK, 2001 in Paderborn, Germany, 2000 in Prague, Czech Republic, 1999 in St. Etienne, France, 1998 in Hagen, Germany, 1997 in Enschede, The Netherlands, 1995 in Roosendaal, The Netherlands, 1994 in Siena, Italy, 1993 in Vevey, Switzerland, 1992 in Teupitz, Germany.

Hence, this year's meeting is continuation of a series of annual international workshops estabilished back in 1992. Continuation of this process is supervised by members of the OWTNM Technical Committee, consisting of Trevor Benson (University of Nottingham, UK), Jiří Čtyroký (IREE AS CR, Czech Republic), Anand Gopinath (University of Minnesota, USA), Hans - Peter Nolting, (HHI Berlin, Germany), Hugo J. W. M. Hoekstra (University of Twente, Netherlands), Olivier Parriaux (University of Saint Etienne, France), Reinhold Pregla (FernUniversität Hagen, Germany), and Christoph Wächter (Fraunhofer Inst. AOT Jena, Germany).

Based on oral contributions and selection of invited talks, it was possible to identify 8

scientific sessions, named

(1) Wave propagation
(2) Photonic bandgap structures I (both jointly with ECIO)
(3) Photonic bandgap structures II
(4) Gratings & subwavelength structures
(5) Laser & nonlinear & meta-material modelling
(6) Modelling methods and tools
(7) Device oriented modelling
(8) Waveguide theory & modelling

In response to the call for papers, total 68 papers have been received. Altogether, OWTNM 2003 includes 9 invited talks, 38 oral contributions (including 10 joint with ECIO program), and 21 posters, making it 68 contributions in total. Authors from 20 countries worldwide contribute, including United Kingdom (number of contributions 10), France (8), The Netherlands (7), Czech Republic (6), Germany (5), Italy (5), Russia (4), Australia (3), Belgium (3), Ukraine (3), Canada (2), Hong Kong (2), Indonesia (2), Spain (2), USA (2), Armenia (1), Japan (1), Sweden (1), Switzerland (1), and Taiwan (1).

Nine invited talks cover almost all topics of interest, and include (in alphabetical order): Henri Benisty from Laboratoire Charles Fabry de l'Institut d'Optique, Orsay cedex, FRANCE (*Planar Photonic Crystals: What are these teenagers capable of ?)*, Peter Bienstman from Ghent University, Dep. of Information Technology, Gent, BELGIUM (*Vectorial eigenmode modelling using perfectly matched layer boundary conditions)*, Gérard Granet, LASMEA, Unité Mixte de Recherche, Université Blaise Pascal, Aubiere Cedex, FRANCE (*Modal analysis of light transmission by subwavelength aperture arrays in metallic films)*, V. Kuzmiak, Institute of Radio Engineering and Electronics, Academy of Sciences of the Czech republic, CZECH REPUBLIC (*Amplification in 1D periodic and random active media near lasing threshold)*, Philippe Lalanne, Institut d'Optique/CNRS, Orsay Cedex, FRANCE (*Bloch wave engineering for applications of subwavelength optical structures,* jointly with ECIO), John Love, Research School of Physical Sciences & Engineering, Australian National University, Canberra, AUSTRALIA (*Passive Planar Devices for Light Processing in Telecommunications)*, Min Qiu, Laboratory of Optics, Photonics and Quantum Electronics, Department of Microelectronics and Information Technology, Royal Institute of Technology, Kista, SWEDEN (*Modelling photonic crystal devices using the finite-difference time-domain method)*, Phillip Russell, Department of Physics, University of Bath, Bath, UNITED KINGDOM (*Photonic crystals as waveguides: beyond total internal reflection*, jointly with ECIO), and C. M. Soukolis, Ames-Laboratory-USDOE and Department of Physics and Astronomy, Iowa State University, USA and Research Center of Crete, FORTH, Heraklion, Crete, GREECE (*Negative Refraction and Left-Handed Behavior in Photonic Crystals*). Most importantly, there are 38 oral contributions and 21 poster presentations to the OWTNM program, covering different areas and aspects of all 8 sessions, mentioned above.

Papers from the Workshop will appear in a Special Issue of Optical and Quantum Electronics Journal on the topic "Optical Waveguide Theory and Numerical Modelling". The papers presented both in oral and poster form at the OWTNM 2003 workshop in Prague will be included. Details about full paper submission will be available on the OWTNM 2003 web site.

This booklet includes abstracts of all contributions presented and consists of three parts. The first part contains the invited talks, the second part contains all accepted regular oral

papers and joint oral papers with ECIO, the third part contains the written versions of the posters accepted for presentation during the workshop.

Information about the OWTNM 2003, including contribution abstracts, downloadable programme, and local travel information can be found at the Workshop's web site
owtnm.fjfi.cvut.cz.

We would like to thank all individuals and institutions that have contributed to the success of the workshop, the invited speakers, authors of papers, sponsors, and the CTU Congress Department, especially.

Prague, April 2003

local organizers

Contents

Workshop Programme

Thursday, April 3, 2003

16.00 – 21.00 Registration

Masaryk College, Entrance Hall

19.00 – 21.00 "Get-together party"

Masaryk College, Entrance Hall

Friday, April 4, 2003

The first two workshop sessions on Friday are joint with the 11th European Conference on Integrated Optics (ECIO'03) which takes place in April 2-4, 2003, at the Faculty of Civil Engineering of the Czech Technical University in Prague.

8.30 – 10.30 Session FrA1: Wave propagation

Joint Session with ECIO'03, Faculty of Civil Engineering of CTU, Prague, Hall A
1 invited (30 min) and 6 regular oral presentations (15 min each)

8.30 – 9.00 Invited 1
Ph. Lalanne
Institut d'Optique/CNRS, Orsay Cedex, FRANCE
Bloch wave engineering for applications of subwavelength optical structures

9.00 – 9.15 Oral 1
M. Gioannini and I. Montrosset
Dip. Elettronica, Politecnico di Torino, Torino, ITALY
Time domain numerical model for linear and nonlinear grating assisted codirectional coupler

9.15 – 9.30 Oral 2
E. A. Romanova and L. A. Melnikov
Saratov State University, Department of Physics, Saratov, RUSSIA
Detailed analysis of spatiotemporal stability of the ultra-short optical pulses propagating in non- linear step-index optical waveguide

9.30 – 9.45 Oral 3
J. Katsifolis, S. Huntington, A. Ankiewicz, J. Love, and L. Cahill
La Trobe University, Dept. of Electronic Engineering, Bundoora, Victoria, AUSTRALIA
University of Melbourne, Dept. of Chemistry, Victoria, AUSTRALIA
Australian National University, Research School of Physical Sciences & Engineering, Canberra, AUSTRALIA
Transition loss in bent waveguides and fibres

9.45 – 10.00 Oral 4
A. Al-Jarro, P. Sewell, T. M. Benson, and A. Nerukh
Nottingham University, School of Electrical and Electronic Engineering, Nottingham, UK
Effective and flexible analysis for propagation in time varying waveguides

10.00 – 10.15 Oral 5
M. Takenaka and Y. Nakano
University of Tokio, Research Center for Advanced Science and Technology, Tokio, JAPAN
Proposal of an all-optical flip-flop using a cross-coupled MMI bistable laser diode

10.15 – 10.30 Oral 6
Hugo J.W.M. Hoekstra, Joris van Lith, Szabolcs B. Gaal and Paul V. Lambeck
University of Twente, MESA+ Research Institute, Lightwave Devices Group, Enschede, THE NETHERLANDS
The Spectral Decomposition Method: a Transparent Theory for Losses in Segmented Waveguides

10.30 – 11.00 Coffee break

Entrance Hall/Exhibition Area

11.00 – 12.30 Session FrA2: Photonic bandgap structures I

Joint Session with ECIO'03, Faculty of Civil Engineering of CTU, Prague, Hall A
1 invited (30 min) and 4 regular oral presentations (15 min each)

11.00 – 11.30 Invited 2
P. Russell
University of Bath, Department of Physics, Bath, UK
Photonic crystals as waveguides: beyond total internal reflection

11.30 – 11.45 Oral 7
R. Iliew, Ch. Etrich, U. Peschel, and F. Lederer
Friedrich-Schiller Uviversität Jena, Institut für Festkörpertheorie und Theoretische Optik, Jena, GERMANY *Efficient waveguide bend design in photonic crystals*

11.45 – 12.00 Oral 8
W. Bogaerts, P. Bienstman, and R. Baets
Ghent University, IMEC, Department of Information Technology, Ghent, BELGIUM
Sidewall roughness in photonic crystal slabs: a comparison of high-contrast membranes and low- contrast III-V epitaxial structures

12.00 – 12.15 Oral 9
D. Michaelis, U. Peschel, C. Waechter, A. Braeuer, and F. Lederer
Fraunhofer Institute for Applied Optics and Precision Engineering, Micro optics Department, Jena, GERMANY
Friedrich-Schiller Uviversität Jena, Institut für Festkörpertheorie und Theoretische Optik, Jena, GERMANY
Photonic crystal waveguides in highly dispersive materials

12.15 – 12.30 Oral 10
M. Hammer and D. Yudistira
University of Twente, MESA+ Research Institute, Department of Applied Physics, Enschede, THE NETHERLANDS
Grating assisted rectangular integrated optical microresonators

12.30 – 14.00 Lunch

Lunch poster preview

14.00 – 16.00 Session Fr3: Photonic bandgap structures II

Congress Hall, Masaryk College
2 invited (30 min each) and 4 regular oral presentations (15 min each)

14.00 – 14.30 Invited 3
H. Benisty
Laboratoire PMC, Ecole Polytechnique, Palaiseau, FRANCE
& Laboratoire Charles Fabry de l'Institut d'Optique, Orsay cedex, FRANCE
Planar photonic crystals: what are these teenagers capable of ?

14.30 – 15.00 Invited 4
M. Qiu
Royal Institute of Technology, Laboratory of Optics, Photonics and Quantum Electronics, Department of Microelectronics and Information Technology, Kista, SWEDEN
Modelling photonic crystal devices using the finite-difference time-domain method

15.00 – 15.15 Oral 11
H.-C. Chang, C.-P. Yu, and Y.-C. Chiang
National Taiwan University, Department of Electrical Engineering, Taipei, TAIWAN
Applications of the finite difference mode solution method to photonic crystal

15.15 – 15.30 Oral 12
S. Helfert and R. Pregla
FernUniversitaet in Hagen, Hagen, GERMANY
Numerical stable determination of Floquet–modes and their application to the computation of band structures

15.30 – 15.45 Oral 13
E. Bekker, P. Sewell, T. Benson, and L. Melnikov
Nottingham University, School of Electrical and Electronic Engineering, Nottingham, UK
Numerical investigation of holey fibres with polygon shaped holes

15.45 – 16.00 Oral 14
E E. Cassan, S. Laval, and L. Vivien
Université Paris-Sud, Institut d'Electronique Fondamentale, UMR CNRS 8622, Orsay, FRANCE
Modeling of optical microcavities in high-contrast index microwaveguides

16.00 – 16.30 Coffee break

Congress Hall, Masaryk College
Coffee break, poster preview

16.30 – 18.00 Session Fr4: Gratings & subwavelength structures

Congress Hall, Masaryk College
1 invited (30 min) and 4 regular oral presentations (15 min each)

16.30 – 17.00 Invited 5
G. Granet
LASMEA, Unité Mixte de Recherche, Université Blaise Pascal, Aubiere Cedex, FRANCE
Modal analysis of light transmission by subwavelength aperture arrays in metallic films

17.00 – 17.15 Oral 15
G. Bao and K. Huang
Michigan State University, Department of Mathematics, East Lansing, MI, USA
Optimal design of guided mode grating resonance filters

17.15 – 17.30 Oral 16
A. Delage and K. Dossou
National Research Council Canada, Institute for Microstructural Sciences, Ottawa, ON, CANADA
PDL calculation for a metalised echelle grating

17.30 – 17.45 Oral 17
B.A. Usievich, V.A. Sychugov, D.H. Nurligareev, and O. Parriaux
Institute of General Physics Moscow, Moscow, RUSSIA
Jean Monnet University, TSI Lab, Saint-Etienne, FRANCE
Grating waveguide resonance makes multilayer resonances sharper

17.45 – 18.00 Oral 18
P. Fernandez, J. C. Aguado, J. Blas, and R. Duran
University of Valladolid, Signal Theory, Communications and Telematic Engineering Department, Valladolid, SPAIN
Apodisation strength optimisation for linearly chirped Bragg gratings

18.00 – 19.30 Poster Session

Congress Hall, Masaryk College
21 posters

Poster 1
M. Montecchi, E. Nichelatti, R. M. Montereali, M. Piccinini, and F. Somma
ENEA, Advanced Physical Technologies Department, Rome, ITALY
INFN-LNF, Rome, ITALY
University of Rome, Department of Physics, Rome, ITALY
Increase of refractive index induced by absorbing centres: homogeneous and inhomogeneous line- broadening cases

Poster 2
L. Kotačka, H. J. W. M. Hoekstra, and J. Čtyroký
Optiwave Corporation, Ottawa, ON, CANADA
University of Twente, MESA+ Research Institute, Department of Applied Physics, Enschede, THE NETHERLANDS
Institute of Radio Engineering and Electronics, Academy of Sciences of the Czech Republic, Prague, CZECH REPUBLIC
Length dependence of the CSHG in planar waveguides: critical assessment

Poster 3
N. Sakhnenko and A. Nerukh
Kharkov National University of Radio Electronics, Kharkov, UKRAINE
Dielectric resonator with time-varying parameters

Poster 4
L. N. Illyashenko, A. I. Nosich, T. M. Benson, and P. Sewell
Institute of Radio-Physics and Electronics NASU, Department of Computational Electromagnetics, Kharkov, UKRAINE
The University of Nottingham, School of Electrical and Electronic Engineering, Nottingham, UK
Modeling of 2D photonic crystals by using the method of integral equations

Poster 5
J. Kašpar, I. Richter, and P. Fiala
Czech Technical University in Prague, FNSPE, Prague, CZECH REPUBLIC
Modeling special properties of subwavelength structures with EMT

Poster 6
W. C.L. Hopman, R. M. de Ridder, P. Pottier, and R. M. de la Rue
University of Twente, MESA+ Research Institute, Lightwave Devices Group, Enschede, THE NETHERLANDS
University of Glasgow, School of Electrical and Electronic Engineering, Scotland, UK
Experimental verification of modelling results of deeply etched Bragg gratings

Poster 7
A. G. Nerukh, F.V. Fedotov, T. M. Benson, and P. Sewell
The University of Nottingham, School of Electrical and Electronic Engineering, Nottingham, UK
Analytic-numerical approach to nonlinear problems in dielectric waveguides

Poster 8
N. Ruzhytska, A. G. Nerukh, and D. Nerukh
Kharkiv National University of Radio Electronics, Kharkov, UKRAINE
University of Cambridge, Department of Chemistry, Cambridge, UK
Dependence of electromagnetic signal complexity on medium disturbances

Poster 9
A. V. Tishchenko, O. Parriaux, and D. Neuschäfer
Jean Monnet University, TSI Lab, Saint-Etienne, FRANCE
Novartis Pharma AG, Basel, SWITZERLAND
Waveguide grating coupling of a 2D focused beam under normal incidence: a phenomenological approach

Poster 10
P. Peterka, B. Faure, W. Blanc, M. Karasek, and B. Dussardier
Université de Nice - Sophia Antipolis, Laboratoire de Physique de la Matičre Condensée CNRS, Nice, FRANCE
Institute of Radio Engineering and Electronics, Academy of Sciences of the Czech Republic, Prague, CZECH REPUBLIC
Theoretical modelling of S-band thulium-doped fibre amplifiers

Poster 11
A. V. Tishchenko
Jean Monnet University, TSI Lab, Saint-Etienne, FRANCE
The generalized source method: a fast numerical method for the analysis of 2D waveguide gratings

Poster 12
E. Romanova and S. Gaal
Saratov State University, Department of Physics, Saratov, RUSSIA
Feasibility of the slowly varying approximation in simulations

Poster 13
N. E. Nikolaev and V.V. Shevchenko
Peoples' Friendship University of Russia, Department of Radiophysics, Moscow, RUSSIA
On capability and accuracy of shift formula method

Poster 14
V. Nemecek, I. Richter, P. Fiala, and J. Kratochvil
Czech Technical University in Prague, FNSPE, Prague, CZECH REPUBLIC
Analysis and design of waveguide grating couplers

Poster 15
M. Novák, I. Richter, and P. Fiala
Czech Technical University in Prague, FNSPE, Prague, CZECH REPUBLIC
PBS Solver – a software tool for calculating photonic band structures of 2D dielectric photonic crystals based on plane-wave method

Poster 16
L. Prkna, J. Čtyroký, and M. Hubálek
Institute of Radio Engineering and Electronics, Academy of Sciences of the Czech Republic, Prague, CZECH REPUBLIC
Microresonator As a Photonic Structure with Complex Eigenfrequency

Poster 17
N. P. Yeung, E. Y. B. Pun, and P. S. Chung
City University of Hong Kong, Department of Electronic Engineering, Hong Kong, HONG KONG
Analysis of a novel broadband Ti LiNbO3 Mach-Zehnder optical modulator using an extended point-matching method

Poster 18
E. I. Smotrova, A. I. Nosich
Institute of Radio-Phisics and Electronics NANU, Kharkov, UKRAINE
Mathematical study of the lasing problem for the whispering-gallery modes in a 2-D circular dielectric microcavity

Poster 19
H. V. Baghdasaryan, T. M. Knyazyan, and A. A. Mankulov
State Engineering University of Armenia, Fiber Optics Communication Laboratory, Yerevan, ARMENIA
Numerical modelling of absorbing and amplifying reflective microinterferometer Fabry – Perot via the method of single expression

Poster 20
H. Alatas, A. A. Iskandar, M. O. Tjia
Institut Teknologi Bandung, Dept. of Physics, Bandung, INDONESIA
University of Twente, Faculty of Applied Physics, Enschede, THE NETHERLANDS
In-gap dark and antidark soliton in deep nonlinear Bragg grating

Poster 21
J. Prawiharjo, A. A. Iskandar, M. O. Tjia, and E. van Groesen
Institut Teknologi Bandung, Dept. of Physics, Bandung, INDONESIA
University of Twente, MESA+ Research Institute, Enschede, THE NETHERLANDS
Band Gap Characterization of One Dimensional Dielectric Omnidirectional Reflector

Poster 22
A. Bertolani, A. Cucinotta, M. Fuochi, F. Poli, S. Selleri, and M. Zobo
University of Parma, Dipartimento di Ingegneria dell'Informazione, Parma, ITALY
University of Modena and Reggio Emilia, Dipartimento di Ingegneria dell'Informazione, Modena, ITALY
Numerical Analysis of Lithium-Niobate Electro-Optical Modulators through a Full-Vectorial Three-Dimensional Finite Element based Beam Propagation Method

20.00 – 22.00 Workshop Dinner

CTU Restaurant, Masaryk College

Saturday, April 5, 2003

Congress Hall, Masaryk College

8.30 – 10.30 Session Sa1: Laser & nonlinear & meta-material modelling

Congress Hall, Masaryk College
2 invited (30 min each) and 3 regular oral presentations (15 min each)

8.30 – 9.00 Invited 6
C. M. Soukolis
Ames-Laboratory-USDOE and Department of Physics and Astronomy, Iowa State University, USA
& Research Center of Crete, FORTH, Heraklion, Crete, GREECE
Negative refraction and left-handed behavior in photonic crystals

9.00 – 9.30 Invited 7
V. Kuzmiak
Institute of Radio Engineering and Electronics, Academy of Sciences of the Czech Republic, Prague, CZECH REPUBLIC
Amplification in 1D periodic and random active media near lasing threshold

9.30 – 9.45 Oral 19
B. Maes, P. Bienstman, and R. Baets
Ghent University IMEC, Department of Information Technology, Ghent, BELGIUM
Rigorous modelling of non-linear structures with mode expansion

9.45 – 10.00 Oral 20
J. Wykes, J. Bonnyman, P. Sewell, T. Benson, S. Sujecki, E. Larkins, L. Borruel, and I. Esquivias
The University of Nottingham, School of Electrical and Electronic Engineering, Nottingham, UK
Utilisation of parallel processing techniques to maximise the computational efficiency of an advanced high power semiconductor laser model

10.00 – 10.15 Oral 21
G. Bellanca, A. Parini, S. Trillo, L. Saccomandi, and P. Bassi
University of Bologna, Dipartimento di Elettronica Informatica e Sistemistica, Bologna, ITALY
Transfer matrix and full Maxwell time-domain analysis of nonlinear gratings

10.15 – 10.30 Oral 22
A. Irman and T. P. Valkering
University of Twente, Applied Physics, Enschede, THE NETHERLANDS
Validity bounds of the coupled mode equations in a Kerr grating

10.30–11.00 Coffee break

Coffee break, informal viewing of posters

11.00 – 12.45 Session Sa2: Modelling methods and tools

Congress Hall, Masaryk College
1 invited (30 min) and 5 regular oral presentations (15 min each)

11.00 – 11.30 Invited 8
P. Bienstman
Ghent University, IMEC, Department of Information Technology, Ghent, BELGIUM
Vectorial eigenmode modelling using perfectly matched layer boundary conditions

11.30 – 11.45 Oral 23
M. Hammer
University of Twente, MESA+ Research Institute, Department of Applied Mathematics, Enschede, THE NETHERLANDS
Quadridirectional eigenmode expansion scheme for 2-D modeling of wave propagation in integrated optics

11.45 – 12.00 Oral 24
S. S. A. Obayya, B. M. A. Rahman, and K. T. V. Grattan
City University London, School of Engineering and Mathematical Sciences, London, UK
Accurate finite element computation of full vectorial modes

12.00 – 12.15 Oral 25
M.A Luque-Nieto, J.G. Wangüemert-Pérez, and I. Molina-Fernández
Malaga University, Dpto. Ingeniería de Comunicaciones, Málaga, SPAIN
A Novel Fourier Based 3D-Full Vectorial Beam Propagation Method

12.15 – 12.30 Oral 26
S. L. Chui and Y. Y. Lu
City University of Hong Kong, Department of Mathematics, Kowloon, HONG KONG
A wide-angle full-vector beam propagation method based on ADI preconditioner

12.30 – 12.45 Oral 27
H. P. Uranus, H. J. W. M. Hoekstra, E. van Groesen
University of Twente, MESA+ Research Institute, Lightwave Devices Group, Enschede, THE NETHERLANDS
Simple high-order Galerkin finite element scheme for the investigation of both guided and leaky modes in axially anisotropic planar waveguides

12.45 – 14.15 Lunch

Lunch, informal viewing of posters

14.15 – 16.00 Session Sa3: Device oriented modelling

Congress Hall, Masaryk College
1 invited (30 min) and 4 regular oral presentations (15 min each)

14.15 – 14.45 Invited 9
J. Love
Australian National University, Research School of Physical Sciences & Engineering, Canberra, AUSTRALIA
Passive planar devices for light processing in telecommunications

14.45 – 15.00 Oral 28
R. Pregla
FernUniversitaet in Hagen, Hagen, GERMANY
Modeling of optical waveguide structures with general anisotropy

15.00 – 15.15 Oral 29
L. Cahill
La Trobe University, Department of Electronic Engineering, Bundoora, AUSTRALIA
The modelling of generalised Mach-Zehnder optical switches and power splitters

15.15 – 15.30 Oral 30
C. Styan, A. Vukovic, P. Sewell, and T.M. Benson
The University of Nottingham, School of Electrical and Electronic Engineering, Nottingham, UK
Adaptive synthesis for optical waveguides: CAD or fad ?

15.30 – 15.45 Oral 31
A. Stump, J. Kunde, U. Gubler, A. - C. Pliska-LeDuff, and Ch. Bosshard
CSEM SA, Alpnach, SWITZERLAND
A microring structure for practical devices

15.45 – 16.00 Oral 32
W. Pascher, J. H. den Besten, D. Caprioli, X. Leijtens, M. Smit, and R. van Dijk
FernUniversität, Elektromagnetische Feldtheorie, Hagen, GERMANY
Eindhoven University of Technology, Opto-Electronic Devices group, Eindhoven, THE NETHERLANDS
TNO Physics and Electronics Laboratory, The Hague, THE NETHERLANDS
Design and optimization of a velocity-matched travelling-wave electro-optic modulator

16.00 – 16.30 Coffee break

Congress Hall, Masaryk College
Coffee break, informal viewing of posters

16.30 – 18.00 Session Sa4: Waveguide theory & modelling

Congress Hall, Masaryk College
6 regular oral presentations (15 min each)

16.30 – 16.45 Oral 33
B. M. A. Rahman, S. S. A. Obayya, N. Somasiri, M. Rajarajan, C. Themistos, and K. T. V. Grattan
City University London, School of Engineering and Mathematical Sciences, London, UK
Polarization issues in optical waveguides and optoelectronic systems

16.45 – 17.00 Oral 34
S.V. Boriskina, T. M. Benson, P. Sewell, and A. I. Nosich
The University of Nottingham, School of Electrical and Electronic Engineering, Nottingham, UK
Integral equation method for studying the resonant spectra

17.00 – 17.15 Oral 35
A. Melloni, F. Morichetti, and M. Martinelli
Politecnico di Milano, Dip. Elettronica e Informazione, Milano, ITALY
An equivalent circuit of partial reflectors for circuit synthesis

17.15 – 17.30 Oral 36
V. Mezentsev, S. Turitsyn, S. Yakovenko, S. Kobtsev, S. Kukarin, and N. Fateev
Aston University, Photonics Research Group, Birmingham, UK
Numerical modal analysis of silica/air-clad dual-core fibres

17.30 – 17.45 Oral 37
A. Cachard, E. Bonnet, A. Tishchenko, O. Parriaux, X. Letartre, and D. Gallagher
Jean Monnet University, TSI Lab, Saint-Etienne, FRANCE Photon Design, Oxford, UK
Anomalously large reflection of a focused free space beam from a high contrast segmented waveguide under normal incidence

17.45 – 18.00 Oral 38
H. B. H. Elforai and H. J. W. M. Hoekstra
University of Twente, MESA+ Research Institute, Lightwave Devices Group, Enschede, THE NETHERLANDS
Exact analytical solution for the local density of modes in planar structures

18.00 – 18.30 Review of the Workshop

Congress Hall, Masaryk College
Review of the Workshop, announcement on the next Workshop, closing

Organization

Conference Chair

Jiří Čtyroký	Institute of Radio Engineering and Electronics, Czech Academy of Sciences, Czech Republic

Technical Committee

Trevor Benson	University of Nottingham, United Kingdom
Jiří Čtyroký	Institute of Radio Engineering and Electronics, Czech Academy of Sciences, Czech Republic
Anand Gopinath	University of Minnesota, USA
Hans-Peter Nolting	HHI Berlin, Germany
Hugo J. W. M. Hoekstra	University of Twente, Netherlands
Olivier Parriaux	University of Saint Etienne, France
Reinhold Pregla	FernUniversität Hagen, Germany
Christoph Wächter	Fraunhofer Inst. AOT Jena, Germany

Local Organizing Committee

Ivan Richter	Faculty of Nuclear Sciences and Physical Engineering, Czech Technical University in Prague, Czech Republic
Petr Honsa	Faculty of Nuclear Sciences and Physical Engineering, Czech Technical University in Prague, Czech Republic
Terezia Němcová	Congress Department, Czech Technical University in Prague, Czech Republic
Václav Němeček, Miroslav Novák, Marek Škereň, Jan Kašpar	Faculty of Nuclear Sciences and Physical Engineering, Czech Technical University in Prague, Czech Republic

Invited Talks

Invited 1 **Ph. Lalanne**
Institut d'Optique/CNRS, Orsay Cedex, FRANCE

Invited 2 **P. Russell**
University of Bath, Department of Physics, Bath, UK

Invited 3 **H. Benisty**
Laboratoire PMC, Ecole Polytechnique, Palaiseau, FRANCE
and Laboratoire Charles Fabry de l'Institut d'Optique, Orsay cedex, FRANCE

Invited 4 **M. Qiu**
Royal Institute of Technology, Laboratory of Optics, Photonics and Quantum Electronics, Department of Microelectronics and Information Technology, Kista, SWEDEN

Invited 5 **G. Granet**
LASMEA, Unité Mixte de Recherche, Université Blaise Pascal, Aubiere Cedex, FRANCE

Invited 6 **C. M. Soukolis**
Ames-Laboratory-USDOE and Department of Physics and Astronomy, Iowa State University, USA and Research Center of Crete, Forth, Heraklion, Crete, GREECE

Invited 7 **V. Kuzmiak**
Institute of Radio Engineering and Electronics, Academy of Sciences of the Czech Republic, Prague, CZECH REPUBLIC

Invited 8 **P. Bienstman**
Ghent University, IMEC, Department of Information Technology, Ghent, BELGIUM

Invited 9 **J. Love**
Australian National University, Research School of Physical Sciences & Engineering, Canberra, AUSTRALIA

Bloch wave engineering for high Q's small V's optical microcavities

Philippe Lalanne, Jean-Paul Hugonin
Laboratoire Charles Fabry de l'Institut d'Optique, Centre National de la Recherche Scientifique, 91 403 Orsay Cedex, France
Philippe.lalanne@ iota.u-psud.fr

Keyword: guided-wave optics, microcavity, radiation losses, Bloch modes

Introduction

Many important devices use periodic microstructures of alternating layers of dielectric materials to enhance reflection. Usually the refractive index contrast of dielectric layers is low, typically 1% in a distributed Bragg reflector, and a large number of small reflections over a long propagation distance are needed to warrant high reflectivity [1]. Alternatively, periodic microstructures deeply etched into a semiconductor waveguide offer high refractive-index contrasts and much shorter interaction lengths. Examples include photonic wires or air-bridge microcavities [2,3] and very compact Bragg reflectors [4,5,6]. Responding to the quest for miniaturization in optoelectronics, these new mirrors implemented in short cavities additionally offer interesting perspectives: large free spectral ranges, small modal volumes as is required for controlling the spontaneous emission of atoms in microcavities [7], and low threshold lasers. However, for strong corrugations, the Bragg mirror cannot be considered as a perturbation of the uncorrugated waveguide and out-of-plane scattering losses (radiation) in the claddings are inevitable. Apparently strong corrugations required for short interaction lengths and small radiation losses required for high performance seems to be two conflicting objectives.

Two routes are known to achieved high Q's and small V's in optics. The first one refers to the complete 3D photonic crystal approach (the cage for light [8]). Another exploits a judicious refractive index engineering of the core and cladding layers [9]. Both approaches provide theoretically lossless operation, but requires a complex 3D refractive-index engineering. *We proposed another approach which can be fully implemented in planar systems*. As shown by numerical computations in [10] and by experimental results in [11], tapered mirrors that incorporate a series of etches whose feature dimensions vary progressively can provide short interaction lengths and low radiation losses.

The radiation-loss problem

To illustrate our purpose, let us consider the one-dimensional photonic-bandgap air-bridge cavity shown in Fig.1. The periodicity constant Λ is 450 nm and the hole diameter w is 250 nm. Hereafter, we assume that the semiconductor bridge (n = 3.48) is 340-nm-thick, 500-nm-wide. Similar microcavities have been studied previously [3], and Q's of ≈ 300 for $V \approx 0.03\ \mu m^3$ have been observed at $\lambda = 1.5\ \mu m$. In the wavelength range of interest, the waveguide supports a single TE-like mode (electric field primarily horizontal at the center of the waveguide) with a double mirror symmetry. For $\lambda = 1.56\ \mu m$, the calculated losses L of

the semi-infinite mirrors illuminated by the fundamental mode of the bridge are 4.5%. Thus one expects that a short microcavity formed by the association of these two mirrors has a Q factor $Q_{FP} = m\pi(R)^{1/2}/L$. For a cavity order $m = 3$ (as it is the case for a single hole defect cavity), one expects that $Q_{FP} \approx 200$.

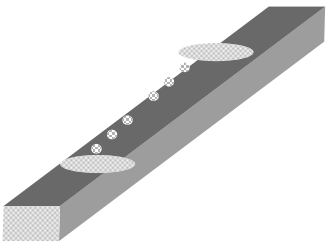

Figure 1. Microcavity discussed in this work. The cavity is formed by two-periodic holes arrays separated by a small defect, typically a single hole defect.

Engineered mirrors and cavities

As shown hereafter, this low Q value can be increased by several orders of magnitude while keeping constant the mode volume V of the cavity. Let us first explain the raison for this low Q value. In [10], the authors propose an approximate model that interpretates the origin of the loss at the interface between the waveguide and the mirror as an impedance mismatch between the incident guided mode and some electromagnetic quantity directly to the fundamental Bloch wave associated to the mirror (we will refer this quantity to as a half-Bloch mode). The losses vary as the square of the integral overlap η between the half-Bloch mode and the incident guided mode [10]. An immediate consequence is that if one desires to reduce the radiation losses to increase the cavity Q, one must engineer the periodic mirrors to taper the incident guided mode into the fundamental Bloch mode of the mirrors. As suggested in [10], a possible solution consists in designing tapered mirrors formed by a series of "segments" whose feature dimensions vary progressively. An illustration of an engineered mirror is shown in Fig. 2, where two "segments" are inserted between the waveguide and the periodic mirror.

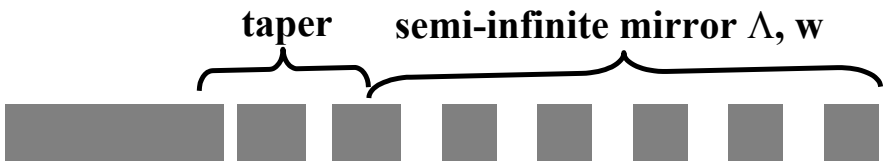

Figure 2. Exemple of tapered mirror obtained by varying the two first hole dimension and spacing of the periodic mirror.

Microcavities with high Q's and small V's

As will be shown at the conference, two different approaches can be used to design microcavities with high Q's and small V's.

The first approach is simple in its principle. It consists in designing mirrors with small radiation losses. At the conference, we will show that the design mainly consists an engineering of the fundamental Bloch mode, and that the main degree of freedom to be used for the design is the length Λ of the segments.

The second approach is more counterintuitive. It can be shown [12] that the performance of microcavities formed by a defect surrounded by two short Bragg mirrors is not ultimately driven by the modal mirror reflectivity and transmission, i.e. by the mirror losses. In other words, cavities formed with quite lossy mirrors can exhibit unexpected high Q factors. As shown in [12], this anomalous Q's of microcavities can be explained by a radiation recycling mechanism, a pure electromagnetism effect on transient fields at subwavelength scale in the cavity defect. Once appropriately engineered, the recycling boosts the Q's and peak transmissions by several orders of magnitude.

The two approaches can cooperate in practice. To illustrate our purpose, we performed calculations for symmetric cavities with slightly different hole geometries. Only two degrees of freedom, namely the location and the diameter of the two inner holes, were varied for optimizing the intrinsic Q factor. Due to the great computational loads, the configuration space was not thoroughly explored, but many cavity geometries with Q's much larger than that achieved with the periodic mirror were obtained. The three-dimensional computation is performed with the frequency-domain Fourier modal method described in [13]. One of the best performance is achieved for a geometry which corresponds to a 30-nm reduction of the hole diameter and to a 65-nm outer displacement of the center hole locations. Circles in Fig. 3 represent the calculated Q's of the engineered cavity for $\lambda = 1.56$ μm and for the third cavity order (m = 3.15) as a function of the number N of holes.

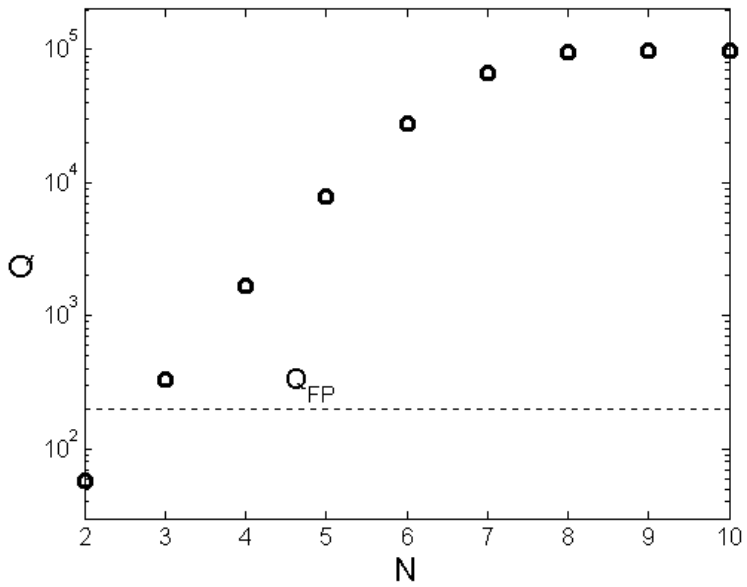

Figure 3. Calculated Q of the engineered cavity as a function of the number of holes. The horizontal dashed line represents the Q factor in the absence of recycling for the cavity formed with the semi-infinite periodic mirrors.

The Q's of the engineered cavity are several order of magnitude higher than the predicted value $Q_{FP} \approx 200$ (horizontal dashed line in the Figure) for the cavity with fully periodic mirrors. This increase has two causes. First, the engineered mirror losses are smaller than those of the periodic mirror increasing the cavity Q from 200 to 750, and secondly, the

radiation recycling is responsible for an other increase by more than a factor one hundred. Finally let us note that, since the modal volume of the engineered cavity is only 6% larger than that of the cavity with fully periodic mirrors, the engineering results in an enhancement of the Purcell factor (Q/V) by a factor 500.

Mirel Palamaru and **Eric Silberstein** were previously involved in this research as master and PhD students. The authors thanks their colleagues **D. Peyrade, A. Talneau, and Y. Chen** from the Laboratoire de Photonique et de Nanostructures at Marcoussis for fruitful discussions and experimental works on the fabrication and characterization of microcavities note reported here in this abstract.

[1] L.A. Coldren and S.W. Corzine, Diode lasers and photonic integrated circuits, First ed. (Wiley, New York, 1995).
[2] J.P. Zhang, D.Y. Chu, S.L. Wu, W.G. Bi, R.C. Tiberio, R.M. Joseph, A. Taflove, C.W. Tu, S.T. Ho, IEEE Photon. Technol. Lett. **8**, 491 (1996).
[3] J.S. Foresi, P.R. Villeneuve, J. Ferrera, E.R. Thoen, G. Steinmeyer, S. Fan, J.D. Joannopoulos, L.C. Kimerling, H.I. Smith and E.P. Ippen, Nature **390**, 143 (1997).
[4] T.F. Krauss and R. M. De La Rue, Appl. Phys. Lett. **68**, 1613 (1996).
[5] T. Baba, M. Hamasaki, N. Watanabe, P. Kaewplung, A. Matsutani, T. Mukaihara, F. Koyama and K. Iga, Jpn. J. Appl. Phys. **35**, 1390 (1996).
[6] T.F. Krauss, O. Painter, A. Scherer, J.S. Roberts, R. M. De La Rue, Opt. Eng. **37**, 1143 (1998).
[7] *Spontaneous emission and laser oscillation in microcavities*, edited by H. Yokoyama and K. Ujihara, Boca raton, FL: CRC Press, 1995.
[8] D. Normile, Science **286**, 1500 (1999).
[9] J. Ctyroky, J. Opt. Soc. Am. A **18**, 435 (2001). See also, M. R. Watts, S.G. Johnson, H.A. Haus and J.D. Joannopoulos, Opt. Lett. **27**, 1785 (2002).
[10] M. Palamaru and Ph. Lalanne, Appl. Phys. Lett. **78**, 1466 (2001).
[11] D. Peyrade, E. Silberstein, P. Lalanne, A. Talneau, Y. Chen, Appl. Phys. Lett. **81**, 829 (2002).
[12] Philippe Lalanne, Jean-Paul Hugonin, « Radiation recycling in microcavities », submitted for publication.
[13] E. Silberstein, Ph. Lalanne, J.P. Hugonin and Q. Cao, J. Opt. Soc. Am. A. **18**, 2865 (2001).

Photonic crystals as waveguides: Beyond total internal reflection

Philip Russell

Optoelectronics Group, Department of Physics
University of Bath, Bath BA2 7AY
United Kingdom
Tel +44 1225 386946; Email p.s.j.russell@bath.ac.uk

Photonic crystals can be viewed as a lattice of identical wavelength-scale dielectric objects – nanostructured sheets, wires or dots. With correct choice of frequency and wave momentum these objects resonate with light. The highly dispersive balance between energy storage and energy flow fundamentally alters the electromagnetic dispersion relation, giving rise to a host of peculiar effects [1]. Examples include negative and zero diffraction, negative Doppler shifts, negative/multiple refraction and reflection, total internal reflection at normal incidence – and of course the photonic band gap.

One example is “photonic crystal film” – a thin layer of dielectric drilled through with a pattern of microscopic holes. Such structures have the potential to confine and direct the flow of light in three dimensions, slowing it down, speeding it up, deflecting it and controlling its dispersion and diffraction. In addition they can function as high quality vertically resonant cavities, with multiple potential applications in sensing and lasers. Given the rapid pace of progress, practical devices seem likely to emerge within the next few years.

Another example is photonic crystal fiber (PCF), sometimes also known as “holey” or “microstructured” fiber [2]. PCF has been the focus of increasing scientific and technological interest since the first working example was produced in late 1995 (reported at the Optical Fiber Communications Conference in March 1996). Although superficially similar to a standard fiber, PCF has a unique microstructure, consisting of an array of microscopic holes (or channels) that run along its entire length. These holes act as optical barriers or scatterers, which suitably arranged can “corral” light within a central core (either hollow or made of solid glass). The holes can range in diameter from ~25 nm to ~50 m. Although most PCF is formed in pure silica glass, it has also recently been made using polymers and non-silica glasses, where it is difficult to find compatible core and cladding materials suitable for conventional total internal reflection guidance. PCF supports two guidance mechanisms: total internal reflection, in which case the core must have a higher average refractive index than the holey cladding; and a two-dimensional photonic bandgap, when the index of the core is uncritical – it can be hollow or filled with material. Light can be controlled and transformed in these fibers with unprecedented freedom, allowing for example the guidance of light in a hollow core, the creation of highly nonlinear solid cores with anomalous dispersion in the visible and the design of fibers that support only one transverse spatial mode at all wavelengths. As the performance of these fibres continues to improve (losses of 13 dB/km for hollow core and 0.58 dB/km for solid core PCFs were reported recently), multiple applications are being found in diverse areas of science and technology.

The enhanced control of light offered by photonic crystals is changing the menu of the possible in optics.

1. P.St.J. Russell, “Designing photonic crystals,” in *Electron and Photon Confinement in Semiconductor Nanostructures* (Ed: P. Schwendimann), Proceedings of International School of Physics (Varenna, Italy, June-July 2002), to be published by Societa' Italiana di Fisica 2003.
2. P.St.J. Russell, “Photonic crystal fibers,” *Science* 299 (358-362) 2003.

Planar Photonic Crystals: What are these teenagers capable of?

H. Benisty

Laboratoire PMC, Ecole Polytechnique, Palaiseau, FRANCE
&
Laboratoire Charles Fabry de l'Institut d'Optique, Orsay cedex, FRANCE

Photonic crystals are now 16 years old on the paper. Their last planar versions (deep-etched on substrate or on membranes) are the more amenable novel and miniature forms of light control applicable to device and integrated optics in particular. However, playing with wavelength-scale cavities and guides in these systems appeared as a very complex game. The cherished rules of "classical" integrated optics give very limited insight and no powerful design rules have emerged to well tackle the simple case of a bend. Furthermore, there are some intrinsic losses in these structures, whatever the design, that add to "unavoidable" losses due to etching irregularities and materials consideration. In view of these elements, one could be doubtful whether these teenagers will become the well behaved adults that were promised originally. I will discuss this issue by addressing the origin of losses of both kinds (intrinsic and irregularities) in a perturbative approach. Based on a proposal by S. Olivier et al. (accepted in the ECIO proceedings) of a novel add-drop filter design tractable with 4x4 coupled-mode theory, we will discuss how to circumvent the hole-to-hole irregularity to a noticeable extent. This gives some hope to get through a possible teenage crisis of this exciting topic.

Modelling photonic crystal devices using the finite-difference time-domain method

Min Qiu
Laboratory of Optics, Photonics and Quantum Electronics, Department of Microelectronics and Information Technology, Royal Institute of Technology (KTH), Electrum 229, 16440 Kista, Sweden
E-Mail: min@imit.kth.se

The present paper shows how the finite-difference time-domain method is used to study photonic crystal devices. Some important numerical issues concerning the method are also addressed.

Keywords: numerical modelling, guided-wave optics, photonic crystals, periodic structures, finite-difference time-domain method

A variety of methods have been used to calculate photonic band structures. Among these there are plane wave expansion method, multiple-scattering theory (Korringa-Kohn-Rostoker method), tight-binding formulation, transfer matrix method, finite difference method, generalized Rayleigh identity method, averaged field approach, and so forth. Each method has its advantages and disadvantages, and one may choose a suitable method depending on particular problems.

The Finite-Difference Time-Domain (FDTD) method is a very often-used approach to solve Maxwell's equations [1]. It can solve a wide variety of problems related to electromagnetic waves, such as wave propagation, scattering, electronic circuits, antenna analysis, etc. It has also been shown that the FDTD method is a powerful method to study the photonic crystal devices.

In the present paper, we show that how the FDTD method is used to compute the band structures of photonic crystals with dielectric and metallic inclusions [2-4], as well as for studying photonic crystal waveguides [5], point defects [6], surface modes [7], and so on. Besides the computations of the eigenmodes, the FDTD method can also be used to study the spectral response of the photonic crystal devices. The effective index method [8] and the effective loss method [9] are also presented when investigating the two-dimensional photonic crystals in slab structures.

Some important numerical issues concerning the FDTD method for photonic crystal devices are also addressed.

References

[1]. K. S. Yee, *IEEE Trans. Antennas Propag.* **14**, 302 (1966).
[2]. C.T. Chan, Q.L. Yu and K.M. Ho, *Phys. Rev. B*, **51**, 16635 (1995).
[3]. M. Qiu and S. He, *J. Appl. Phys*., **87**, 8268, (2000).
[4]. M. Qiu and S. He, *Phys. Lett. A,* **278***,* 6, (2001).
[5]. M. Qiu and S. He, *Phys. Lett. A,* **266***,* 425, (2000).
[6]. M. Qiu and S. He, *Phys. Rev. B.,* **61**, 12871, (2000).
[7]. M. Qiu and S. He, *Phys. Lett. A,* **282***,* 85, (2001).
[8]. M. Qiu, *Appl. Phys. Lett.* **81**, 1163, (2002).
[9]. M. Qiu, B. Jaskorzynska, M. Swillo, and H. Benisty, *Microwave Opt. Techn. Lett.,* **34**, 387 (2002).

Modal analysis of light transmission by subwavelength aperture arrays in metallic films

Gérard Granet

LASMEA, Unité Mixte de Recherche, Université Blaise Pascal, Aubiere Cedex, FRANCE
granet@lasmea.univ-bpclermont.fr

Nowadays, opticians are greatly interested in structures that exhibit anomalous behaviour because of their potential applications in novel photonic devices. The extraordinary enhanced transmission by sub wavelength metallic hole arrays is one such phenomenon. Since the publication of Ebbesen et al., many experimental and theoretical studies have been carried out in order to determine the physical origin of the observed enhanced transmission. Several authors attributed it to the excitation of surface plasmons, others related the effect to cavity resonances. It is now established that both horizontal and vertical resonances play a role in the extraordinary transmission. It is then of importance to characterise and to understand the electromagnetic behaviour of the channel through which the light propagates inside the metallic film. Numerical simulations have recently shown that a transmission as high as 80 % can be obtained with annular apertures. The aim of the present communication is to study the spectral response of metallic films with coaxial apertures.

Although general methods, like FDTD (for example), allow to calculate rigorously the reflection and transmission of a plane wave by a periodical structure in the resonance domain, modal methods are best suited for analysing the physical behaviour of such structures. The problem is indeed to asses which kind of modes are supported by the structure and which of them are responsible for the resonant transmission. Because of the periodicity of the problem, we use the Fourier modal method. It is known to offer computational simplicity since only basic linear algebra operations are required: seeking eigenvalues and eigenvectors and solving linear systems. The accuracy of the results is linked with the number of spatial harmonics retained in the calculation. For diffraction by crossed grating structures, the size of the matrices involved in computation is squared in comparison with that of the corresponding one-dimensional problem. It is therefore of crucial importance to derive the smallest possible eigenvalue problem. We have shown in previous work that highly improved convergence rates could be obtained by using an adaptive coordinate system such that spatial resolution was increased around the discontinuities of the permittivity function. Another reason for using adaptive spatial resolution is that we are interested in the spatial distribution of the field inside the metallic hole. We have therefore to be sure that we have achieved convergence. A S matrix approach is used to write the coupling between the modes located inside the hole and the free space spectrum.

The first part of this talk is devoted to the numerical method itself. Our opinion is indeed that the concept of adaptive spatial resolution is relevant for all Fourier based methods. We will show that this approach is even absolutely necessary for problems in the optical domain as soon as metals are involved. In the second part, we will investigate the spectral behaviour of some coaxial waveguides with sub wavelength apertures and we will study the influence of the various geometrical parameters of the structure on its transmission spectrum.

Negative Refraction and Left-Handed Behavior in Photonic Crystals

C. M. Soukoulis

Ames-Laboratory-USDOE and Department of Physics and Astronomy,
Iowa State University, Ames, IA 50011

Research Center of Crete, FORTH, Heraklion, Crete, Greece

The conditions of obtaining left-handed (LH) behavior in a photonic crystal (PC) are examined systematically. For that purpose we use the Finite Difference Time Domain (FDTD) technique to study the propagation of electromagnetic (EM) waves through PC structures. Our results show that the existence of negative refraction does not guarantee the existence of negative index of refraction and so LH behavior. We propose a wedge type of experiment that can distinguish between cases of negative refraction that occur when left-handed behavior is present, from cases that show negative refraction without LH behavior. We also study with the FDTD, a case where an EM wave undergoes a negative refraction , at the interface between a positive and negative refractive index material. We observe that the wave is temporarily trapped on the interface, gradually reorganizes itself and after a long time, eventually propagates in the negative direction. This shows how negative refraction can occur in the realistic PC system without violating causality and the speed of light limit.

Amplification in one-dimensional periodic and random active medium near lasing threshold

Vladimir Kuzmiak
Institute of Radio Engineering and Electronics AS CR, Chaberská 57, 182 51 Praha 8, Czech Rep.
kuzmiak@ure.cas.cz

By using analytical expressions that have been derived by means of the Chebyshev identity we study properties of the transmittance $|t_N|^2$ of one-dimensional periodic medium with gain that resemble the transmittance of a single slab both of which reveal maximum as a function of the length L and number of layers N, respectively. We show that the effects associated with the presence of the gain in a one-dimensional periodic medium, such as enhanced amplification near the band edges, can be described in terms of the components of the complex Bloch wave vector that is determined from the eigenvalue equation for the transfer matrix. To examine the behaviour of the periodic amplifying medium near the lasing threshold we employ the convergence criterion proposed by Nam and Zhang[Phys. Rev. B **66**, 73101(2002)], and the transmittance is monitored as a function of the imaginary part of the dielectric function $\epsilon^{''}$ and the number of layers N. By varying $\epsilon^{''}$ we determine the relative position of the transmittance of the system with respect to the pole of the transmittance at which $d|t_N|^2/d\epsilon^{''} = 0$ and beyond which the system becomes anticausal and corresponds the diverging solution of the time-dependent Maxwell's equation. We show that the random active media in contrast to periodic media do not possess an unambiguos critical number of layers N_c that separates the physical system from an unphysical one. To study the behaviour of the random system near the lasing threshold we inspect the relation for the critical length L_c, that is defined in statistical terms as the length for which probability of finding of the physical solution $P(\Lambda_c) = 0.5$, where $\Lambda_c \equiv L_c/\xi_0$ and ξ_0 is a localization length in the absence of gain. The relation for L_c can be within two-parameter scaling model obtained from the slope of $\Lambda_c = \Lambda_c(q)$, which leads to the relation $L_c \simeq q^{-2/3}$ where $q \equiv \xi_0/l_g$ denotes a dimensionless gain length and $l_g = 2/\omega\epsilon^{“}$ is gain length. In this paper we extend the study of the relation for the critical size L_c with respect to the strength of randomness σ by inspecting the dependence of the slope on the strength of the randomness we interpret its behaviour in terms of the statistical properties of the localized states. Namely, by inspecting of the variance of the Lyapunov coefficient λ(inverse of the localization length ξ_0) we have found that the slope of the $\ln\Lambda_c(q)$ reflects the transition between two different regimes of localization known as Anderson- and Lifshits-like behaviour that is known to be indicated by peak in $var(\lambda)$. Deych *et* al.[Phys. Rev. Lett. **81**, 5390(1998)].

Vectorial Eigenmode Modelling using Perfectly Matched Layer Boundary Conditions

Peter Bienstman, Roel Baets
Department of Information Technology, Ghent University / IMEC,
Sint-Pietersnieuwstraat 41, B-9000 Gent, Belgium
Peter.Bienstman@rug.ac.be

Keywords: eigenmode expansion, boundary conditions

Abstract

We will present an efficient and flexible method for the calculation of guided wave and photonic crystal structures. The method is based on the principle of vectorial eigenmode expansion. Rather than spatially discretising the structure under study, the electromagnetic field is expanded into the eigenmodes of each longitudinally invariant layer. Subsequently, scattering matrices are computed to describe the behaviour of the entire component. The method can be used equally well to model infinite and finite structures.

For infinite structures and band structure calculations, the model has the advantage that it can easily be applied to dispersive media, which will be illustrated with examples. Also, because it uses eigenmodes rather than plane waves as basis functions, it converges faster than more conventional approaches.

For the modelling of finite structures containing periodic sections, the method has the advantage that computation times are logarithmic in the number of periods, rather than linear. Also, the use of advanced absorbing boundary conditions like PML (perfectly matched layer) means that the method is able to model radiation loss accurately, which is important for practical applications.

The extension to three-dimensional problems will be discussed as well. More specifically, we will illustrate how a two-stage procedure can be very efficient in finding the eigenmodes of waveguides with an arbitrary 2D cross-section. Once again, radiation loss can be accounted for using PML boundary conditions, and the materials can have complex refractive indices.

The modeling code (called CAMFR or Cavity Modelling FRamework) is freely available from http://camfr.sourcefore.net .

Passive Planar Devices for Light Processing in Telecommunications

John D. Love

Australian Photonics Cooperative Research Centre
Research School of Physical Sciences & Engineering
Australian National University
Canberra ACT 0200
Australia

(E-mail: jdl124@rsphysse.anu.edu.au)

There is a wide variety of passive guided wave devices that enable light signals in an optical communications sytem to be manipulated in various ways, including splitting, attenuation, spot-size variation, coupling, wavelength multiplexing and demultiplexing, polarisation, and wavelength filtering. An overview of a variety of these types of devices and their physical functionality will be presented.

A subset of these devices includes low-loss, approximately adiabatic devices that rely solely on the variation in the geometrical and refractive index configurations along their length for the desired functionality. These devices include, for example, couplers, splitters and mode converters. They can also be combined with other physical phenomena, such as Bragg reflection gratings, to produce novel wavelength filtering devices. Recent research into planar adiabatic wavelength multiplexers and demultiplexers, as well as fibre and waveguide bends that are free of transition loss will be presented.

Regular Papers

Papers presented at joint sessions with ECIO'03

Oral 1 **M. Gioannini and I. Montrosset**
Dip. Elettronica, Politecnico di Torino, Torino, ITALY

Oral 2 **E. A. Romanova and L. A. Melnikov**
Saratov State University, Department of Physics, Saratov, RUSSIA

Oral 3 **J. Katsifolis, S. Huntington, A. Ankiewicz, J. Love, and L. Cahill**
La Trobe University, Dept. of Electronic Engineering, Bundoora, Victoria, AUSTRALIA
University of Melbourne, Dept. of Chemistry, Victoria, AUSTRALIA
Australian National University, Research School of Physical Sciences & Engineering, Canberra, AUSTRALIA

Oral 4 **A. Al-Jarro, P. Sewell, T. M. Benson, and A. Nerukh**
Nottingham University, School of Electrical and Electronic Engineering, Nottingham, UK

Oral 5 **M. Takenaka and Y. Nakano**
University of Tokio, Research Center for Advanced Science and Technology, Tokio, JAPAN

Oral 6 **Hugo J.W.M. Hoekstra, Joris van Lith, Szabolcs B. Gaal and Paul V. Lambeck**
University of Twente, MESA+ Research Institute, Lightwave Devices Group, Enschede, THE NETHERLANDS

Oral 7 **R. Iliew, Ch. Etrich, U. Peschel, and F. Lederer**
Friedrich-Schiller Uviversität Jena, Institut für Festkörpertheorie und Theoretische Optik, Jena, GERMANY

Oral 8 **W. Bogaerts, P. Bienstman, and R. Baets**
Ghent University, IMEC, Department of Information Technology, Ghent, BELGIUM

Oral 9 **D. Michaelis, U. Peschel, C. Waechter, A. Braeuer, and F. Lederer**
Fraunhofer Institute for Applied Optics and Precision Engineering, Micro optics Department, Jena, GERMANY
Friedrich-Schiller Uviversität Jena, Institut für Festkörpertheorie und Theoretische Optik, Jena, GERMANY

Oral 10 **M. Hammer and D. Yudistira**
University of Twente, MESA+ Research Institute, Department of Applied Physics, Enschede, THE NETHERLANDS

Time Domain Numerical Model for linear and nonlinear Grating-Assisted Codirectional Coupler

Mariangela Gioannini, Ivo Montrosset
Dept. of Electronic Engineering, Politecnico di Torino, C.so Duca degli Abruzzi, 24, Torino, Italy.
ivo.montrosset@polito.it

A time domain model is presented for the dynamic analysis of linear and nonlinear devices based on coupled modes propagating with different group velocities. As a test, the numerical algorithm is applied to the analysis of a linear grating assisted co-directional coupler and the limitation of the method are investigated.

Keywords: linear and nonlinear co-directional coupling, GACC filter, TDTW model, simulation

Introduction

Narrow band filters, tunable over a wide wavelength range and integrated with other photonic devices, are important elements for WDM multi/demultiplexing systems. Apart from the distributed Bragg reflectors based on contra-directional coupling, linear and nonlinear filters having a Grating Assisted Codirectional Coupler (GACC) [1] have also been used in many laser and integrated optic structures [2]-[5]. Fig. 1(a) show the typical GACC structure with the two waveguides coupled through a long period grating with pitch Λ_{coupl}. As shown in Fig. 1(b) the modes of the two waveguides, coupled through the perturbation created by the grating, propagate co-directionally with different propagation constants, $\beta_1(\omega)$ and $\beta_2(\omega)$. The different dispersion of the two propagation constants gives different group velocities, v_{g1} and v_{g2}, and the group velocity difference determines the GACC filter bandwidth and tuning capability [6]. Several papers have been published in the literature on the spectral domain analysis and design of these filters [5]-[7], but, to our knowledge, there is not any model that analyze dynamically the propagation of two coupled modes having different group velocities. Furthermore this kind of simulation is essential whenever waveguide nonlinear effects have to be included [5]. The purpose of this paper is to present an extension of the Time Domain Travelling Wave (TDTW) model [8] applied to this case. The TDTW equations and the numerical algorithm for their solution presented in the literature concern indeed only with the case of two coupled modes travelling with the same group velocity, v_g, as for example in DFB and DBR lasers [8],[9]. For these devices the TDTW equations are numerically solved using a space-time discretization grid, defined to satisfy the condition $\Delta z = v_g \Delta t$, where Δz and Δt are respectively the space and time discretization steps. This condition allows the field samples to propagate according to the differential equation characteristic lines, keeping null the numerical error accumulated during the propagation [9]. We have observed that the the standard TDTW approach [8],[9] can not take into account the case of modes with different group velocities and this leads, for example, to significant errors in the simulated GACC filter bandwidth and tunability. A proper numerical method and the conditions to solve correctly the TDTW system of coupled mode equations with different group velocities is thus presented. The numerical errors that result moving away from these proper working conditions are also evaluated.

Model and numerical algorithm

The GACC TDTW equations can be obtained from the spectral domain equations that result from coupled mode theory [1]. To define the notations we report the final equations for

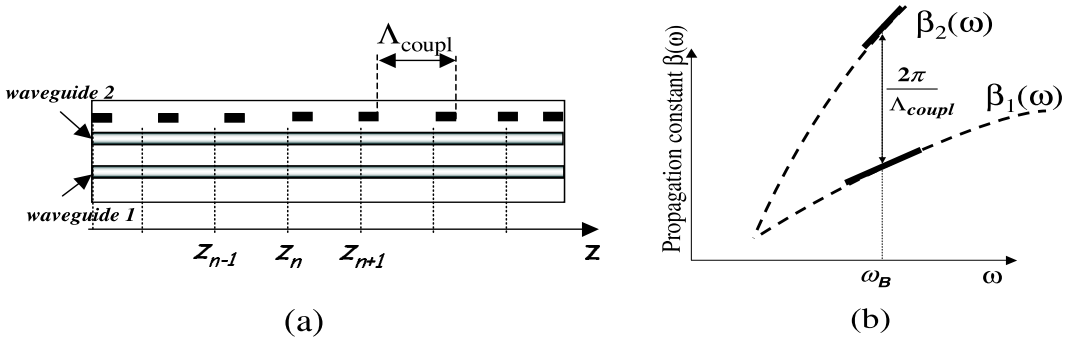

Fig.1. (a) GACC structure with the spatial discretization grid and (b) scheme of the dispersion of the propagation constants.

the slow varying forward components, $\mathcal{A}_1^+(z,t)$ and $\mathcal{A}_2^+(z,t)$, of the electric field.

$$\begin{cases} \dfrac{\partial \mathcal{A}_1^+(z,t)}{\partial z} + \dfrac{1}{v_{g1}} \dfrac{\partial \mathcal{A}_1^+(z,t)}{\partial t} = -j\,\widetilde{\delta}_1\,\mathcal{A}_1^+(z,t) + j\,k\,\mathcal{A}_2^+(z,t) \\ \dfrac{\partial \mathcal{A}_2^+(z,t)}{\partial z} + \dfrac{1}{v_{g2}} \dfrac{\partial \mathcal{A}_2^+(z,t)}{\partial t} = -j\,\widetilde{\delta}_2\,\mathcal{A}_2^+(z,t) + jk\,\mathcal{A}_1^+(z,t) \end{cases} \tag{1}$$

These slow varying components have been obtained for each waveguide, i, extracting from the time domain electric field an arbitrary reference pulsation, ω_0, and a reference propagation constant $\beta_{i0} = \omega_0/c \cdot n_{eff\,i0}$, with c the light velocity and $n_{eff\,i0}$ the effective refractive index of waveguide i. In equation (1) k is the mode coupling coefficient and $\widetilde{\delta}_1$ and $\widetilde{\delta}_2$ are in general complex detuning terms that take into account the detuning of the reference pulsation ω_0 from the Bragg condition, the waveguide loss, gain and nonlinear effects. Analogous equations can be also obtained for the backward components. For the numerical solution the coupler structure has been divided in slices $\Delta z = v_{g_{num}}\,\Delta t$ (Fig. 1a), having chosen $v_{g_{num}} = \max\{v_{g\,1}, v_{g\,2}\}$ for convergency reasons [10]. In the following we will assume that $v_{g\,1}$ is the maximum group velocity. The system of equations (1) has then been solved with a split step algorithm. For each spatial node z_n, we have calculated the field propagation from time instant t_m to t_{m+1} in two steps. In the first step we have solved the temporal propagation equation, obtaining, as shown in equations (2) and (3), the field samples $\overline{\mathcal{A}}_{1\,n,m+1}^+$ and $\overline{\mathcal{A}}_{2\,n,m+1}^+$

$$\frac{\partial \mathcal{A}_1^+(z,t)}{\partial z} + \frac{1}{v_{g\,1}} \frac{\partial \mathcal{A}_1^+(z,t)}{\partial t} = 0 \implies \overline{\mathcal{A}}_{1\,n,m+1}^+ = \mathcal{A}_{1\,n-1,m}^+ \tag{2}$$

$$\frac{\partial \mathcal{A}_2^+(z,t)}{\partial z} + \frac{1}{v_{g\,2}} \frac{\partial \mathcal{A}_2^+(z,t)}{\partial t} = 0 \implies$$

$$\overline{\mathcal{A}}_{2\,n,m+1}^+ = \mathcal{A}_{2\,n,m}^+ - \frac{v_{g\,2}\Delta t}{2\,\Delta z}[\mathcal{A}_{2\,n+1,m}^+ - \mathcal{A}_{2\,n-1,m}^+] + \frac{1}{2}\left(\frac{v_{g\,2}\,\Delta t}{\Delta z}\right)^2[\mathcal{A}_{2\,n+1,m}^+ - 2\mathcal{A}_{2\,n,m}^+ + \mathcal{A}_{2\,n-1,m}^+] \tag{3}$$

Since $\Delta z = v_{g_1}\,\Delta t$, equation (2) is solved exactly [9] whereas equation (3) have been solved numerically using a second order Lax-Wendroff scheme [10]. In the second step we have then included the coupling and the complex detuning, $\widetilde{\delta}_1$ and $\widetilde{\delta}_2$, solving the following equations:

$$\frac{\mathrm{d}\,\mathcal{A}_1^+}{\mathrm{d}\,z} = -j\,\widetilde{\delta}_1\,\mathcal{A}_1^+(z) + jk\,\mathcal{A}_2^+(z) \quad \text{and} \quad \frac{\mathrm{d}\,\mathcal{A}_2^+}{\mathrm{d}\,z} = -j\,\widetilde{\delta}_2\,\mathcal{A}_2^+(z) + jk\,\mathcal{A}_1^+(z) \tag{4}$$

The transfer matrix for the solution of (4) can be easily obtained from the calculation of eigenvalues and eigenvectors of (4). Thus we obtain:

$$\begin{pmatrix} \mathcal{A}_1^+{}_{n,m+1} \\ \\ \mathcal{A}_2^+{}_{n,m+1} \end{pmatrix} = \begin{pmatrix} T_{11}(\Delta z) & T_{12}(\Delta z) \\ \\ T_{21}(\Delta z_2) & T_{22}(\Delta z_2) \end{pmatrix} \begin{pmatrix} \overline{\mathcal{A}}_1^+{}_{n,m+1} \\ \\ \overline{\mathcal{A}}_2^+{}_{n,m+1} \end{pmatrix} \tag{5}$$

We have observed that evaluating the matrix elements T_{11}, T_{12} in $\Delta z = v_{g\,1}\,\Delta t$ and T_{21}, T_{22} in $\Delta z_2 = v_{g\,2}\,\Delta t$, the solution obtained is less affected by numerical errors respect to the solution calculated evaluating all the elements in the same $\Delta z = v_{g\,1}\,\Delta t$, as done in a standard split-step TDTW approach [9].

Numerical results

To demonstrate the accuracy and efficiency of the proposed time-domain method, we analyze a 540 μm long GACC, with a grating coupling coefficient of 29 cm^{-1} and group refractive index $n_{g1} = 3.524$ and $n_{g2} = 3.867$. We show in Fig.2a and 2b the power distribution of the CW fields $\mathcal{A}_1^+(z,t)$ and $\mathcal{A}_2^+(z,t)$ when the GACC Bragg pulsation is equal to the reference pulsation ω_0. The boundary conditions are $\mathcal{A}_1^+(0,t) = 1$ and $\mathcal{A}_2^+(0,t) = 0$. Fig. 2a shows that, evaluating all the transmission matrix elements in the same $\Delta z = v_{g\,1}\,\Delta t$ the solution is not correct because the upper waveguide receives too much power from the lower one and the total power is not conserved. On the contrary, as demonstrated in Fig. 2b, the total power maintains constant along z, if the transfer matrix is calculated as indicated in (5). To test the method also in a

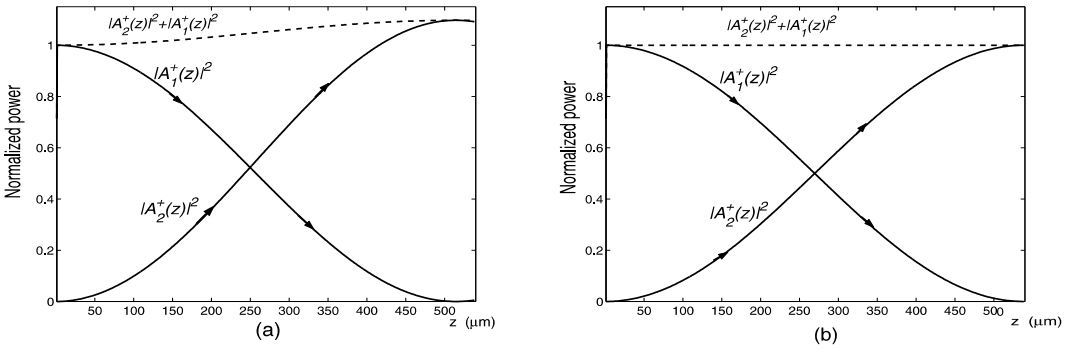

Fig. 2. Normalized power distribution, along the GACC, of the CW forward fields at the Bragg wavelength. Simulation evaluating (a) all the transfer matrix elements in $\Delta z = v_{g1}\Delta t$ and (b) as indicated in equation (5).

wide wavelength range, we compare in Fig. 3a-b the GACC transmission spectrum, obtained with our TDTW analysis, with the exact result obtained with a spectral domain analysis. Fig. 3a shows that in case of zero detuning, $\Delta\lambda$, between the numerical procedure extracted reference wavelength (λ_0=1570 nm) and the GACC Bragg wavelength, λ_B, the two solutions practically overlap. However the error becomes significant when we move away from $\lambda_B = \lambda_0$, as shown in Fig. 3b for $\Delta\lambda = 20$ nm. This leads to errors in the simulated GACC Bragg wavelength and maximum transmission coefficient. We have observed that these numerical errors are mainly due to the dispersion and distortion introduced by the Lax-Wendroff scheme [10] and can be partially compensated at λ_B since they can be analytically evaluated [10] for each wavelength component of the fields. Fig. 3c-d report, as an example, the errors on GACC Bragg wavelength and peak transmissivity versus the detuning $\Delta\lambda$ when the numerical algorithm is applied without and with the application of a simple error correction scheme at λ_B.

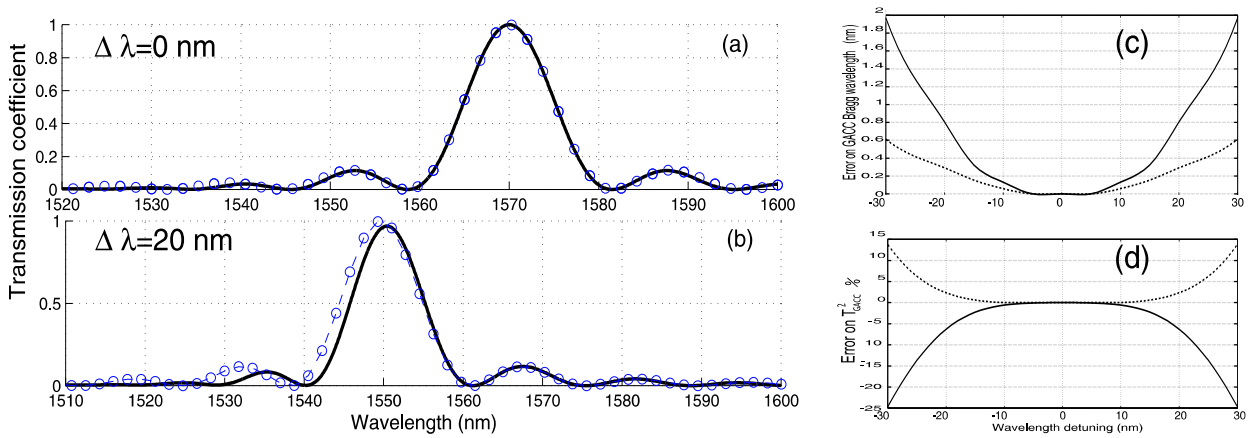

Fig. 3. GACC transmission coefficient versus wavelength for the cases we choose (a) zero and (b) 20 nm detuning of the extracted λ_0=1570 nm from the Bragg wavelength. Solid line: TDTW solution, Circle: exact reference solution. (c) Error in the GACC Bragg wavelength and (d) maximum transmissivity versus wavelength detuning without (solid line) and with (dash line) error correction.

Conclusion

We have presented a numerical method for the solution of the TDTW equations of two co-directionally coupled modes travelling at different group velocities. As a reference case to validate the proposed algorithm, we have considered a GACC filter. It has been shown that with a proper choice of the reference pulsation the numerical error is practically null over a wide wavelength range. Furthermore, for non zero detuning in the device selected reference pulsation, it can be partially compensated around ±10 nm with a simple error correction procedure. The model proposed can find interesting applications in the time-domain analysis of photonic integrated devices that include a GACC such as active and nonlinear filters, lasers and whenever the nonlinearity does not allow a straightforward application of the spectral domain approach.

[1] D.Marcuse, *IEEE J. Lightwave Technol.*, **LT-5**, 268–273, 1987.

[2] R.C. Alferness et alii, *Appl. Phys. Lett.*, **APL-60**, 3209–3211, 1992.

[3] M. Oberg et alii, *IEEE Photon. Tech. Lett.*,**PTL-5**, 735–738, 1993.

[4] S. Illek et alii *Electron. Lett.*, **EL-27**, 920–924, 1989.

[5] B.E. Little et alii, *IEEE J. Lightwave Tech.*, **LT-11**, 1990–1997, 1993.

[6] G.Griffel et alii, *IEEE J. Quantum Electron.*, **QE-27**, 1115–1118, 1991.

[7] Z.M. Chuang et alii, *IEEE J. Quantum Electron.*,**QE-29**, 1071–1080, 1993.

[8] J. Carroll et alii, *Distributed feedback semiconductor lasers*, Ed. The institution of Electrical Engineers, London, 1998.

[9] B.S. Lim et alii, *IEEE J. Quantum Electron.*,**QE-36**, 787–794, 2000.

[10] J.C. Strikwerda, *Finite difference schemes and partial differential equations*, Wandroff and Brook/Cole Advanced Books and Software, Pacific Grove, California, 1989.

Detailed analysis of spatiotemporal stability of the ultra-short optical pulses propagating in non-linear step-index optical waveguide

Elena A.Romanova, Leonid A.Melnikov
Saratov State University, Astrakhanskaya 87, 410026 Saratov, Russia
romanova@optics.sgu.ru

Propagation of the ultra-short optical pulse through a boundary of linear and non-linear segments of planar dielectric waveguide with step-like distribution of the refractive index is simulated numerically. Impact of self-steepening and normal dispersion effects as well as role of retarded non-linear response of the waveguide material are analysed separately in detail. Solution of the paraxial wave equation with non-linear susceptibility is shown to be stable in space in time provided that the quasi-static approximation is used.

Keywords: optical waveguides, ultra-short pulses, Kerr-like non-linearity, spatiotemporal dynamics

Recent experiments with propagation of femtosecond optical pulses in fused silica has demonstrated a complicated dynamics of both spatial and temporal pulse distribution that reveal itself in splitting of the pulse and filamentation of the gaussian beam [1]. These effects are mainly due to the high peak intensities of the beam focused on a bulk silica with a relatively small Kerr-constant $n_2 \approx 10^{-16} cm^2/W$. In optical waveguides, self-action of ultra-short pulses was considered before predominantly as a temporal self-action but the self-focusing effect was assumed to be negligibly small [2]. However the above mentioned experiments with fused silica as well as design of new glasses with greater non-linearity [3] show that there is a need to consider both the spatial and temporal effects of high-intensity pulse propagation through dielectric waveguiding structures.

In our previous works, we studied spatial transient process of fundamental mode propagation through a boundary between linear and non-linear segments of step-index waveguide [4]. Behind a region of spatial transient process in the non-linear segment, a steady-state field distribution was obtained as a numerical solution of paraxial wave equation with non-linear susceptibility (so-called "non-linear mode"). This effect depends on geometry of the guiding structure and can be used to manage parameters of the propagating radiation. However these CW results can be generalised onto the pulsed power propagation provided that the pulse duration is much greater than period of optical oscillations and non-linear response of the waveguide material.

In this work, we simulate numerically propagation of femtosecond optical pulse in planar step-index waveguide with the Kerr-like non-linearity embedded and analyse spatiotemporal dynamics of slowly varying envelope $A(x,z,t)$ of the total filed $E(x,z,t) = A(x,z,t)\exp(i\omega t - i\beta z)$ in the quasi-static approximation and with account of self-steepening effect and finite non-linear response as well as second-order dispersion of the waveguide material.

Numerical modeling is based on solution of the (2+1) paraxial wave equation written in a moving-frame coordinate system ($z = z,\ t = t_0 - z/u$) :

$$2i\beta\frac{\partial A}{\partial z}+\frac{\partial^2 A}{\partial x^2}+\varepsilon_1\frac{\partial^2 A}{\partial t^2}+(k^2n^2(x)-\beta^2)A+2i\varepsilon_2\frac{\partial(|A|^2 A)}{\partial t}+\varepsilon_3\left(|A|^2 A-\tau_R\frac{\partial|A|^2}{\partial t}A\right)=0 \qquad (1)$$

where $\varepsilon_1 = k_2 k/\tau^2(0)$, $\varepsilon_2 = n_2 k/(c\tau(0))$, $\varepsilon_3 = n_2 k^2$, k_2 is dispersion coefficient, n_2 is the Kerr constant, k is the mean wave number, c is the light velocity in vacuum, β is longitudinal propagation constant of the TE_0 mode, τ_R is the retarded non-linear response, $\tau(0)$ is initial pulse duration (time coordinate t and τ_R are normalised to $\tau(0)$). The waveguide is assumed to have step-index distribution of the refractive index: $n(x) = n_{co}$ ($|x| \le d$), n_{cl} ($|x| > d$), where d denotes half-width of the waveguide core (in our simulations we used $n_{co} = \mathbf{1.491}$, $\mathbf{n_{cl} = 1.487}$, $\mathbf{d = 3\mu m}$). The alternative-direction implicit method was used to solve the six-point finite-difference equations obtained from Eq.(1) with improved interface conditions [5]. Non-linear part of the dielectric permittivity was

inserted into the finite-difference scheme in such a way that the value of *A(x,z,t)* obtained on a previous layer was used as a zero approximation for the next layer. In order to avoid the boundary reflection problem, complex scaling of coordinates was applied near the grid edges [6] beginning from $x=X_b=15d$. Initial field distribution $A(x,0,t)=A_0\psi(x)\exp(-t^2/2)$ with transverse profile $\psi(x)$ of linear TE_0 mode (Fig.1,a) was launched numerically into a non-linear waveguide segment where a spatial transient process was observed (Fig.1,b).

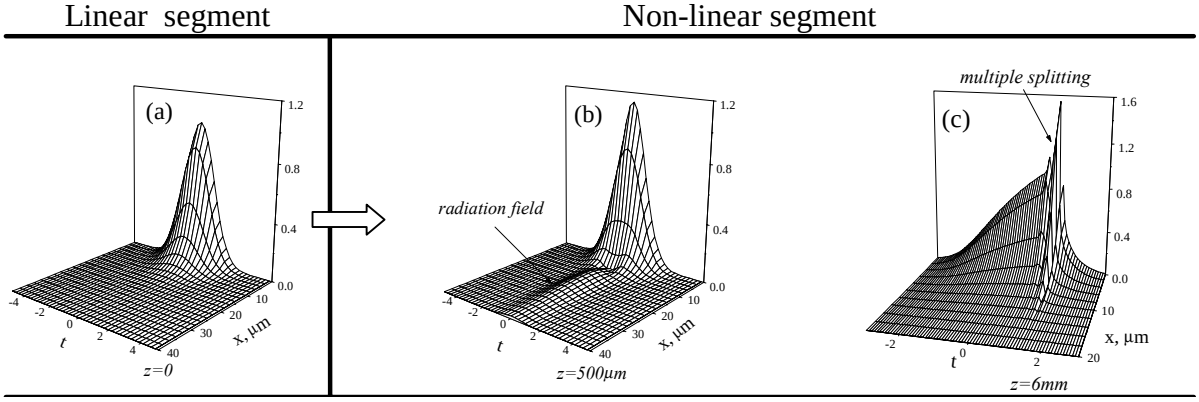

Fig.1 Spatiotemporal distribution of the pulse intensity

In the quasi-static approximation ($\varepsilon_1=0$, $\varepsilon_2=0$, $\tau_R=0$), we assume that only self-focusing and temporal self-action determine non-linear dynamics of the total field so that its spatial and temporal distribution depends on input power and doesn't depend on the initial pulse duration (Fig.2). Similarly to CW propagation [4], total losses resulting from the leakage of radiation field outside the guiding region grow with input power (in our simulations we used the output parameter $T(X,z)=\int_{-X}^{X} dxdt\,|A(x,z,t)|^2 \,/\, \int_{-X}^{X} dxdt\,|A(x,0,t)|^2$).

Behind the region of spatial transient process, stable spartiotemporal field distribution is observed with increased power flow propagating inside the core ($T(d,z)>1$). Pulse duration on the waveguide axis $\tau_a(z)$ is less than its initial value ($\tau_a(z)/\tau(0)<1$) and increases with transverse coordinate tending to $\tau(0)$ in the cladding. The beam width also is minimal at the pulse peak. In general, the stable field distribution is consistent with "non-linear mode" or "spatial soliton" representation.

Self-steepening effect and retarded non-linear response are the factors which destroy stability of the solution so that constant leakage of the power outside the guiding region is observed along the propagation distance (Fig.3).

The self-steepening effect results from intensity dependence of the group velocity and manifests itself through a shift of the pulse peak and optical shock in the trailing edge of the pulse (Fig.4). This variation of the temporal (longitudinal) pulse distribution influences the transverse profile and cancels balance between self-focusing and diffraction so that stable distribution is no longer obtained.

The retarded non-linear response similarly shifts the pulse peak to the trailing edge however don't disturb symmetry of the frontal and trailing parts. With $\tau_R=0.1$ that is typical for femtosecond pulse propagation at $1.53\mu m$ in fused silica, this effect is much less than the self-steepening one.

In the far-field, mutual action of the self-steepening and retarded non-linear response results in the pulse splitting (Fig1,c). For increasing input power or decreasing pulse duration, the splitting moves to the near field.

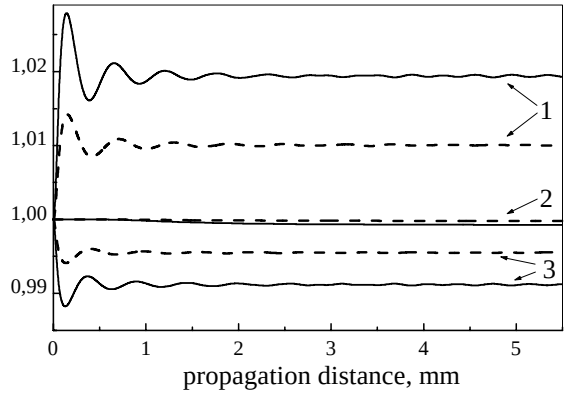

Fig.2 Quasi-static approximation: 1 - *T(d,z);* 2 - *T(X$_b$,z)*; 3- $\tau_a(z)/\tau(0)$; solid curves – $n_2I=0.002$; dashed curves - $n_2I=0.001$.

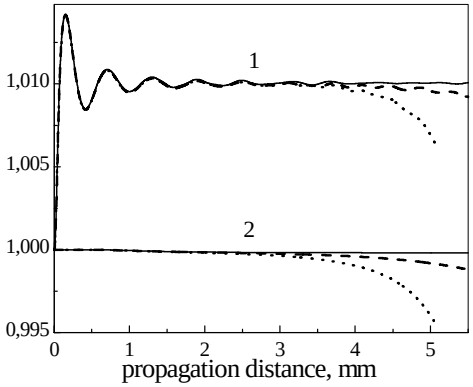

Fig.3 Self-steepening effect: 1 – *T(d,z);* 2 – *T(X$_b$,z)*; $n_2I=0.001$; dashed curves- $\tau(0)=30fs$, dotted ciurves - $\tau(0)=20fs$.

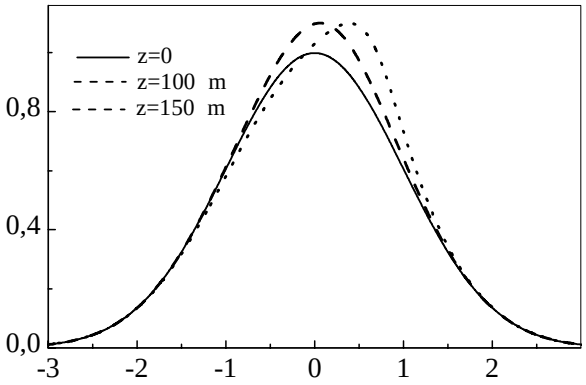

Fig.4 Displacement of the pulse peak due to the self-steepening effect. $n_2I=0.001$, $\tau(0)=20fs$

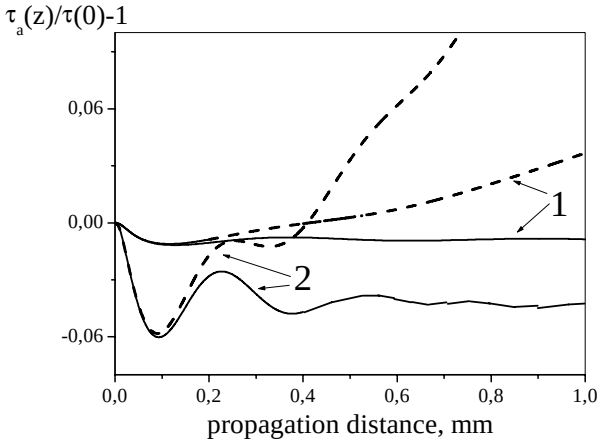

Fig.5 Relative variation of the pulse duration with account of normal dispersion (dashed curves) and in quasi-static approximation (solid curves):
1 - $n_2I=0.002$, $\tau(0)=30$ fs, $k_2 = -0.001$ fs^2/μm;
2 - $n_2I=0.01$, $\tau(0)=10$ fs, $k_2 = - 0.036$ fs^2/μm.

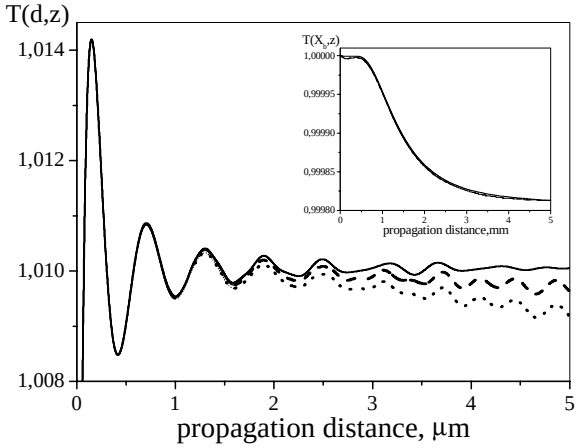

Fig.6 Effect of normal dispersion: dashed curves - $\tau(0)=30fs$, dotted curves - $\tau(0)=10$ fs; $n_2I=0.002$, $k_2 = - 0.036$ fs^2/μm.

Normal group velocity dispersion ($k_2<0$) plays an important part in propagation of ultra-short pulses. In idealized model based on non-linear Schrodinger equation, the self-phase modulation and the second-order dispersion are accounted for. As a result of balance between non-linear and dispersion effects, this model gives a stable solution (soliton) for space-time field distribution [2]. If diffraction term is taken into consideration, the normal group velocity dispersion prevents catastrophic collapse of high-power beam in a uniform Kerr medium via multi-splitting of the pulse, however the self-focusing and splitting events are spatially separated [1]**.** In the step-index waveguide, character of spatiotemporal dynamics of the total field depends also on magnitudes of the dispersion and diffraction lengths: $l_{ds}=\tau^2(0)k/(k_2\beta)$ and $l_{df}=\beta d^2/2$. If $l_{ds}>> l_{df}$ that is typical for picosecond pulse propagation in optical waveguide, the pulse broadening is small over the region of spatial transient process initiated by the self-focusing effect (Fig.5,curves 1). In this case, the self-focusing and the dispersion broadening are separated in space and can be treated independently. If a femtosecond pulse is taken into consideration, the characteristic lengths can be of the same order, $l_{ds}\sim l_{df}$, so that significant variations of the pulse duration along the propagation distance are observed (Fig.5,curves 2). These variations of the pulse duration change in turn the spatial distribution of the field leading to constant leakage of the power outside guiding region along the propagation distance (Fig.6). Contrary to the self-steepening effect, the frontal and trailing parts of the pulse keep symmetric. Comparison of the parameter $T(X_b,z)$ (Fig.3 and Fig.6) shows that the radiation field excited as a result of dispersion effect is more paraxial than the radiation field leaking from the guiding region due to the self-steepening effect.

In summary, simulations of the modal field transformation behind the boundary of linear and non-linear segments of planar waveguide has demonstrated that the self-steepening effect, retarded non-linear response of the waveguide material and normal material dispersion create instability in the high-power ultra-short pulse spatiotemporal dynamics. This results in constant leakage of the power outside the guiding region. The self-steepening effect leads also to multiple pulse splitting in the far-field.

This results can be generalized on any irregular guiding structures of integrated circuits where spatial and temporal transformation of high-intensity pulsed power takes place.

The work was supported in part by Award No.REC – 006 of the U.S.Civilian Research & Development Foundation for the Independent States of the Former Soviet Union (CRDF).

[1] A.A.Zozulya, S.D.Diddams, A.G.Van Engen, T.S.Clement, *Phys.Rev.Lett.*,**82**(7),1430-1433, 1999.
[2] S.A.Akhmanov, V.A.Vysloukh, A.S.Chirkin, Optics of Femtosecond Laser Pulses, American Institute of Physics. NY,1992.
[3] S.Smolorz, I.Kang, F.Wise, B.G.Atiken, N.F.Borrelli, *Journ.of Non-Crystalline Solids*, **256&257**, 310-317, 1999.
[4] E.A.Romanova, L.A.Melnikov, E.V.Bekker, *Microwave and Opt. Technol. Lett*.,**30(**3),212-216, 2001.
[5] Y-P. Chiou, Y-C. Chiang and H-C. Chang, *Journ. of Lightwave Technol*.,**18**(2),243-249, 2000.
[6] C.W. McCurdy and C.K. Stroud, *Computer Phys. Commun.*, **63**, 323-328,1991.

Transition Loss in Bent Waveguides and Fibres

Jim Katsifolis
Dept. of Electronic Engineering, La Trobe University, Bundoora, Victoria 3083, Australia
j.katsifolis@ee.latrobe.edu.au

Shane Huntington
School of Chemistry, University of Melbourne, Parkville, Victoria 3010, Australia

Adrian Ankiewicz, John Love
Research School of Physical Sciences, Australian National University, ACT 0200, Australia.

Laurie Cahill
Dept. of Electronic Engineering, La Trobe University, Bundoora, Victoria 3083, Australia

We determine the origin of transition loss in bent waveguides and fibres. We show that transition loss can be suppressed, even in very tight bends provided that, in the geometrical transition from the straight to the bent waveguide or fibre, the local curvature is increased sufficiently slowly along the bend. Experimental results demonstrate this effect and are shown to be consistent with numerical simulations.

Keywords: bend loss, transition loss, beat length

Introduction

When a straight single-mode fibre or waveguide enters a bend, it is well known that power is radiated from the fundamental mode into the cladding as it propagates along the bend. The total radiated power along the bend can be expressed in terms of a superposition of two physically different effects, namely pure bend loss and transition loss. Pure bend loss is associated with the radiation of fundamental mode power from each position along the bend and is independent of the transition from the straight to the bent waveguide [1]. Conversely, transition loss is normally associated with the abrupt change in curvature between the straight and bent waveguides and its contribution to overall bend loss occurs over a relatively short distance along the bend.

Pure bend loss has been investigated in detail by many authors and can be quantified using a number of different analytical techniques. As a result, approximate analytical expressions are available for pure bend loss from e.g. step-profile slab waveguides [2] and fibres [1].

Transition loss arises from the mismatch between the fundamental mode fields of the straight and bent waveguides or fibres. For a bent waveguide, the effect of curvature is to introduce a small offset in the fundamental mode that displaces its field slightly outwards relative to the centre of the bend in the plane of the bend. As a result of this shift, not all of the incident mode power of the straight waveguide is transmitted into the fundamental mode on the bend. The power that is lost excites the non-guided field and thus forms part of the radiation field of the bent fibre.

Although the radiation loss from the fundamental mode is continuous along the bend, the superposition of the transition loss can lead to the generation of discrete beam radiation within the bend region. This effect was first reported by Gambling et al [3] using a coiled fibre stripped of its coating and immersed in a cladding-index matching liquid. It was subsequently investigated by others during an early study of loss from curved single mode fibres [4][5]. Their analyses suggested that; (i) the beam phenomenon was due to a beating effect between the fundamental mode and a dominant higher-order leaky mode that is quasi-guided by the bend, and (ii) the coupling between the fundamental and leaky modes was caused by the constant-radius bend.

In this paper we show that, although the beams are due indeed to a beating effect as previously observed, the effect is actually induced by the relatively rapid increase in curvature from the beginning of the bend, rather than by the constant-radius bend itself. We also show that it is possible to suppress excitation of the leaky mode and therefore the discrete beams, even in a tight bend, by introducing a transition region leading into the bend with a sufficiently slow increase in curvature.

Numerical Simulation

Bend loss in fibres and waveguides occurs predominantly in the plane of the bend. Accordingly it is adequate for the present investigation to model bend loss from a single-mode bent waveguide and thereby simplify the complexity of the numerical simulation. The 2-dimensional bent step-profile waveguide is then replaced by a straight graded 1-dimensional waveguide using a standard conformal transformation. The effect of this transformation is to tilt the refractive index profile. Thus, by varying the tilt of the profile either abruptly or continuously along the waveguide, the effect of a jump or continuous increase in curvature on propagation can be quantified. The numerical quantification of bend loss and the radiation field along the bends was simulated using Olympios BPM software. In each case the fundamental mode field of the straight waveguide was launched at the beginning of the bend.

Results showed the presence of discrete beam radiation occurred along bends where there was an abrupt or relatively fast change in curvature. Where the change of radius of curvature was minimized, the discrete beam radiation was also minimized or effectively suppressed. These results are plotted in Figure 1 for a bend radius of 2.1mm.

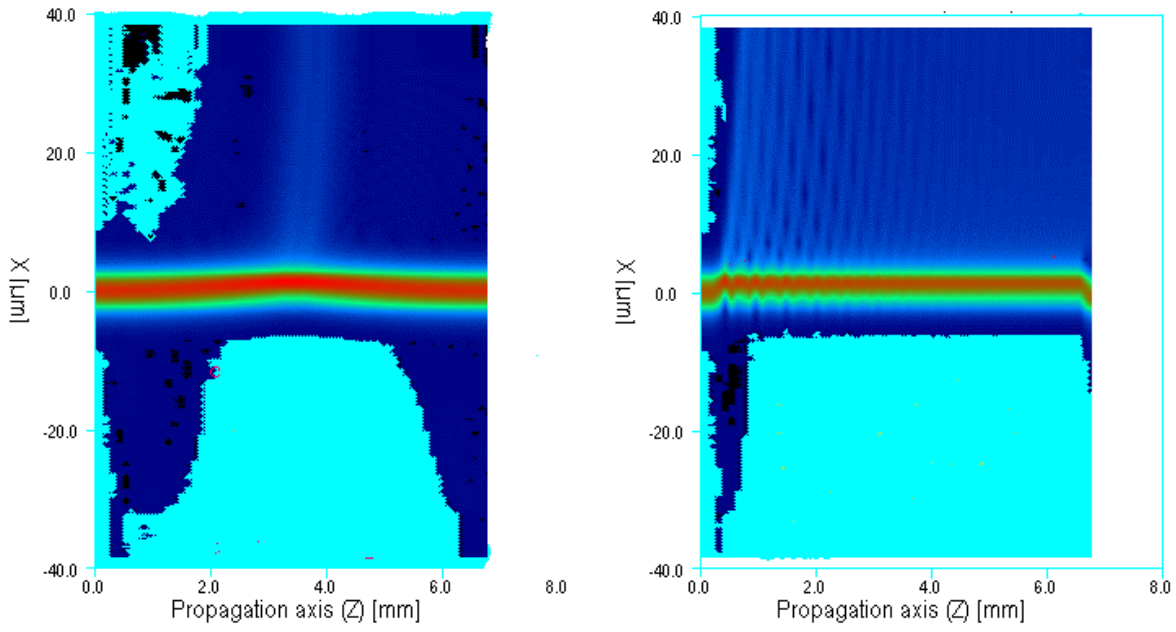

(a) (b)

Figure 1: Simulation results for slab waveguides. In (a), the waveguide is bent into a parabolic curve with a low rate of curvature change everywhere along its length, and no discrete beam radiation is present. In (b) the parabolic curve has a more rapid change in curvature at the beginning of the bend, and discrete beam radiation is now present.

The simulation results in Figure 1(a) show that even for a tight parabolic bend there are no discrete beams generated, since there is only a low rate of change in the radius of curvature. Only continuous radiation due to pure bend loss is present. In the case where there is a more abrupt change in curvature radius, as in Figure 1(b), the higher-order leaky mode is excited at this transition point, and the resultant beating between this mode and the fundamental along the bend generates the set of discrete beams.

Experimental Investigation

Several single-mode fibres were bent into different radii and, after removal of the coating, were immersed in an oil medium with a slightly higher refractive index than the cladding in order to view any discrete radiation. In each experiment only the fundamental mode of the fibre was excited.

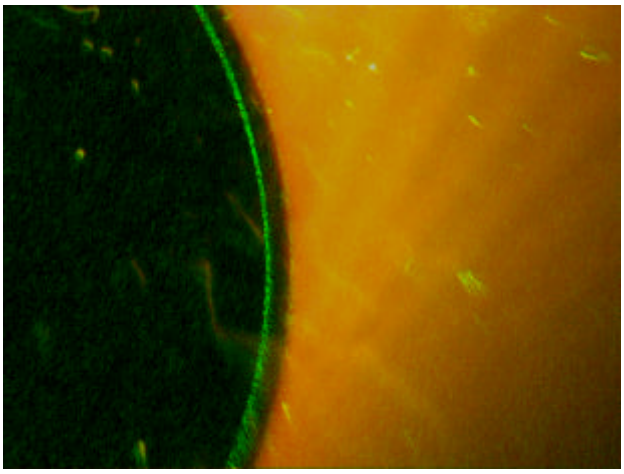

Figure 2. Discrete beam radiation from a single-mode fibre bent into a semi-circular arc of 1.5mm radius.

Figure 2 shows the discrete beam radiation from a single-mode fibre bent in a semi-circular arc with uniform radius of 1.5mm. The measured beat length between the beams is approximately 180 microns and is consistent with the numerical simulation, allowing for the difference between modal effective indices between the fibre and slab geometries. The discrete beams can be accounted for by the fairly abrupt change of curvature between the straight part of the fibre and the circular bend. The abruptness couples power from the fundamental mode into the leaky second mode and the two modes beat together to generate the discrete beams.

This phenomenon is illustrated better in Figure 3, where a near single-mode fibre is bent into a 180º parabolic-shape bend with a low rate of curvature change at any point along its length. Using a fibre with a higher V-value allows discrete beam radiation to be observed at larger bend radii for the same excitation wavelength. Only the fundamental mode is excited in the straight part of the fibre.

In Figure 3(a), no discrete beams are present and only the expected continuous radiation due to pure bend loss from the fundamental mode is present. In Figure 3(b), the lead-in fibre is straightened slightly so that a small transition region with more abrupt change in curvature is introduced close to the beginning of the parabola. In this case, discrete beam radiation is again clearly evident.

A more detailed and quantified analysis of transition loss will be presented at the conference, including a criterion for minimising transition loss.

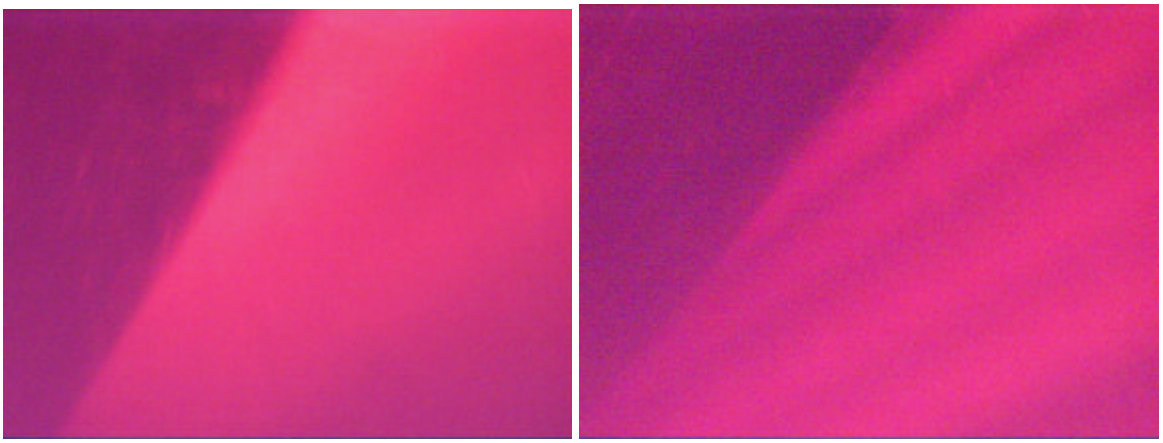

(a) (b)

Figure 3 A fibre bent into a 180º parabolic bend shape. In (a), no discrete beam radiation is present due to the low rate of change in curvature along the fibre. In (b) the lead in fibre is straightened slightly to give a more abrupt change in curvature and discrete beam radiation is now present.

Conclusions

The origin of discrete beams observed in the radiation field of bent single-mode waveguides and fibres has been shown to be due to the coupling of power from the fundamental mode to the first leaky along the bend. Such coupling only occurs when the bend curvature changes rapidly along the bend and can be virtually suppressed by introducing a sufficiently slow change in curvature.

This prescription allows, in particular, for the design of transition-loss free waveguide bends with a smooth variation in curvature, and provides an alternative to the standard practice of inserting an offset between the straight and bent waveguide cores in the case of an abrupt change in curvature.

Acknowledgements

This research was supported by the Australian Photonics Cooperative Research Centre.

References

[1] A. W. Snyder and J.D. Love, ”Optical Waveguide Theory”, Chapman and Hall, 1983, Chapter 23.

[2] D. Marcuse, “Light Transmission Optics”, Bell Laboratories Series, Section 9.6, 398–406, 1972.

[3] W.A Gambling, D. N. Payne and H. Matsumura, “Radiation from curved single-mode fibres”, Electronics Letters, Vol. 12, No. 21, 567 – 569, 1976.

[4] R. A. Sammut, “Discrete radiation from curved single-mode fibres”, Electronics Letters, Vol.13, No.14, 418-419, 1977.

[5] C. G. Someda, “Radiation of discrete beams from curved single-mode fibres”, Electronics Letters, Vol. 13, No.14, 712-713, 1977.

Effective and Flexible Analysis for Propagation in Time Varying Waveguides

A Al-Jarro, P Sewell, TM Benson, A Nerukh
Electromagnetics Research Group, School of Electrical and Electronic Engineering, The University of Nottingham, University Park, Nottingham, NG7 2RD, UK.
eexaa@nottingham.ac.uk

The equivalence between the propagation of dispersive modal fields in two and three dimensional waveguides, and plane waves in a one dimensional plasma is presented. A computationally efficient time domain integral equation is discussed for this important practical case and its stability is improved by means of both a semi-implicit formulation and the use of rectangular meshing.

Keywords: time domain analysis, numerical algorithm, dimensionality reduction.

Introduction

Recently, significant interest has been focused upon the interaction of electromagnetic signals and time varying media, [1,2]. The motivation for studying such phenomena include, wavelength shifting and terahertz wave generation applications, as well as gaining insight into the behaviour of high speed switches and lasers. In contrast to the early research in this area, which concentrated upon plane waves, the leading edge of this work is now considering the effects of time varying materials upon optical fields transversely confined by waveguide geometries.

Computational methods that can account for time varying and inhomogeneneous media, include the finite difference time domain method, FDTD, the transmission line method, TLM as well as time domain integral equation techniques. A particular advantage of the latter approach is that it can often identify the general properties of a particular class of problems rather than just solving specific instances, [3]. Unfortunately in all cases, the move from 1D plane wave problems to 2D, let alone 3D waveguide configurations severely increases the computational overhead incurred. However, for initial design purposes, it is recognised that it is not strictly necessary to model the complete 2D or 3D nature of the structure, rather it is sufficient to consider just the fundamental modal fields which indicate the presence of the waveguide confinement by possessing frequency dependent propagation constants and modal impedances. Exclusively concentrating upon the fundamental modes is justifiable given that the temporal changes in the waveguide parameters are usually small in practice so that excitation of higher order transverse modes is of secondary importance to the overall behaviour observed. The significant advantage gained by this approach is a reduction in the dimensionality of the problem that needs to be simulated.

Theory

If the transverse mode shape is frequency independent, which is a reasonable engineering approximation for semiconductor slab waveguides confined by large refractive index steps such as occur in SOI structures, then it is straightforward to demonstrate that the dispersive effects exhibited by a waveguide mode whose cutoff frequency is ω_c, are the same as those observed for plane waves in a 1D plasma defined by the following relationship between electric field and electric flux density, $D(t) = \varepsilon_o \varepsilon_1 E(t') + \int^{t} dt' \ (t-t')\omega_c^2 E(t')$ where ε_1 is the relative permittivity of the material filling the guide. The electric field in a 1D structure satisfies Volterra integral equation, [3],

$$E(t,z) = E_o(t,z) - \frac{1}{2\varepsilon_o \varepsilon_b}\frac{d}{dt}\int_0^t dt' \int_0^a dz' \ \delta\left(t - t' - \frac{|z-z'|}{v_b}\right)\left[P(t',z') - \varepsilon_o(\varepsilon_b - 1)E(t',z')\right] \qquad (1)$$

where ε_b is a background relative permittivity, P is the polarisation of the media, E_o is the excitation field and t and z are the time and space coordinates. It is a significant advantage of the approach, compared to FDTD for example, that the domain of the spatial integration only encompasses the discontinuity, i.e. the region whose properties differ from the background medium, here taken as 0<z<a. Similarly, there is no need to terminate the calculation window with artificial absorbers as the kernel of the integral equation intrinsically contains the correct asymptotic behaviour at infinity. To perform the simulation of the modal fields in a 2D waveguide as introduced above, E is now interpreted as the modal amplitude and the equivalent 1D material modelling the modal dispersion is defined by the polarisation function,

$$P(t,z) = \varepsilon_o(\varepsilon_1 - 1)E(t,z) + \varepsilon_o\omega_c^2 \int_o^t dt'(t-t')E(t',z) \qquad (2)$$

In previous simulations of 1D plasmas using Volterra equations, [4], the field was discretised in space-time using a square mesh with respect to the speed of light in the background material, i.e. $\Delta z = v_b \Delta t$. Furthermore, the integration over t' in (1) was performed using a semi-open integration scheme and the derivative with respect to t evaluated using a backward difference. Given that using $\Delta z = v_b \Delta t$ is tantamount to operating at precisely the Courant condition, these features give rise to a slightly explicit scheme which causes problems for stability and accuracy. To overcome these problems, a very simple Crank-Nicolson approach is adopted; a central difference formula is used for the derivative with respect to t, coupled with $E(t - dt/2) = \alpha E(t) + (1-\alpha)E(t - dt)$. Using α=0.5 ensures maximal accuracy and theoretical stability, but in practice α is set slightly larger than 0.5 to compensate for rounding error induced instability. As shall be shown below, this revised implementation of the algorithm, reported here for the first time, significantly enhances its utility.

A second novel and complimentary change to the algorithm is to relax the need for a square mesh in space-time, which effectively allows Δt to be lower than that of the Courant condition. Evaluating the numerical quadratures along lines of constant z±vt which are required in (1), involves interpolation for non-square meshes, although this is straightforward to implement in practice. Here we specifically demonstrate the stability and accuracy improvements that can be obtained by using a rectangular mesh with $\Delta t = \Delta z/(2v_b)$.

Results

First, the equivalence between modal propagation in waveguide and 1D propagation in a plasma as well as the efficacy of our improved algorithm shall be shown. In figure 1, an incident pulse, with a Gaussian distribution in both time and space, strikes a section of waveguide sandwiched between 2 free space regions and frequency dependent reflection and transmission occurs. The problem parameters used here and below have been chosen to clearly demonstrate the approach and are therefore not necessarily realistically achievable.

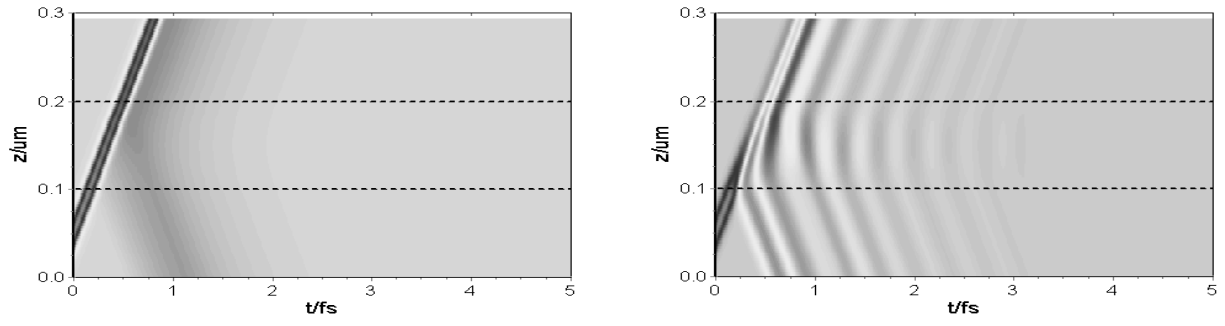

Figure 1: The modal amplitude excited by a Gaussian pulse striking a section of waveguide, 0.1μm<z<0.2 μm with (a) f_c=500THz and (b) f_c=2500THz. Here, $\varepsilon_1 = \varepsilon_b$=1, $\Delta t = \Delta z/v_b$=0.01fs and α=0.6.

To precisely quantify the accuracy of the numerical implementation, figure 2 compares the transmission coefficient obtained by Fourier transforming the time dependent field just before and after the waveguide with the exact theoretical result.

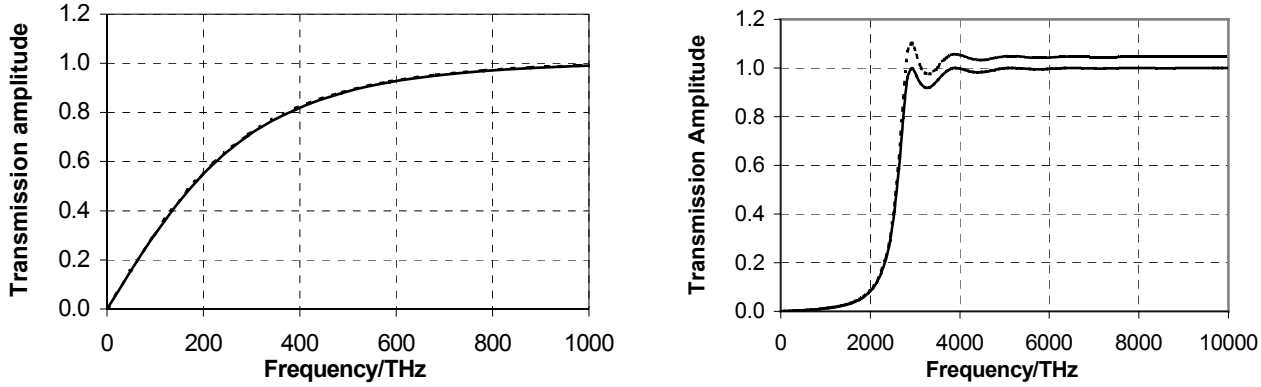

Figure 2: The numerical (dotted) and theoretical (solid) transmission coefficient obtained for the examples of figure 1

Although the agreement is excellent for the case of relatively weak dispersion, for the case of more severe dispersion there is both an overshoot at the cutoff frequency as well as a "steady state" pass band amplitude error. This is attributable to the use of a stability factor of α=0.6 and a fairly large time step. To illustrate this, the pass band error is plotted in figure 3(a) against α for different Δt.

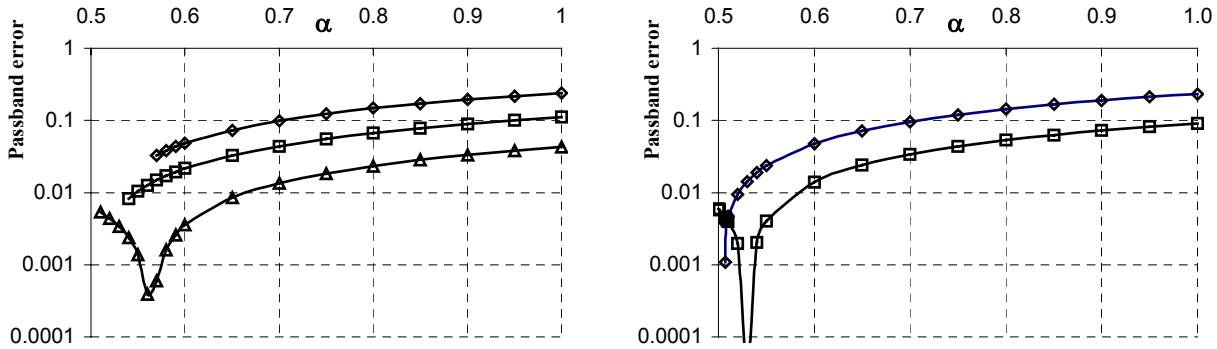

(a) (b)

Figure 3: The effect of α and Δt on the errors for a Square (a) and Rectangular (b) mesh for the example of figure 1b: (a) diamonds ($\Delta t=\Delta z/v_b$ =0.01fs), squares ($\Delta t=\Delta z/v_b$=0.005fs) and triangles ($\Delta t=\Delta z/v_b$=0.0025fs); (b) diamonds ($\Delta t=\Delta z/v_b/2$=0.005fs) and squares ($\Delta t=\Delta z/v_b/2$=0.0025fs).

It is clear that this measure of error is significantly reduced as both α approaches 0.5 and by using a smaller time step. However, it is also observed that each of the curves starts at a value α which is greater than 0.5, as below this value instability occurs. Therefore it is not possible to obtain the accuracy that would appear asymptotically available for a given value of Δt. As using smaller Δt implies using smaller Δz in a square mesh, improving the accuracy this way incurs an undesirable increase in numerical effort. This is precisely the reason for considering rectangular meshing as it moves the algorithm away from the accuracy-stability knife-edge associated with the Courant condition. Figure 3(b) shows the same measure of error obtained from a mesh with $\Delta t=\Delta z/(2v_b)$.

As a further visual illustration of the wavguide-plasma equivalence we consider the case of a rib waveguide resonator. A section of waveguide is sandwiched between two sections of waveguide having a higher cutoff frequency, and this combination is surrounded by free space. Modelling each waveguide as an appropriate 1D plasma (without consideration of the mismatch in modal profiles)

is in essence a time domain effective index model, the frequency domain a of which has achieved widespread acceptance as a fast initial design tool. Figure 4 shows the fields excited by a Gaussian pulse incident from free space and the frequency dependent confinement and resonances are plainly seen.

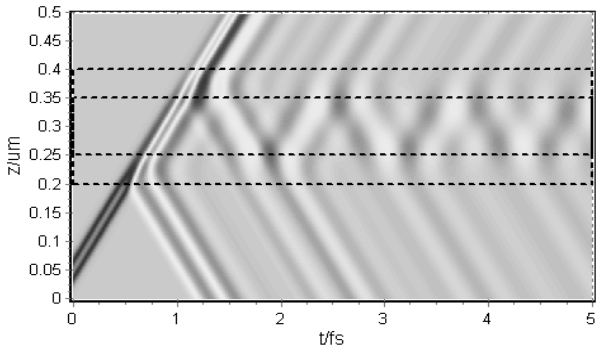

Figure 4: The modal amplitude excited by a Gaussian pulse striking a cascade of three waveguides with f_c=2500THz for 0.2μm<z<0.25μm and 0.35μm<z<0.40μm and f_c=1000THz for 0.25μm<z<0.35. $\Delta t=dz/v_b$=0.005μm, α=0.6 and $\varepsilon_1=\varepsilon_b$=1.

Finally, attention is focused on the case of a time jump in the waveguide parameters. Figure 5 shows the effect of switching the cutoff frequency of the waveguide region as the field passes through it, the reflection at the instant of switching, t=4fs, being clearly visible.

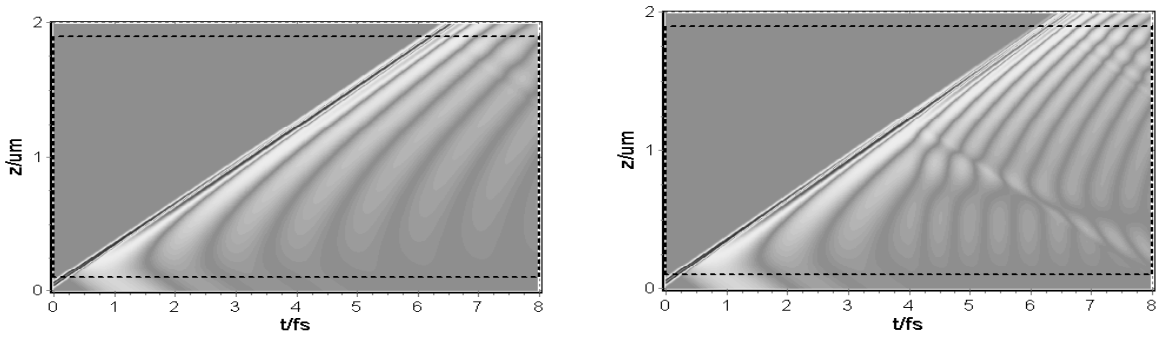

(a) (b)

Figure 5: The modal amplitude excited by a Gaussian pulse striking a section of waveguide, 0.1μm<z<1.9 μm with f_c=500 THz, $\varepsilon_1=\varepsilon_b$=1, $\Delta t=\Delta z/v_b$=0.01fs and α=0.6. In (b) f_c is switched to 2500THz at t=4fs.

Conclusion

In this paper we have presented and demonstrated two practical improvements for time domain simulations. Firstly, that simulations of 2D and 3D waveguide structures can be efficiently performed using a time domain effective index approach, which promises fast initial design tools. Secondly, for Volterra integral equation formulations, both the use of stabilised algorithms and non-square meshes have been quantifiably shown to substantially improve the accuracy that can be obtained. Finally, qualitative examples of dealing with more complex geometries as well as time variant cases have been presented to illustrate the flexibility of the approach.

References

[1] J.W.D. Chi, L. Chao, M.K.Rao, *IEEE J. Quantum Electronics*, vol. 37, No 10, 1329-1336, 2001
[2] Y. Jeong, B. Lee, *IEEE J. of Quantum Electronics*, vol. 37, No 10, 1292-1300, 2001.
[3] A.G Nerukh, I.V. Scherbatko, M. Marciniak, *National Institute of Telecommunications Publishing House*, Warsaw, 2001.
[4] K.M.Yemelyanov, F.V. Fedotov, A.G. Nerukh, *Transparent Optical Networks conf*. 226 –229, 2001.

Proposal of an All-Optical Flip-Flop Using a Cross-Coupled MMI Bistable Laser Diode

Mitsuru Takenaka and Yoshiaki Nakano
Research Center for Advanced Science and Technology, University of Tokyo, JST-CREST
7-3-1 Hongo, Bunkyo-ku, Tokyo, 113-8656, Japan
takenaka@hotaka.t.u-tokyo.ac.jp

We propose a novel bistable laser diode (BLD) with active multi-mode interference (MMI) cavity. Using FD-BPM, we predict that the MMI-BLD shows bistable switching between two cross-coupled modes, which can be utilized as an all-optical flip-flop or an optical memory.

Keywords: bistable laser diode, MMI coupler, two-mode bistability, all-optical flip-flop, FD-BPM

Introduction

Bistable laser diodes (BLDs) are expected to be important elements of future optical communications such as packet buffering, bit-length conversion, retiming, reshaping, demultiplexing, and wavelength conversion. However, conventional absorptive BLDs [1] have the difficulty of optical reset. To overcome this problem, two-mode intensity bistability [2], which originate from cross gain saturation between the two lasing modes, have been investigated. Although this type of bistability has been demonstrated by cross-coupled bistable laser diodes (XCBLDs) [3], they had a bit complicated waveguide structures.

In this paper, we propose a novel two-mode BLD including an active multi-mode interference (MMI) cavity (Fig.1). An all-optical flip-flop will be realized by the MMI-BLD whose simple structure is matched to the conventional LD fabrication technique. Moreover, it gets the benefits of the MMI's features, i.e, compactness, high design tolerances, a large optical bandwidth and polarization insensitivity. We design a 2 × 2 MMI which couples light signal from an input port totally into a cross output port. Two-mode bistability between two cross-coupled modes will occur in this configuration due to cross gain saturation. The static characteristics of the MMI-BLD are investigated using a finite difference beam propagation method (FD-BPM).

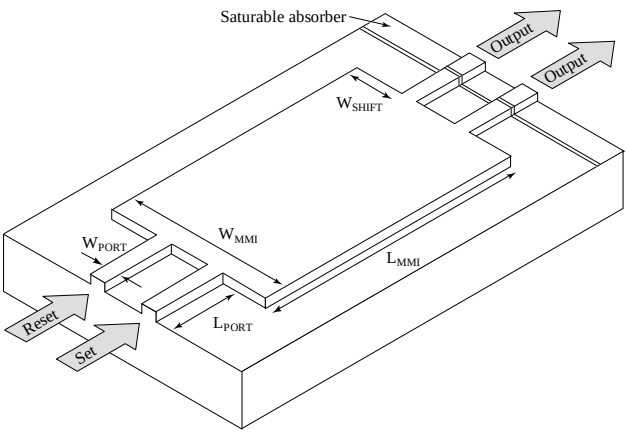

Fig. 1 Schematic view of MMI-BLD.

Simulation Method

The modeling of an MMI coupler requires special attention because several modes inside the coupler interfere with each other. Moreoever, the behavior of an active MMI coupler has been not well know yet. Therefore, we chose FD-BPM [4] which can treat complex distributions of photon, refractive index, and gain inside the cavity. However, the BPM models only take forward propagating lights into account, thus reflections inside the cavity are neglected. In this paper, we analyse uni-directionally forward and backward propagating lights, respectively, and only reflections from the cleaved facets of LDs [5] are considered.

In describing light propagation through the waveguides, the wave equation for a TE mode derived from Maxwell's equations is solved. The scalar Helmholtz equation for a TE-polarized light propagating a planar waveguide in the direction of *z* axis becomes:

$$\frac{\partial^2 E}{\partial z^2}+\frac{\partial^2 E}{\partial x^2}+k_0^2 n^2 E=0 \tag{1}$$

where $E(x, z)$ is the space-dependent electric field, $n(x, z)$ the space-dependent refractive index, k_0 the wave vector in vacuum and a temporal dependence of $\exp(j\omega t)$ is assumed. This equation can be reduced to the paraxial wave equation:

$$E(x,z)=\phi(x,z)\exp(-j\beta_0 z) \tag{2}$$

$$2j\beta_0\frac{\partial\phi}{\partial z}=\frac{\partial^2\phi}{\partial x^2}+(k_0^2 n^2-\beta_0^2)\phi \tag{3}$$

where β_0 is a reference propagation constant. Equation (3) is obtained by a slowly varying envelope approximation. It is solved using finite differences in the transverse (x) direction and a Cranck-Nicolson scheme for the longitudinal (z) coordinate. In order to avoid nonphysical reflections from the computational window edges, Hadley's transparent boundary condition [6] is implemented.

We also take photon-carrier interactions into account. To evaluate the carrier density $N(x, z)$, the steady-state carrier rate equation is expressed as:

$$\frac{J}{ed}=R(N)+\Gamma v_g g_1 S_1+\Gamma v_g g_2 S_2 \tag{4}$$

where J is the current density, e the electron charge, d the thickness of the active layer, R the recombination rate, Γ the confinement factor, v_g the group velocity, g the material gain and S the photon density (the subscripts 1 and 2 refer to the two cross-coupled modes in the MMI cavity respectively).

Using a detailed model including Auger recombination [7], the recombination rate is written as:

$$R(N)=c_1 N+c_2 N^2+c_3 N^3 \tag{5}$$

where c_1, c_2, and c_3 are recombination constants.

For the unsaturated material gain g_0, a linear dependence on carrier density is assumed:

$$g_0(N)=a(N-N_0) \tag{6}$$

where a is gain constants, N_0 the carrier density at transparency.

As two-mode bistability originates in cross gain saturation, it is necessary that this effect is included in bistability analysis. The saturated gains for the cross-coupled modes are related to the unsaturated gain g_0 through the photon densities of the two modes as follows:

$$g_1(N)=\frac{g_0}{1+\varepsilon_{11}S_1+\varepsilon_{12}S_2},\quad g_2(N)=\frac{g_0}{1+\varepsilon_{22}S_2+\varepsilon_{21}S_1} \tag{7}$$

where ε_{11}, ε_{22} and ε_{12}, ε_{21} are the self-saturation and the cross-saturation coefficients, respectively.

To take into account the refractive index dependence on carrier density, a linearly dependent equation is assumed:

$$n=n_0+\frac{dn}{dN}N \tag{8}$$

where n_0 is the refractive index without carrier injection, and dn/dN is refractive index shift coefficient, which is taken to be negative. We only consider the refractive index change of the waveguide's core, whereas the refractive index of the clad is assumed to be fixed.

Bistability Analysis

An InGaAsP multiple quantum well (MQW) structure whose band gap energy is around 1.55 μm is studied. We assume that the self-saturation coefficient is 8.0×10^{-17} cm^3 and the cross-saturation coefficient is 1.6×10^{-16} cm^3. The other parameters are shown in [8].

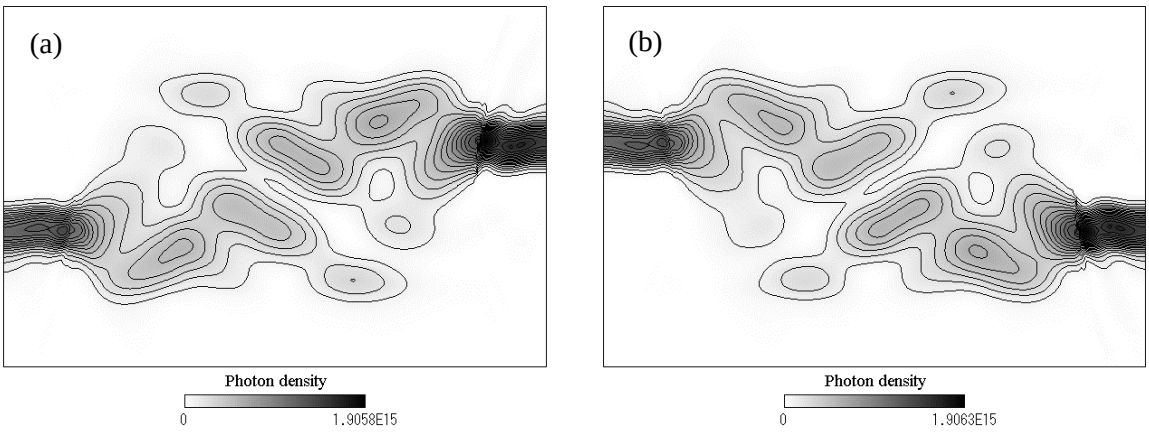

Fig. 2 Photon density [cm^{-3}] distributions of the MMI-BLD at (a) mode-1 and (b) mode-2.

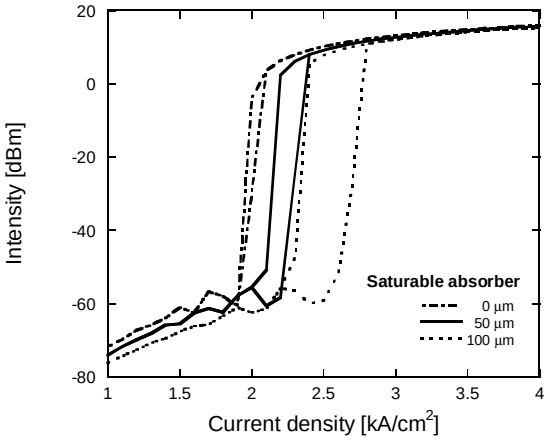

Fig. 3 L-I characteristics of the MMI-BLD with saturable absorber, 0, 50, and 100 μm.

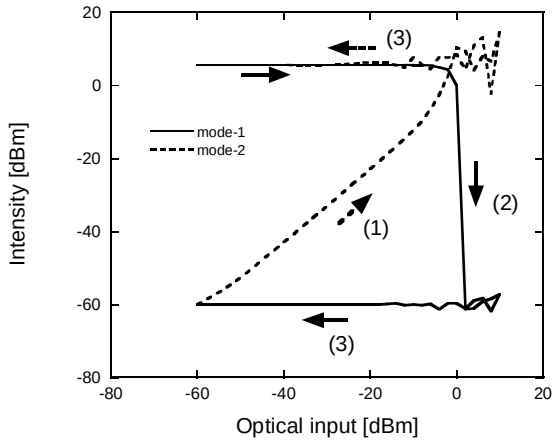

Fig. 4 Bistable switching characteristics of the MMI-BLD.

The 2 × 2 MMI coupler section should be designed in such a way that the input light totally couples into the cross output port. In the case of ridge waveguides whose refractive indices of core and clad are 3.255 and 3.24, respectively, the cross-coupled MMI coupler assumes the following physical dimensions: W_{MMI} = 12 μm, L_{MMI} = 540 μm, and W_{SHIFT} = 2.7 μm. The port width W_{PORT} and length L_{PORT} are 2 μm and 100 μm, respectively. In this design, the MMI-BLD has two cross-coupled lasing modes as shown in Fig. 2.

The saturable absorbers are equipped at the end of the output ports. Figure 3 shows L-I characteristics with the lengths of the saturable absorber (biased at 0.1 kA/cm^2) being 0, 50, and 100 μm, respectively. By increasing the saturable absorber length, the lasing threshold and the width of the hysteresis loop increase due to nonlinear absorption. The injection current of the gain region should be within the hysteresis loop in order to make use of the two-mode bistability. We adopt 50 μm as the saturable absorber length and 2.1 kA/cm^2 as the bias current density of the gain region.

External light injection of a set-signal saturates the absorption to mode-1, causing mode-1 to start lasing (ON state). At the same time cross gain saturation and the absorption to mode-2 by the saturable absorber suppress mode-2. In a similar manner, light injection of a reset-signal at the ON state suppresses mode-1 through cross gain saturation, therefore stopping laser oscillation in mode-1. Simultaneously, the absorption of mode-2's saturable absorber is decreased by the light injection to mode-2, resulting in lasing of mode-2 (OFF state). Even when the light injection is terminated, cross gain saturation and recovered absorption of the mode-1's absorber prevent mode-1 from

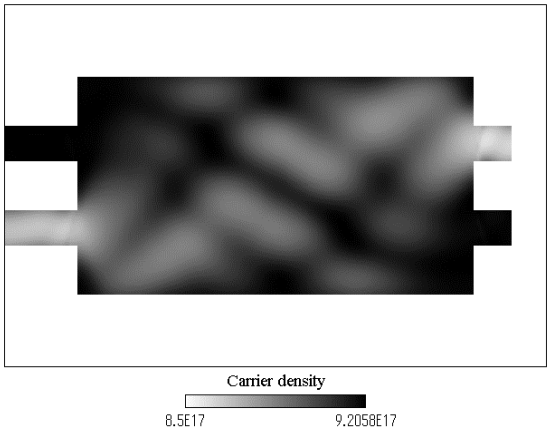

Fig. 5 Carrier density [cm^{-3}] distribution of the MMI-BLD lasing at mode-1.

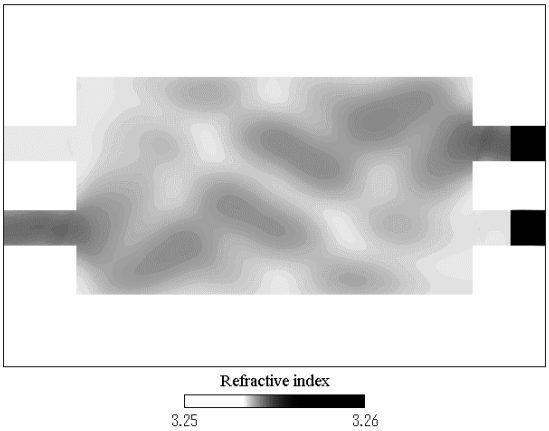

Fig. 6 Refractive index distribution of the MMI-BLD lasing at mode-1.

lasing again. Figure 4 shows this bistable switching characteristics. The MMI-BLD is set to the ON state by set-pulse at the beginning of the calculation. Increasing the optical injection to mode-2 (1) suddenly results in extinction of mode-1 (2) at around 0 dBm, thus switching MMI-BLD into the OFF state. When the optical injection is eliminated, the OFF state is maintained (3). As shown in Fig. 4, the two-mode bistability overcomes the optical reset problem of the absorptive BLDs, and the all-optical flip-flop operation will be realized using the MMI-BLD.

Figure 5 and 6 show the distributions of carrier density and refractive index in the case of the ON state, respectively. Because there were strong stimulated emission at the large optical intensity regions, the carrier distribution becomes uneven, i.e., spatial hole-burning occurs. Inside the MMI coupler, the range of the carrier density is 8.8×10^{17} to 9.2×10^{17} cm^{-3}. This difference of carrier density leads to the uneven distribution of refractive index, 3.2535 to 3.254 inside the MMI coupler. The range of refractive index is small enough for the tolerance of the MMI coupler, so the spatial hole-burning does not make some unstable operation, and the laser radiations of the mode-1 and mode-2 exist stably.

Conclusion

We have proposed and investigated a novel BLD with an active 2×2 MMI coupler. The static characteristics of the MMI-BLD have been simulated by using FD-BPM which takes into account the photon-carrier interaction through the carrier rate equation. We have predicted that the MMI-BLD shows bistable switching between the two cross-coupled modes by 0 dBm external light injection, which can be used as an all-optical flip-flop or an optical memory.

[1] G. J. Lasher, *Solid-State Electronics*, vol. 7, pp. 707-716, 1964.
[2] C. L. Tang, A. Schremer, and T. Fujita, *Appl. Phys. Lett.*, vol. 51, pp. 1392-1394, 1987.
[3] B. B. Jian, *Electron. Lett.*, vol. 32, no. 20, pp. 1923-1925, 1996.
[4] Y. Chung, and N. Dagli, *IEEE J. Quantum Electronics*, vol. 26, pp. 1335-1339, 1990.
[5] H. K. Bissessur, F. Koyama, and K. Iga, *IEEE J. Select. Topics in Quantum Electronics*, vol. 3, pp. 344-352, 1997.
[6] G. R. Hadley, *IEEE J. Quantum Electronics*, vol. 28, pp. 363-370, 1992.
[7] R. Olshansky, C. B. Su, J. Manning, and W. Powazinik, *IEEE J. Quantum Electronics*, vol. QE-20, pp. 838-854, 1984.
[8] M. Takenaka, and Y. Nakano, *COIN+PS2002*, PS.TuB5, pp. 78-80, Cheju Island, July, 2002.

The Spectral Decomposition Method: a Transparent Theory for Losses in Segmented Waveguides

Hugo J.W.M. Hoekstra, Joris van Lith, Szabolcs B. Gaal and Paul V. Lambeck
Lightwave Devices Group, MESA$^+$ Research Institute, Faculty EWI, University of Twente,
Po box 217, 7500 AE Enschede, The Netherlands. h.j.w.m.hoekstra@tn.utwente.nl

An approximate theory, giving insight into the effects of device parameters on loss in segmented waveguides, is presented. Computational results on low and high loss structures, and structures showing anomalous length dependence of the loss are discussed.

Keywords: guided wave optics, segmented waveguides, gratings, theory.

Introduction

Segmented waveguides (SWs) have raised a lot of interest due to their potential as devices for quasi-phase matching in second harmonic generation (SHG)[1], for tuning the size of the modal field [2] and for sensing [3,4]. In the latter use is made of the dependence of the loss on the index of the segments. Optimization of SWs for any of these or other purposes involves many parameters, related to both the basic structure of the waveguide (WG) and its segmentation, i.e., the distribution of transitions along the propagation direction. In order to be able to get insight into the effects of these device parameters we have developed the spectral decomposition method (SDM). This 2D method, which is correct only in the limit of low losses, leads to analytical expressions for the relative loss in terms of the segmentation and the parameters describing the basic structure.

The rest of the paper is organized as follows: below the main features of the SDM are introduced. This is followed by a section in which results are shown, discussed and compared with that of the finite difference beam propagation method (BPM) [5] and the mode expansion method (MEM)[6]. The paper ends with conclusions.

Theory

Below analytical expressions will be given for modal losses in a 2D SW for an arbitrary segmentation. The polarization is assumed to be TE, TM polarization can be treated along the same lines. A time-dependence $\exp(iwt)$ is assumed but suppressed. The wave equation to be solved is given by (see also figure 1):

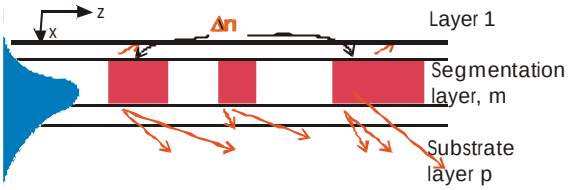

Figure 1. *Schematic picture of the considered waveguide, with segmentation in one of the layers.*

$$\{\partial_{xx} + \partial_{zz} + k_0^2 e(x,z)\}E_y = 0\,. \qquad (1)$$

Here $k_0 (\equiv 2p/l)$ is the wavenumber and $e(x,z)(\equiv n^2(x,z))$ is the relative permittivity. In the below it is assumed that we may write

$$e(x,z) = e_b(x) + h(x)g(z)\Delta e\,, \qquad (2)$$

where e_b describes the so-called basic structure, assumed to be mono-modal, Δe describes the change in permittivity, which is here assumed to occur in one layer, layer m, for which $h(x)=1$; $h(x)=0$ in the other layers. The segmentation is described by $g(z)$, which may be of any form. It is assumed that the segmentation occurs for, say $z \geq 0$, and that for $z<0$ the incoming field is that of the fundamental mode, corresponding to the basic structure, given by:

$$E_0 = e_0(x)\exp(-ib_0 z)\,, \qquad (3)$$

with propagation constant $b_0 \equiv k_0 N_0$, where N_0 is the modal index. It is assumed that the fundamental mode propagates undepleted along z. The total field is written as

$$E_y = E_0 + E_r, \tag{4}$$

where E_r is the field excited by the perturbation. Below we will concentrate on solving the radiative part of it. Substituting (4) into (1) leads to:

$$\{\partial_{xx} + \partial_{zz} + k_0^2 e_b\} E_r = A(E_0 + E_r) \approx A E_0;\ A \equiv -g(z)h(x)k_0^2 \Delta e\ . \tag{5}$$

Here we used the modal field equation for E_0, and for the second equality that the effect of modulation is weak. In the SDM (5) is solved by taking the Fourier transform of (5) with respect to z, and solving the resulting equation for each value of the spatial frequency, k_z, corresponding to radiation modes.

A lengthy but rather straightforward derivation [3] leads to the following expression for the power, radiated into the substrate and the cladding, P_p and P_1, respectively:

$$P_p + P_1 = \int_{-K}^{K} |\, G_0 H_p \,|^2\, dk_z + \int_{-K_1}^{K_1} |\, G_0 H_1 \,|^2\, dk_z \equiv \int_{-K}^{K} H\, |\, G_0 \,|^2\, dk_z\ , \tag{6}$$

with $K_1 \equiv k_0 n_1$, $K \equiv k_0 n_p$ and $H \equiv |\, H_1 \,|^2 + |\, H_p \,|^2$. The relative loss, h, is given by:

$$h = (P_p + P_1)/P_0, \tag{7}$$

with P_0 the power of the incoming fundamental mode. The characteristic functions, $H_{1/p}$, introduced in (6) are given by:

$$|\, H_p \,|^2 \equiv |\, a_p \,|\, t_{mp}(T_1 + S_1)/\{2D(k_z^2 - b_0^2)\}\,|^2\ /(2k_0 Z_0) \tag{8}$$

and

$$|\, H_1 \,|^2 \equiv |\, a_1 \,|\, t_{m1}(T_2 + S_2)/\{2D(k_z^2 - b_0^2)\}\,|^2\ /(2k_0 Z_0), \tag{9}$$

with $H_{1/p} = 0$ if $|\, k_z \,| > k_0 n_{1/p}$. In the above the following notations have been used:

$a_l \equiv \sqrt{k_z^2 - k_0^2 n_l^2}$, $l = 1, p, m$; $D \equiv \exp(a_m d_m) - r_{m1} r_{mp} \exp(-a_m d_m)$; $Z_0 \equiv \sqrt{m_0 / e_0}$;

$T_1 \equiv \partial_x e_{0,m}(0)(1 + r_{m1})/a_m - e_{0,m}(0)(1 - r_{m1})$; $T_2 \equiv \partial_x e_{0,m}(d_m)(1 + r_{mp})/a_m + e_{0,m}(d_m)(1 - r_{mp})$;

$S_1 = \{\exp(a_m d_m) - r_{m1} \exp(-a_m d_m)\} e_{0,m}(d_m) - \{\exp(a_m d_m) + r_{m1} \exp(-a_m d_m)\} \partial_x e_{0,m}(d_m)/a_m$

$S_2 = -\{\exp(a_m d_m) - r_{mp} \exp(-a_m d_m)\} e_{0,m}(0) - \{\exp(a_m d_m) + r_{mp} \exp(-a_m d_m)\} \partial_x e_{0,m}(0)/a_m$.

d_m is the thickness of segmentation layer m, reflection and transmission coefficients are denoted by r and t, respectively and should be evaluated for k_z. The field of the incoming zero-order mode in layer m is denoted by $e_{0,m}(x)$, and we have used a local coordinate system for layer m ($x = 0 - d_m$). The function G_0 corresponds to the Fourier transform of $g(z)$ as follows:

$$G_0(k_z) \equiv k_0^2 \Delta e \int_0^{\infty} g(z) \exp\{i(k_z - b_0)z\} dz / \sqrt{2p} \tag{10}$$

Results and discussion

To illustrate the above we consider a three-layer structure, with refractive indices of 1, 1.8 and 1.457. The wavelength is chosen to be $l = 1mm$. The central layer is segmented, and its thicknesses are chosen to be either $d_2 = 500nm$ or $d_2 = 591nm$, corresponding to modal indices of $N_0 = 1.6795$ and $N_0 = 1.7034$, respectively. The thickness $d_2 = 591nm$ corresponds to a special situation (see below) for which the first order mode is just below cut-off, i.e., $|\, D \,| \sim 0$ at $k_z \sim\!< k_0 n_3$.

The characteristic functions H as a function of $n_{eff}\,(\equiv k_z / k_0)$ are given, for both considered thicknesses, in figure 2. As follows from the above H is an even function of n_{eff}. For the relatively simple (three-layer) structure the functions H are also simple showing only a few maxima and minima. Choosing $n_p \geq n_1$, the large values at $|n_{eff}| <\sim n_p$ (note here p=3) are typical, and are

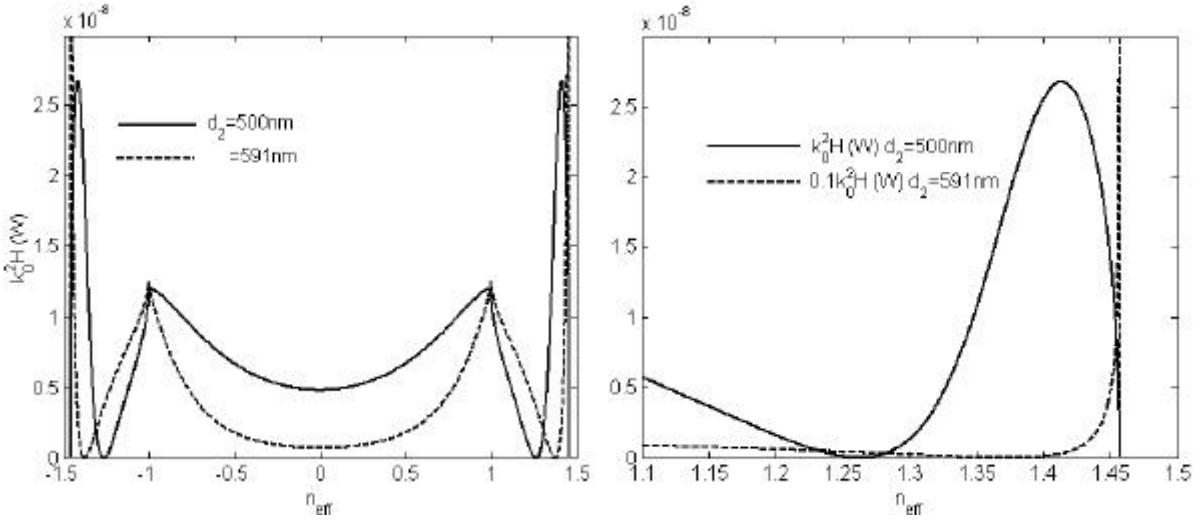

Figure 2. Characteristic functions H, for the two considered thicknesses and a modal power of $P_0 = 1W/m$ (left hand side). The right hand side shows a detail.

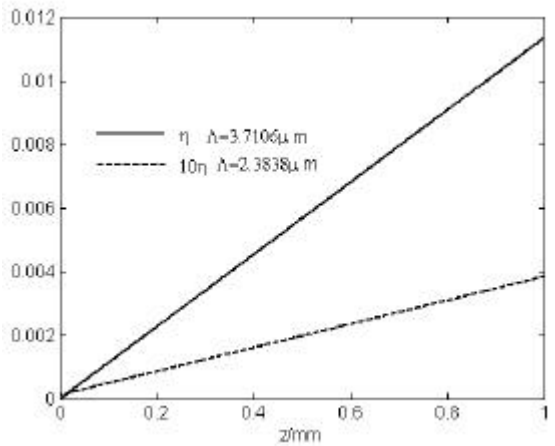

Figure 3. *Relative loss as a function of z for two different grating periods (see text, $\Delta e = 0.01$).*

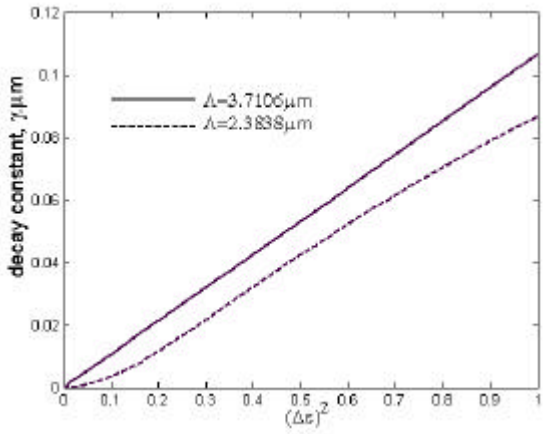

Figure 4. *Decay constant, g, as a function of $(\Delta e)^2$ for two different grating periods (see text).*

related to the term $(k_z^2 - b_0^2)^2$ occurring in the denominator of (8). At $|n_{eff}| = n_p$ usually $H = 0$, as there $a_p = 0$, unless there is a resonance (i.e., $D = 0$) exactly at that position. Then it can be shown [3] that $H \propto 1/\sqrt{K^2 - k_z^2}$. This explains the strong enhancement of H at $|n_{eff}| <\sim n_3$ in figure 2, for $d_2 = 591nm$, for which the resonance (i.e. $|D| \sim 0$), occurs just below cut-off.

In this paper we consider gratings with segments of equal lengths (duty cycle 0.5; period Λ). From (10) it can be shown that then $|G_0^2|$ consists of a central peak at $n_{eff} = N_0$ and peaks at

$n_{eff} = N_0 + (2m+1)\,l/\Lambda$, where m is an integer. The weight of the latter peaks is proportional to $1/(2m+1)^2$. All peaks narrow if the length of the grating is increased.

The above features in H can be utilized to design low-loss or, as desired for SW sensors, high-loss SWs. Examples thereof are given in figure 3, showing the relative loss, h, as a function of z according to the SDM for the cases of indicated grating periods, both calculations used $\Delta e = 0.01$. The considered grating periods correspond to a first-order ($m = -1$) peak of $|G_0^2|$ coinciding with the peak in H at $n_{eff} = 1.41$ and with the zero of H at $n_{eff} = 1.26$, leading, as expected, to high and low loss SWs, respectively.

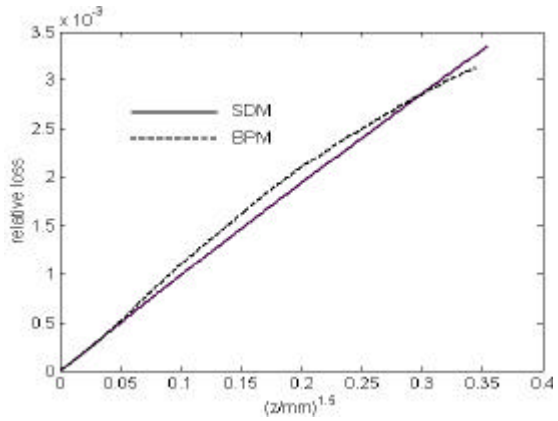

Figure 5. *Anomalous length dependence in the SW, with* $d_2 = 591nm$ *and* $\Delta e = 0.0036$.

If the index contrast increases the large difference between the losses for the two grating periods remains until $\Delta e \approx 0.3$. This can be seen from the MEM calculations given in figure 4, showing the decay constant g, defined by $P_0(z) = P_0(0)\exp(-gz)$.

If there is a resonance at cut-off and if also the 1st order peak of $|G_0^2|$ is also positioned exactly with $n_{eff} = n_p$ it can be shown with the SDM [3] that $h \propto z^{1.5}$. Hereby the relatively small effect of the other peaks in $|G_0^2|$ has been neglected. The above behaviour is similar to the anomalous length dependence of Cerenkov SHG [7,8]. Figure 5 shows the approximate $h \propto z^{1.5}$ dependence, according to both SDM and BPM, for the case that $d_2 = 591nm$ and a grating period of $\Lambda = 4.0577\,mm$, corresponding to a 1st order peak in $|G_0^2|$ at $n_{eff} = n_3$. This remarkable result is slightly counterintuitive, but well understandable in the light of the above: on increasing the length of a grating the k_z-region of the excited radiation modes (i.e., peaks of $|G_0^2|$) always narrows; if the excitation to these modes (i.e., H) in the considered region is peaked the relative loss will increase faster than linearly with the length.

Conclusions

An approximate theory, leading to analytical expressions for the loss in SWs has been presented. The theory opens the way to study the effect of device parameters on all kind of phenomena that may play a role in SWs

Acknowledgments

The presented work was supported by STW, project number TOE.5071

[1] J. Webjorn, F. Laurell, G. Arvidsson, *J. Lightw. Technol.* **7**, 1597-1600, 1989.
[2] Z. Weisman, A. Hardy, *J. Lightw. Technol.* **11**, 1831-1838, 1993.
[3] S.B. Gaal, thesis, Twente, 2002. H.J.W.M.Hoekstra, S.B. Gaal, P.V. Lambeck, to be published.
[4] J. van Lith, P.V. Lambeck, H.J.W.M. Hoekstra, R.G. Heideman, submitted to ECIO '03.
[5] H.J.W.M. Hoekstra, *Opt. Quant. Electron.* **29**, 157-171, 1997.
[6] OlympIOs; *C2V software*, version 5.1.12
[7] J. Ctyroky, L. Kotacka, *Opt. Quant. Electron.* **32**, 799-818, 2000.
[8] H.J.W.M. Hoekstra, J. Ctyroky, L. Kotacka, *J. Lightw. Technol.* January 2003.

Efficient Waveguide Bend Design in Photonic Crystals

Rumen Iliew, Christoph Etrich, Ulf Peschel, and Falk Lederer,
Institut für Festkörpertheorie und Theoretische Optik,
Friedrich-Schiller-Universität Jena, Max-Wien-Platz 1, 07743 Jena, Germany
Rumen.Iliew@uni-jena.de

By interpreting line defects in photonic crystals as strongly coupled point defects we predict basic properties of the waveguide modes from the properties of the point defects and compare the results with rigorous calculations.

Keywords: guided-wave optics, photonic crystals, periodic structures, waveguide modes

The realization of efficient sharp and compact waveguide bends is still a challenging task in microoptics. With the introduction of photonic crystals (PCs) major interest has also focused on the issue of efficient waveguide bends embedded in PCs. There are various proposals for bend design in order to minimize losses. Examples are smoothening the sharp bends [1], introducing cavities or intermediate straight sections [2] or placing smaller holes around the bend [3]. To inhibit the modal mismatch at a Y splitter [4] an additional hole has been added at the bend. On the other hand, it has been shown that a coupled-defect waveguide (CDW) composed of a chain of point defects in a PC can also have a very high transmission for a certain wavelength range at sharps bends [5] when the single defect is single moded. In that case it can be shown that for the single point defect in a square or hexagonal lattice this mode is invariant under all symmetry operations of the C_{4v} or the C_{6v} point group of the underlying crystal, respectively.

The aim of this contribution is to put forward an efficient tool for bend optimization. In our approach we start from the localized modes of a single point defect (e. g. a removed rod or a filled air hole) in a photonic crystal lattice at frequencies within the bandgap. Grouping such defects separated by a few lattice constants into a chain leads to the well-known CDW whereby it is assumed that the modal field of the single defect is not changed significantly and hence the properties of the modes in the arising miniband are determined by the properties of the single defect. This is validated by the good agreement of coupled-mode description and rigorous treatment.

Here we apply this approach to strongly coupled defects where the spacing is one lattice constant and arrive at a W1 line defect waveguide. The complete electromagnetic fields of the waveguide in Fourier domain are again written by means of a superposition of the modal fields of the single point defect located at the individual defect sites l and modified with a complex amplitude a_{kl}:

$$\mathbf{E}(\mathbf{r},\omega)=\sum_{k,l} a_{kl}(\omega)\,\mathbf{e}_k(\mathbf{r}-\mathbf{R}_l),\quad \mathbf{H}(\mathbf{r},\omega)=\operatorname{sgn}(\omega)\sum_{k,l} a_{kl}(\omega)\,\mathbf{h}_k(\mathbf{r}-\mathbf{R}_l) \tag{1}$$

Here $\mathbf{e}_k$ and $\mathbf{h}_k$ denote the orthogonal electric and magnetic field of the k-th mode of the single defect, respectively and $\mathbf{R}_l$ is the l-th defect site. For a wave-like excitation $a_{kl}=a_{k,0}\exp(ilKa)$ (K…Bloch wave vector, a…lattice pitch) for the case where we have a twofold degenerate point defect mode we get two decoupled minibands as solutions for the defect chain. This fact we identify as one cause of reduced bend transmission due to coupling to the respectively other mode at the bend.

When instead we have only one point defect mode, that necessarily then bears the full symmetry of the underlying lattice there occurs only one miniband with the following dispersion relation

obtained from coupled mode analysis (CMA) for only nearest neighbor interaction describing the relation between the excitation frequency ω and the Bloch vector K:

$$\omega(K) = \frac{1 + 2\beta\cos(Ka)}{1 + \frac{1}{2}\gamma_0 + (2\beta + \gamma_1)\cos(Ka)} \tag{2}$$

with $\beta, \gamma_0, \gamma_1$ being overlap integrals of the electric field of the single point defect with the spatial distribution of the dielectric constant for the line defect. For describing bends sections of line defect waveguides must be put together at different angles and additional terms in the equations for the coefficients occur [5] modifying the transmission characteristics.

Plane-wave calculations [6] of the line defect reveal that for square or hexagonal lattices inside the occuring miniband the field structure is still mainly given by the superposition of the field of the single defects shifted by the defect distance. This is also confirmed by the good agreement of the dispersion relation of the miniband obtained from rigorous planewave calculations and from equation (2) as shown in Figure 1 for a sample structure composed of a two-dimensional hexagonal array of dielectric (semiconductor) cylinders in air with removed cylinders as defects and for TM polarization of the electromagnetic field.

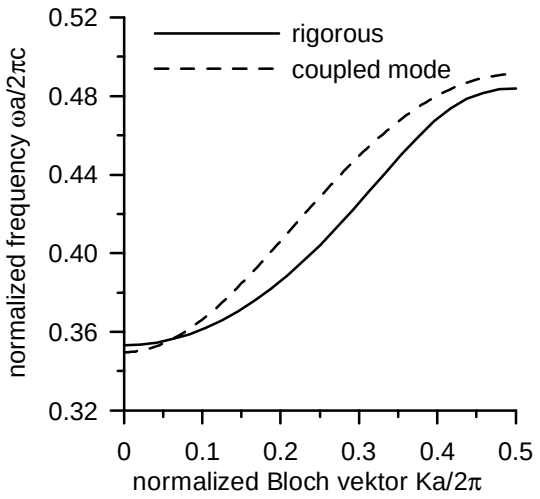

Figure 1. Comparison of the dispersion relations obtained from rigorous (planewave) and coupled mode calculations for a line defect in the TM example structure.

We will utilize this knowledge for designing efficient waveguide bends by following the idea that a point defect mode with the full symmetry of the point group will have the same coupling strength into all equivalent lattice directions. For instance, for point defects arranged in ΓK direction in a hexagonal lattice this would mean there are six equivalent directions for coupling to a second point defect. Exploitation of this idea leads us to a geometry of hexagonally arranged dielectric rods with a double bend where we expect a high transmissivity within a reasonable wavelength range. The result of a two-dimensional finite-difference time-domain (FDTD) calculation of this double bend for a continuous wave excitation at the left end is shown in Figure 2.

In Figure 3 we show the result of the respective FDTD transmissivity calculation for the interesting wavelength range confirming the expected high efficiency of the bend. If we have instead a doubly degenerate point defect mode with a twofold symmetry both of the point defect modes have two different coupling constants to the modes of neighboring defects, depending

whether it is a straight line or a bend. Additionally, it will couple to both modes of the next defect resulting in mode mixing and hence to reduced transmission into the original mode of the waveguide.

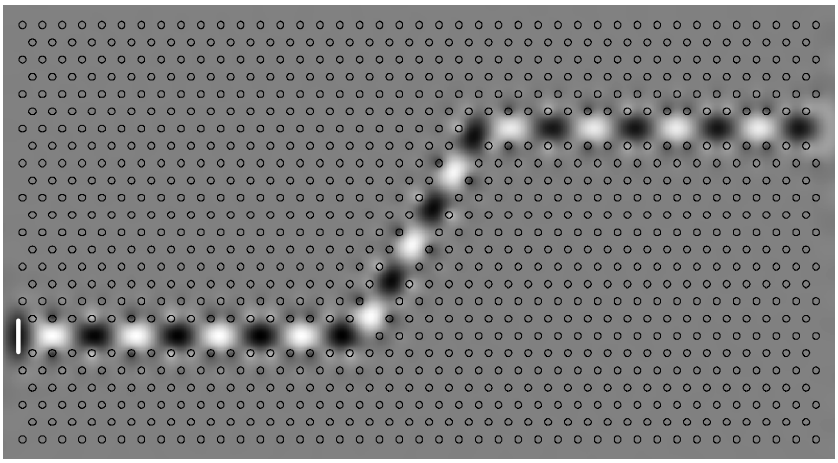

Figure 2. Image plot of the *z* component of the electric field of a W1 waveguide double bend realized in a 2D photonic crystal for TM polarization. The excitation is shown as a white line in the left part.

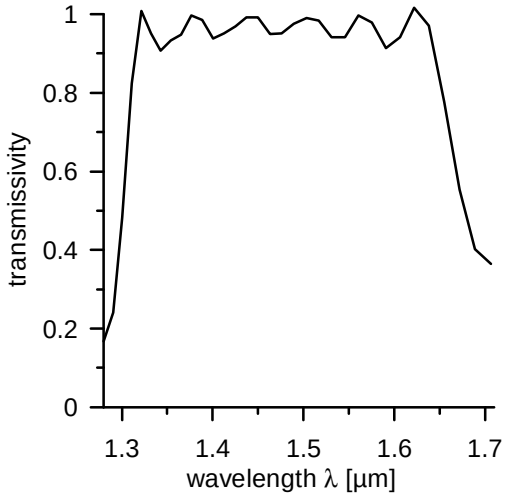

Figure 3. Transmissivity (intensity transmission) obtained for the structure in Fig. 2 from 2D FDTD calculations.

In our paper we will predict the bending performance of W1 line defect waveguides in PCs from the behavior of the single defect for different geometries and compare with FDTD calculations. We will explore the reliability of quantitative predictions based on a CDW description for different geometries.

References

[1] J. Moosburger, M. Kamp, A. Forchel, S. Olivier, H. Benisty, C. Weisbuch, U. Oesterle, "Enhanced transmission through photonic-crystal-based bent waveguides by bend engineering," *Appl. Phys. Lett.* **79**, 3579-3581, 2001.

[2] S. Olivier, H. Benisty, C. Weisbuch, C. J. M. Smith, T. F. Krauss, R. Houdré, and U. Oesterle, "Improved 60° Bend Transmission of Submicron-Width Waveguides Defined in Two-Dimensional Photonic Crystals," *J. Lightwave Technol.* **20**, 1198-1203, 2002.

[3] A. Talneau, Ph. Lalanne, M. Agio, and C. M. Soukoulis, "Low-reflection photonic-crystal taper for efficient coupling between guide sections of arbitrary widths," *Opt. Lett.* **27**, 1522-1524, 2002.

[4] S. Boscolo, M. Midrio and T. F. Krauss, "Y junctions in photonic crystal channel waveguides: high transmission and impedance matching," *Opt. Lett.* **27**, 1001-1003, 2002.

[5] U. Peschel, A. L. Reynolds, B. Arredondo, F. Lederer, P. J. Roberts, T. F. Krauss, and P. J. I. de Maagt, "Transmission and Reflection Analysis of Functional Coupled Cavity Components," *IEEE J. Quantum Electron.* **38**, 830-836, 2002.

[6] S. G. Johnson and J. D. Joannopoulos, "Block-iterative frequency-domain methods for Maxwell's equations in a planewave basis," *Opt. Express* **8**, 173-190, 2001.

Sidewall Roughness in Photonic Crystal Slabs: A Comparison of High-Contrast Membranes and Low-Contrast III-V Epitaxial Structures

Wim Bogaerts, Peter Bienstman, Roel Baets
Ghent University – IMEC, Dept. of Information Technology (INTEC)
Sint-Pietersnieuwstraat 41, B-9000 Gent, Belgium
wim.bogaerts@intec.rug.ac.be

We have simulated sidewall roughness in photonic crystal slabs. Structures with a low vertical index contrast (like III-V waveguides) are shown to be more prone to scattering at sidewall roughness than membranes or SOI-like structures.

Keywords: photonic crystals, scattering, roughness, silicon-on-insulator

Introduction

Today's photonic crystal slab waveguides are limited in their performance by propagation losses. A large fraction of these losses can be attributed to out-of-plane scattering. While in-plane scattering in photonic crystal slabs is prevented by the photonic bandgap effect, in the vertical direction the light is only bound by a vertical index contrast. Most photonic crystal structures consist of a lattice of holes etched into a slab waveguide structure. These holes break the vertical confinement, allowing the light to radiate to the top or bottom cladding. Evidently, the amount of scattering is highly dependent on the refractive index profile of the layer structure in which the photonic crystals are fabricated. One can use a conventional III-V grown layer structure in the GaAs or InP material system. These structures have a low index contrast between the guiding core and the cladding. Alternatively, photonic crystals can be made in a layer structure with a high index contrast, like silicon-on-insulator (SOI) or semiconductor membranes. Both systems have their merits, but exhibit a drastically different behaviour with respect to out-of-plane scattering losses.

Out-of-plane scattering accounts for a large fraction of the losses in photonic crystals. Current state-of-the-art single-mode photonic crystal waveguides have losses of 6dB/mm in SOI [1], and 11dB/mm in III-V materials [2]. These losses are orders of magnitude larger than those of classical waveguides. To reduce these losses, good management of out-of-plane scattering is needed.

Intrinsic Out-of-Plane Scattering

Out-of-plane scattering in photonic crystal slabs has a number of different causes. Even in perfect photonic crystal slabs light is not necessarily confined vertically, and can leak away gradually as it propagates through the structure. This is true for modes located above the light line in the dispersion diagram. These modes extend into the top and bottom cladding and have a radiation component. As is discussed in [3] and [4], these losses increase strongly with the index contrast between core and cladding. Therefore, III-V semiconductors with a low index contrast are a good material system to keep these losses low. On the other hand, when the photonic crystal waveguide modes are located below the light line, they propagate without loss as long as the periodicity is not disturbed. However, it is only possible to construct such a photonic crystal when it has a cladding with a low refractive index and therefore a light line with a steep slope. This implies a high vertical refractive index contrast, as found in SOI or semiconductor membranes.

To reduce intrinsic losses one can either use a low refractive index contrast, so the intrinsic losses are kept low (but not zero) or use a high refractive index contrast, designing a waveguide with a guided Bloch mode. However, in the latter case, careful engineering is needed for defects, as these might cause large scattering losses [3].

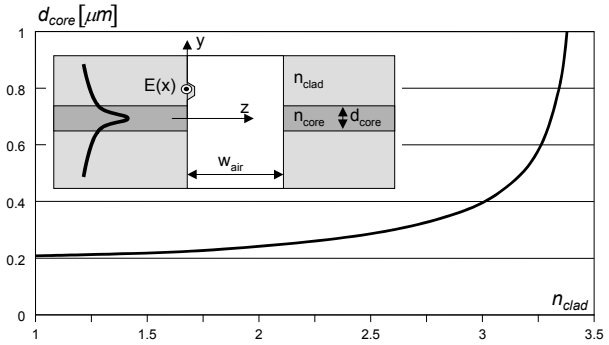

Figure 1: 3-layer slab waveguide with air slot. To guarantee single-mode behaviour, the thickness of the slab core is dependent on the refractive index of the cladding.

Out-of-Plane Scattering at Sidewall Roughness

Although one can design photonic crystal waveguides that are intrinsically lossless, this will never be the case for fabricated structures. The most common fabrication technique for photonic crystals consists of high-resolution lithography combined with dry etching. Although the quality of this technology is improving steadily, a certain amount of roughness due to the etching process is unavoidable. These irregularities, mostly located on the sidewalls of the holes, can scatter light and give rise to losses. Again, we expect the vertical index profile to play a role.

To model the out-of-plane scattering caused by sidewall roughness, we used a 2-D approximation of a photonic crystal slab: 1-D air slots etched into a slab waveguide (Figure 1). We then modelled the scattering roughness by a dipole excited by the incident electromagnetic field, i.e. the mode of the slab waveguide. Because the scatterer radiates in all directions, a fraction of the light will be recaptured by the slab waveguide core. This fraction is of course dependent on the index profile of the slab waveguide and the position of the roughness on the sidewall. We calculated a measure for the losses by averaging over position y of the irregularity on the sidewall:

$$L_{tot} \sim \int_{y} P(y)L(y)dy\,, \tag{1}$$

with $P(y)$ the power radiated by the dipole and $L(y)$ the fraction not recovered by the slab waveguide core. We calculated this using CAMFR [5][6], a vectorial eigenmode expansion tool with PML absorbing boundary conditions. Along the propagation axis, the structure is cut into sections with a constant index profile, in which the electromagnetic field is expanded into the local eigenmodes. Radiation modes are supported through PML absorbing boundary conditions. At the interface between sections, mode matching is used to decompose the field into the eigenmodes of the new section. This way, a scattering matrix describing the entire structure is obtained.

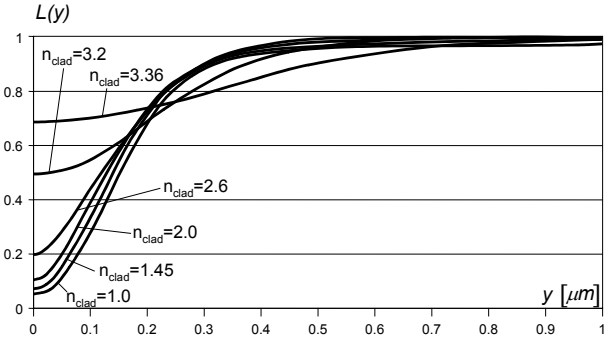

Figure 2: Fraction of light radiated by a dipole in position y that is not recaptured by the waveguide core.

To compare structures with a different refractive index contrast, we defined a slab structure with a constant *v*-number of 2.79. Because the *v*-number depends on the cladding index and core thickness, the core will be thicker for lower cladding index. The core thickness is plotted in Figure 1 as a function of cladding index. For the slab core a refractive index of 3.45 was chosen. The air slots in the slab waveguide are considered to be etched through completely and have a width of 280nm.

Using CAMFR, we then calculated the excitation of the dipole, as well as the fraction of light that can be recovered. This was done in a rigorous way, taking into account the effects of the surroundings on the radiation pattern of the dipole. Because in a photonic crystal, backward and forward propagating light is coupled, we consider the radiated light coupled into the forward and backward propagating mode as *not* lost. Figure 2 plots the lost fraction $L(y)$ of the light as a function position y of the dipole for different values of the cladding index. We see that for low cladding indices (i.e. high vertical index contrast) much light is recovered when the dipole is near the cladding. This can be explained by the fact that a narrow waveguide with high index contrast automatically has a large numerical aperture and can capture much light.

The integrand of equation (1) also contains the power of the radiating dipole. This power depends on two factors: The field strength in position y and the geometry of the roughness on the material-air interface. In a first-order approximation, the incident field strength can be derived from the slab waveguide guided mode. The excitation of the dipole by this incident field is determined by the geometry of the sidewall roughness, as well as by the refractive index contrast along the material-air interface. We can write the radiated power of the dipole $P(y)$ as

$$P(y) = \eta(y)^2 . \frac{E^2(y)}{2.Z_{rad}(y)}, \tag{2}$$

with $E(y)$ the field in position y, $\eta(y)$ describing the effect of the roughness and $Z_{rad}(y)$ the radiative impedance of the environment in position y. The first and last term are easily calculated using CAMFR. To study the effect of the geometry $\eta(y)$ we simulated the scattering of a plane wave incident on an irregularity on a smooth interface between a homogeneous material and air. We did this for different material refractive indices and found that $\eta(y)$ behaves very much like

$$\eta^2 = \gamma . (\Delta\varepsilon_h)^2, \tag{3}$$

with $\Delta\varepsilon_h$ the difference in dielectric constant (i.e. the square of the refractive index) at the interface. If we use this result in our slab waveguide configuration we see that $\eta(y)$ is indeed dependent on the position y, as the index contrast along the interface changes from core to cladding.

Taking into account these results, we can now calculate the integrand in equation (1). $P(y).L(y)$ is

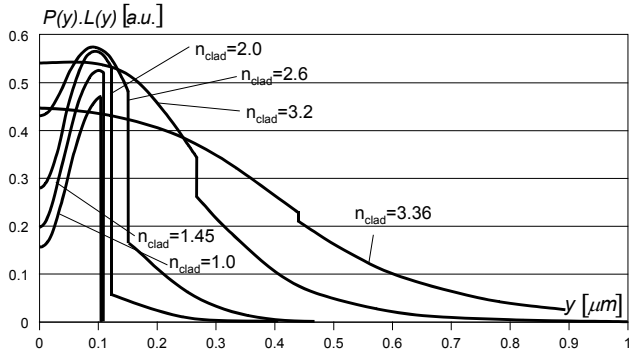

Figure 3: Power lost by radiation caused by an irregularity as a function of position y for different values of the cladding refractive index.

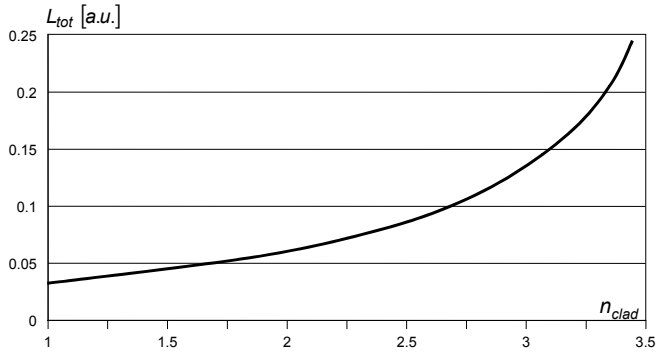

Figure 4: A measure for the average power lost due to sidewall roughness as a function of the refractive index of the slab waveguide cladding.

plotted in Figure 3 for different values of the cladding index. The discontinuity in the curves is caused by the discontinuity in $\eta(y)$ at the core-cladding interface. We see that the amount of scattering is significantly lower for structures with a high refractive index contrast.

Figure 4 plots the measure for scattered light as described in equation (1). We see that for low refractive index contrast, like in III-V, losses due to scattering are considerably higher than in the case of SOI or membranes, and this for a similar amount of sidewall roughness.

Conclusion

Out-of-plane scattering is the major loss mechanism in photonic crystals, and scattering at sidewall roughness can contribute to these losses. Although there are two beneficial regimes for intrinsic losses, i.e. the very high and the very low index contrast, only the high vertical index contrast promises to alleviate these losses for the same level of manufacturing technology.

This advantage with respect to out-of-plane scattering losses might provide an explanation as why photonic crystal waveguides in SOI seriously outperform their III-V competitors [1][2]. Also, these results again show the importance of high-quality fabrication technology. Especially when photonic crystal-based structures are to be commercialised, reproducible mass-fabrication techniques are required.

Acknowledgements

Part of this work was carried out in the context of the European IST-PICCO project. Part of this work was carried out in the context of the Belgian IAP PHOTON network.

Wim Bogaerts thanks the Flemish Institute for the Industrial Advancement of Scientific and Technological Research (IWT) for a specialisation grant.

Peter Bienstman acknowledges the Flemish Fund for Scientific Research (FWO-Vlaanderen) for a postdoctoral fellowship.

References

[1] M. Notomi, A. Shinya, et al., *IEEE J. Quant. Electron.* 38(7), p.736, 2002
[2] Talneau, L. Le Gouezigou, N. Bouadma, *Opt. Lett.* 26(16), p. 1259, 2001
[3] W. Bogaerts, P. Bienstman, D. Taillaert, R. Baets, D. De Zutter, *IEEE Phot. Technol. Lett.* (13), p.565 (2001)
[4] H. Bénisty, D. Labilloy, C. Weisbuch, et al., *Appl. Phys. Lett.* (76), p. 532 (2000)
[5] P. Bienstman and R. Baets, *Opt. Quant. Electron.* 33(4-5), p. 327 (2001)
[6] CAMFR website: http://camfr.sourceforge.net

Photonic crystal waveguides in highly dispersive materials

D. Michaelis, U. Peschel*, C. Waechter, A. Braeuer, and F.Lederer*
Fraunhofer Institute for Applied Optics and Precision Engineering Jena, Micro Optics Department,
Winzerlaer Str. 10, 07745 Jena, Germany
dirk.michaelis@iof.fraunhofer.de

*Friedrich-Schiller-University Jena, Institute for Solid State Theory and Optics,
07743 Jena, Max-Wien-Platz 1, Germany

We derive a reciprocity theorem for photonic crystal waveguides (PCWs) which can be used for analytical descriptions of perturbed PCWs. Especially we analytically investigate polaritons in PCWs and transmission-reflection problems between PCWs and conventional waveguides.

Keywords: photonic crystals, waveguides, polaritons, transmission – reflection analysis

Introduction

Due to their potential applications photonic crystals (PCs) are intensively studied in the last decade. In particular photonic crystal waveguides (PCWs) are of great interest because they allow for an efficient transport of optical signals in highly integrated all-optical circuits. However, there is still a strong need in both numerical modelling as well as fundamental understanding of the field dynamics in these sub-wavelength structures. The frequencies and modes of straight, ideal PCWs are usually calculated by means of plane-wave expansion methods or band structure calculations. However, the field distribution in perturbed, bended or mutually interacting PCWs has still to be determined by solving the complete set of Maxwell's equation via a Finite Difference Time Domain (FDTD) simulations. The latter one is extremely time- and memory consuming and do often not provide for a deeper insight into the physics of the investigated structures. Therefore some simpler modelling or even analytical descriptions of the field dynamics in perturbed PCWs are desirable.

Here we derive a reciprocity theorem and a orthogonality relation for PCW modes starting from Maxwell's equations. Using the reciprocity theorem a set of strongly coupled discrete equations for the field amplitudes in the PC unit cells is deduced. This equations can be used for the modelling or even analytical description of PCWs with arbitrary perturbations. As an example, the theory is applied to the investigation of the influence of polaritons on the band structure of a PCW. Furthermore, the new orthogonality relation is used to derive the coupling coefficients between different PCWs or between a PCW and a conventional waveguide.

Orthogonality relation and coupling coefficients

Starting from Maxwell's equation and using the symmetries of Bloch modes of a PCW in *z*-direction (electric field: $\vec{E}_q = \vec{e}_q(x,y,z)\exp(iqz)$, magnetic field: $\vec{H}_q = \vec{h}_q(x,y,z)\exp(iqz)$, Bloch vector: q) a orthogonality relations for the eigenmodes can be derived

$$\int_{-\infty}^{+\infty} dx \int_{-\infty}^{+\infty} dy \left[\vec{e}_{q_2} \times \vec{h}^*_{q_1} + \vec{e}^*_{q_1} \times \vec{h}_{q_2}\right]_z = \delta_{q_1 q_2}\, s(q_1), \tag{1}$$

which generalize the well known formulas for conventional waveguides of integrated optics [1]. δ is the Kronecker symbol and *s* denotes the energy flux in the respective mode. This orthogonality relation is different to the common, well known orthogonality relation of PCs where a integration over the whole volume of the PC has to be carried out $\iiint_{PC} dx\,dy\,dz\, \vec{H}^*_{q_1} H_{q_2} \sim \delta_{q_1 q_2}$. Because the new orthogonality relation only needs an integration over a plane it can be used for the description of coupling between different waveguides where a mode decomposition in the coupling plane has

to be carried out. Because of the lack of space we concentrate here on approximation formulas for one of the most important case of coupling problems, where both the left and the right waveguide have only one bound mode of a given symmetry. Additionally, for an efficient coupling the transverse shape of both modes has to be similar. Therefore, only a small amount of radiation and evanescent modes is excited. In this case the field structures can be approximated by the left and right bound mode respectively and the following simple approximation formulas yields for the reflectivity:

$$R = -\frac{\iint\limits_{\text{coupling plane}} d\vec{A}\left[\vec{E}^{(t)}_{\text{left}} \times \vec{H}^{(t)}_{\text{right}} - \vec{E}^{(t)}_{\text{right}} \times \vec{H}^{t}_{\text{left}}\right]}{\iint\limits_{\text{coupling plane}} d\vec{A}\left[\vec{E}^{(t)^*}_{\text{left}} \times \vec{H}^{(t)}_{\text{right}} + \vec{E}^{(t)}_{\text{right}} \times \vec{H}^{(t)^*}_{\text{left}}\right]} \tag{2}$$

Similar equations can be derived for the transmission. They can be considered as generalizations of the well known coupling formulas in integrated optics deduced by Marcuse [2]. By means of these formulas approximations for the transmission – reflection – analysis can be obtained very simply. The physics of the coupling can be easily discussed by means of symmetries, phase relations and overlaps of the eigenmodes. Here we only demonstrate the validity of such approximations by means of an example shown in fig. 1. Light couples from a potentially displaced, conventional monomode waveguide to a monomode PCW. In fig. 1c the transmission, obtained by above approximations, is compared to Finite-Difference Time-Domain simulations and shows a good agreement even for a rather large displacement.

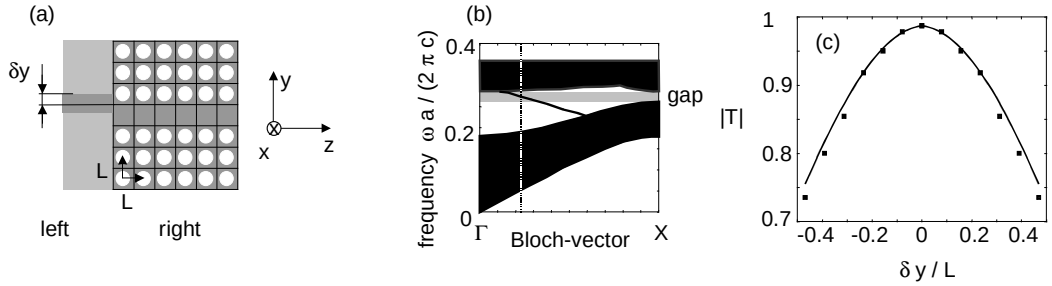

Fig. 1: Coupling of light from a conventional waveguide ($\varepsilon_{\text{guide}}$ = 12, $\varepsilon_{\text{layer}}$ = 9, width / L = 0.4) to a PCW (subtsrate: ε = 12, holes: ε = 1 radius / L = 0.4), (a) scheme of system under consideration, (b) band structure of the PCW, (d) Transmission of the light from the conventional waveguide to the PCW for q = 0.11, solid line: approximation formulas, points: FDTD – simulations.

Photonic crystal waveguides as strongly coupled discrete systems

Using eq. (1) for a mode decomposition $\vec{E} = \sum_q a_q(z)\,\vec{e}_q(\vec{r}) + b_q(z)\,\vec{e}^{\,*}_q(\vec{r})$ $\vec{H} = \sum_q a_q(z)\,\vec{h}_q(\vec{r}) - b_q(z)\,\vec{h}^{\,*}_q(\vec{r})$ of a field in a PCW in the presence of an arbitrary perturbation $\vec{P}_{\text{pert}}$ a set of strongly coupled discrete equations for the amplitudes of the forward $a(z)$ and backward $b(z)$ propagating eigenmodes can be derived from Maxwell's equations:

$$\begin{aligned} &a_q[(k+1)L]\exp[-iq(k+1)L] - a_q[kL]\exp[-iqkL] \\ &= \frac{i\omega}{s(q)} \int_{-\infty}^{\infty} dx \int_{-\infty}^{\infty} dy \int_{kL}^{(k+1)L} dz\, \vec{e}^{\,*}_q\, \vec{P}_{\text{pert}}\, \exp(-iqz) \end{aligned} \tag{3}$$

$$b_q\left[(k+1)L\right]\exp\left[iq(k+1)L\right]-b_q\left[kL\right]\exp\left[iqkL\right]$$
$$=-\frac{i\omega}{s(q)}\int_{-\infty}^{\infty}dx\int_{-\infty}^{\infty}dy\int_{kL}^{(k+1)L}dz\;\vec{e}_q\;\vec{P}_{\text{pert}}\exp(iqz)$$

,

where we have assumed the k^{th} unit cell to extend between $kL \le z = (k+1)L$. Here the mutual coupling between distant unit cells is of great importance and no nearest neighbour approximation holds. The above discrete set of equation can be used to describe a variety of problems with linear and/or nonlinear perturbations. In particular the most significant frequency dependence is incorporated into the Bloch vector $q(\omega)$.

Polaritons in photonic crystal waveguides

Here we apply eq. (3) to one of the simplest examples, namely a spatially constant but dispersive perturbation $\vec{P}_{\text{pert}} = \varepsilon_0\,\Delta\varepsilon(\omega)\left[a_q(z)\,\vec{e}_q(\vec{r}) + b_q(z)\,\vec{e}_q(\vec{r})^*\right]$. Band structure calculations usually do not take into account the dispersion of the dielectric function of the PC materials. This dispersion can be regarded as a perturbation of the nondispersive PC. Therefore eqs. (3) represent an ideal tool to include the dispersion. Here we analytically discuss the influences of a two level systems $\Delta\varepsilon(\omega) = \dfrac{f\,(\omega_0-\omega)}{(\omega_0-\omega)^2+\gamma^2}$ (ω_0 : resonsance frequency, γ: line width, f ~ oscillator strength) on the band structure of a PCW of fig. 2a. A homogenously doped PC with quantum dots represents an example for such a configuration. Applying a slowly varying envelope approximation eq. (3) results in a matrix equation for the amplitudes of the modes in the k^{th} unit cell (a_k , b_k) and $(k+1)^{\text{th}}$ unit cell (a_{k+1} , b_{k+1}):

$$\begin{pmatrix} a_{k+1} \\ b_{k+1} \end{pmatrix} = \hat{M}\begin{pmatrix} a_k \\ b_k \end{pmatrix}$$
$$\hat{M} = \frac{1}{1+\kappa^2-|c|^2}\begin{pmatrix} \left[(1+i\kappa)^2+|c|^2\right]\exp(iqL) & 2c\exp(iqL) \\ 2c^*\exp(-iqL) & \left[(1-i\kappa)^2+|c|^2\right]\exp(-iqL) \end{pmatrix}, \tag{4}$$

where the coefficients read as $\kappa=\Delta\varepsilon(\omega)\kappa'(\omega)$ and $c=\Delta\varepsilon(\omega)c$ with $\kappa' = \dfrac{\omega\varepsilon_0}{2\,s(q)}\displaystyle\int_{-\infty}^{\infty}dx\int_{-\infty}^{\infty}dy\int_0^L dz\;\;|\vec{e}|^2$ and $c' = \dfrac{i\omega\varepsilon_0}{2\,s(q)}\displaystyle\int_{-\infty}^{\infty}dx\int_{-\infty}^{\infty}dy\int_0^L dz\;\;\vec{e}^{*2}\exp(-2iqz)$. κ' and c' do not depend on the perturbation. They are exclusively determined by the band structure of the unperturbed PCW and represent the quantities which describe the sensitivity for a deformation of the band due to perturbations. Fig. 2b shows these parameters for the PCW of fig. 2a. The eigenvalues analysis of the matrix $\hat{M}$ gives the new eigenmodes of the perturbed PCW. A field in the perturbed waveguide can be written as:

$$\begin{pmatrix} A_k \\ B_k \end{pmatrix} = \alpha_+\lambda_+^k\begin{pmatrix} 1 \\ e_+ \end{pmatrix} + \alpha_-\lambda_-^k\begin{pmatrix} 1 \\ e_- \end{pmatrix}, \tag{5}$$

where the eigenvalues read as $\lambda_\pm = \pm\sqrt{[\text{Re}(\eta)]^2-1}+\text{Re}(\eta)$ with $\eta = \dfrac{(1+i\kappa)^2+|c|^2}{1+\kappa^2-|c|^2}\exp(iqL)$.

$\alpha_{\pm}$ are the amplitudes of the new forward and backward propagating mode. For $\mathrm{Re}(\eta) \le 1$ the eigenvalues are complex $\lambda_{\pm} = \mathrm{Re}(\eta) \pm i\sqrt{1-[\mathrm{Re}(\eta)]^2}$. Their amounts are equal to unity. Therefore they can be written as $\lambda_{\pm} = \exp(iqL)$, where the new Bloch vector reads as $q = \arctan\left(\sqrt{1-\mathrm{Re}(\eta)}/\eta\right)/L$. In this case the mode dynamics is given by a simple phase evolution, i.e. eq. (5) describes the mode propagation in the perturbed PCW. For $|\mathrm{Re}(\eta)| > 1$ the eigenvalues become purely real. Thus the former propagating modes pass over to evanescent modes. A closer look at eq. (5) reveals the physical meaning of the parameters κ and c. Depending on the sign, κ shifts the band towards larger or smaller Bloch vectors, whereas c leads to a band shrinkage. For a strong enough of Δε of the two level system the PCW band structure is not only deformed, there could be even a splitting of the original band and a new gap is created (evanescent modes appear). The sensitivity of the PCW – band for a creation of a new gap depends strongly on the corresponding frequency. A new gap is created for $|\mathrm{Re}[\eta(\Delta\varepsilon_{crit})]| = 1$ which defines the critical value of perturbation $\Delta\varepsilon_{crit}$ for band splitting (see fig. 2c). Close to the Γ – point the band is very sensitive for a negative $\Delta\varepsilon$, whereas for increasing frequencies the sensitivity becomes larger for positive $\Delta\varepsilon$ - values. In our case for a normalized resonance frequency of 0.32 (see fig. 2d) close to the Γ – point the gap emerges for negative $\Delta\varepsilon$, i.e. above the resonance frequency. The situation reverses for larger resonance frequencies, i.e. the gap appears below the resonance. This is in contrast to the common dispersion relations of polaritons in bulk media. The backward bended branch in fig. 2d occurs in the resonance of the two level system. In this frequency range strong absorption is present. Thus no ideal band can be defined in this region.

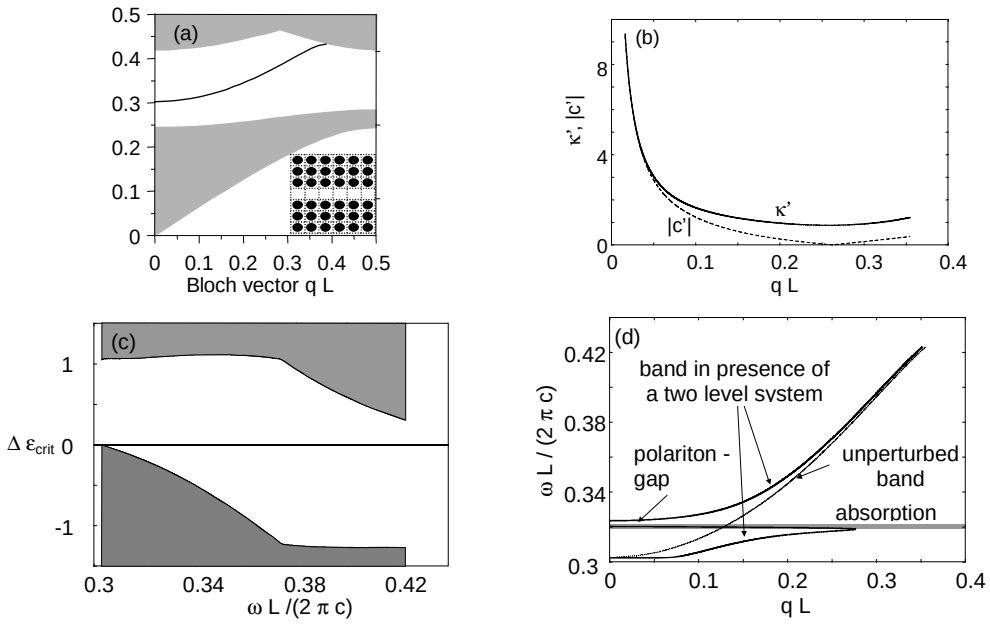

Fig. 2: Polaritons in a PCW (rods: ε = 12, radius / L = 0.2), (a) band structure (b) coefficients for the perturbation theory describing perturbation induced band deformations (c) critical perturbation for band splitting (shaded regions: band splitting - evanescent modes) ,(d) unperturbed and perturbed band structure due to the existence of polaritons

[1] R. März, 'Integrated Optics, desing and modeling', Artech House, Boston London (1994).

[2] D. Marcuse, 'Theory of Dielectric Optical Waveguides', Academic Press, New York, (1974).

Grating assisted rectangular integrated optical microresonators

Manfred Hammer*, Didit Yudistira
MESA+ Research Institute, University of Twente, The Netherlands

A wide, multimode segment of a dielectric optical waveguide, enclosed by Bragg reflectors and evanescently coupled to adjacent port waveguides, can constitute the cavity in an integrated optical microresonator. We outline a design strategy for these devices and give results of numerical simulations by means of mode expansion techniques, that exemplify the specific spectral response of the standing wave resonators.

Keywords: integrated optics, numerical modeling, optical microresonators, rectangular microcavities.

Introduction

Optical microresonators are at present discussed as basic elements for large scale integrated optics [1, 2], typically for applications in optical wavelength division multiplexing. The focus is on compact cylindrical disk- or ring shaped structures, designed for material systems with high refractive index contrast, where the technological implementation or the application itself usually requires a facility for post fabrication adjustment. If the tuning is to be realized by electrooptical means, a major obstacle may be encountered in the form of the strong anisotropy of some of the most promising electrooptic materials [3, 2]. The birefringence must be suspected to lead to a pronounced modulation, if not to leakage, of the circulating optical waves, i.e. to a lossy cavity.

These problems can be avoided in standing wave resonators, where the light propagation is restricted basically to one axis. Integrated optical microresonators with square or rectangular cavities have attracted attention only quite recently [4, 5, 6, 7]. In their conventional form, also these concepts have a severe technological disadvantage: An extremely high refractive index contrast is required for the total reflection effect at the facets of the waveguide segments [8] that serve as cavities; with the presently available materials a realization seems to be difficult.

A way out is found by replacing the waveguide facets by Bragg reflectors. This leads to a concept for a standing wave resonator in the form of a Fabry-Perot cavity with lateral, evanescent coupling. Fig. 1 sketches the structure and introduces the relevant parameters. While a parameterized time-domain coupled mode theory model is given in Ref. [4], so far apparently neither rigorous nor approximate simulations of these devices exist. This is what we would like to provide with this paper.

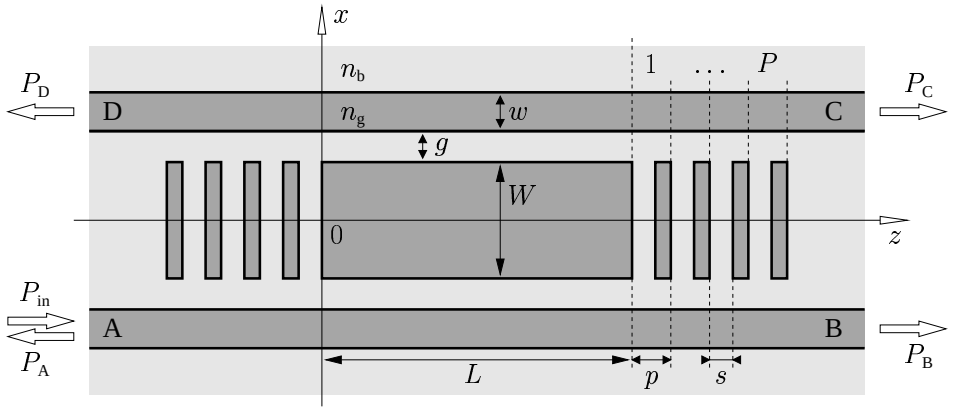

Fig. 1. Grating assisted rectangular resonator: Two parallel waveguide cores of width w are coupled by a cavity of width W and length L, separated by gaps g. Gratings with P periods of length p with a spacing s enclose the cavity. The guiding regions with refractive index n_g are embedded in a background medium with index n_b. Capital letters A to D denote the input and output ports.

* Manfred Hammer, Department of Applied Mathematics, University of Twente, P.O. Box 217, 7500 AE Enschede, The Netherlands. Phone: ++31(0)53/489-3448, Fax: ++31(0)53/489-4833, E-mail: m.hammer@math.utwente.nl

Design strategy

Assuming that the hypothetical device will be realized on the basis of rectangular Si_3N_4 cores (refractive index 1.98) surrounded by a SiO_2 background medium, we fix a common channel thickness of $0.223\,\mu$m. Then the values given in Table 1 correspond to the effective index projection of the realistic 3D structure, at a design wavelength of $\lambda_0 = 1.55\,\mu$m. For simplicity, all considerations are restricted to this 2D model and to TE polarization.

As a starting point of the resonator design we choose the width w of the port waveguides, such that these are single mode in a suitable wavelength region around λ_0; the values of Table 1 lead to an effective mode index $n_{\text{eff}} = 1.540$ at λ_0.

Reasoning along the coupled mode model of Ref. [6], only few (one or two) guided modes of the cavity segment are likely to be relevant for specific standing wave resonances. These modes are to be excited in the cavity; hence, to satisfy the phase matching condition, we adjust W such that the cavity waveguide supports a guided mode that is degenerate with the port fields. In the present case, W should be among the discrete values $(1.0 + j\,1.791)\,\mu$m, for integer j.

As a second condition, pronounced resonances require a reflectivity close to unity for the relevant modes at the ends of the cavity [6]. In contrast to an ordinary high contrast waveguide facet, where two cavity modes are necessary [8], with the present gratings a single cavity mode is sufficient. The corresponding Bragg reflectors can be constructed on the basis of a model of tilted plane wave incidence on a multilayer stack with equivalent refractive index composition. We consider an incidence angle θ that corresponds to the angle of the relevant mode in the cavity, defined by $\cos\theta = n_{\text{eff}}/n_{\text{g}}$. Optimization of the layer stack for the present mode angle of 15.69° at λ_0 leads to the grating parameters p and s as given in Table 1.

To select a suitable cavity width W, we computed single mode reflectivities for Bragg gratings according to the specification of Table 1 and Fig. 1, for $P = 5$ and $W = (1.0 + j\,1.791)\,\mu$m, in each case for incidence of the j-th order mode. Levels of 0.17, 0.21, 0.23, 0.24, 0.25, 0.26 were observed for $j = 1, 2, \ldots, 5$, with the last value already close to the limiting level of 0.28, the reflectivity of a plane wave, incident under an angle of 15.69° on a laterally unbounded equivalent multilayer stack. Obviously the reflectivity is the higher, the larger the fraction of the mode profile is that actually encounters the corrugation of the Bragg reflector. Therefore a width W corresponding to a higher order mode is preferred, (such that the phase matching condition is still sufficient to distinguish the cavity modes, the propagation constants of which become closer for large W). We set W to the value for order $j = 5$ for the present simulations. Fig. 2 shows that in this way indeed a suitable Bragg grating can be designed, with a spectral response that resembles the curve expected from the plane wave model surprisingly well.

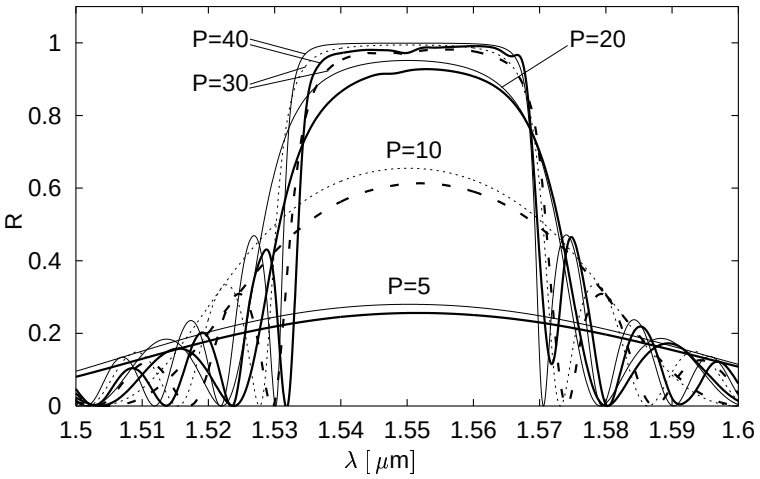

Fig. 2. Reflectivity R of Bragg-reflectors according to the specification of Table 1, versus the vacuum wavelength, for different numbers of grating periods P. The guided 5th order mode is launched in the wide cavity waveguide segment; the thick lines show the relative power levels that are reflected into that specific mode. The thin curves indicate the plane wave reflectivity of an equivalent multilayer stack for wave incidence under the respective mode angle (15.69° at $\lambda = 1.55\,\mu$m).

Given the complex valued amplitude reflection coefficient $r\ \exp \mathrm{i}\varphi$ of the Bragg gratings, a resonance at λ_0 requires the total phase gain along one propagation cycle through the cavity to match an integer multiple of π. This amounts to a condition $L = (m\pi + \varphi)\lambda_0/(2\pi n_{\text{eff}})$ for the cavity length [6], with integer m. Neglecting the wavelength dependence of n_{eff} and assuming a long cavity $m\pi \gg \varphi$, one obtains $\Delta\lambda = \lambda_0/m = \lambda_0^2/(2Ln_{\text{eff}})$ for the spectral distance of two neighboring resonances. L, or m, respectively, is to be selected such that there is a chance for pronounced resonances in the window of high Bragg reflectivity around the design wavelength (m is about 119 and 159 in Fig. 3).

The gap width g is to be determined such that on the one hand there is a sufficient power transfer between the port waveguide and the cavity along the long unfolded light path in case of a resonance, while on the other hand the level of direct, unidirectional coupling (as in a conventional three-guide directional coupler, without a pronounced wavelength dependence) remains negligible. This parameter is selected finally on the basis of numerical experiments.

Numerical results

The design procedure leads to simulation parameters as listed in Table 1. The devices were simulated by means of the mode expansion techniques as described in Refs. [9, 5]; Fig. 3 shows the spectral response obtained in this way. We verified the results using an only recently released commercial simulation tool [10], based on bidirectional eigenmode propagation.

Table 1. Geometrical and material parameters for the simulations of Fig. 3. Including two Bragg reflectors and the cavity, the overall lengths of the devices are 182 μm and 203 μm.

n_{g}	n_{b}	$w/\ \mu$m	$g/\ \mu$m	$W/\ \mu$m	$L/\ \mu$m	$p/\ \mu$m	$s/\ \mu$m	P	$\lambda/\ \mu$m
1.60	1.45	1.000	1.600	9.955	59.860, 79.985	1.538	0.281	40	$\in [1.5, 1.6]$

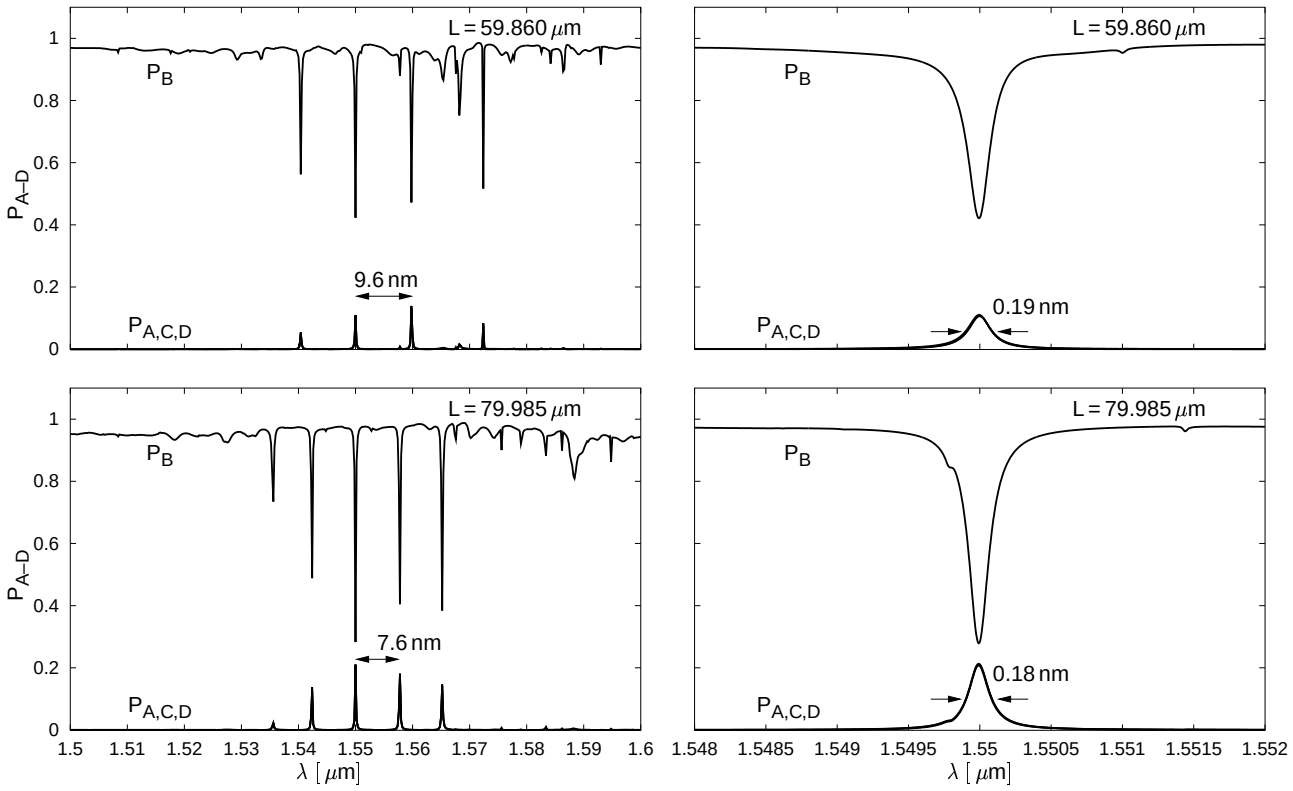

Fig. 3. Spectral responses of resonators according to Fig. 1, with the parameters of Table 1, for cavity lengths $L = 59.860\,\mu$m (top) and $L = 79.985\,\mu$m (bottom). P_{A} to P_{D} are the relative power fractions that are reflected or transmitted into ports A to D. The curves related to P_{A}, P_{C}, and P_{D} are almost completely superimposed.

The resonators are excited in port A by the right traveling guided mode of the lower core. For most wavelengths, the major part of the input power is directly transmitted to port B. Resonant states appear as a drop in P_{B} and a simultaneous increase of the reflected and dropped power fractions P_{A}, P_{C}, and P_{D}. As expected, the resonances are restricted to the range of high reflectivity of the Bragg gratings (cf. Fig. 2). The finesse for the two resonators is 51 (top) and 42 (bottom), here defined as the ratio between the free spectral range and the width at half maximum.

While at resonance the present device distributes the input among all four ports, a filter that properly drops the power into a single output channel can be realized with two cascaded single cavity resonators at a specific distance [4, 5]. The total length of the add-drop filter could be about $500\ \mu$m.

Remarks and conclusion

Based on quite simple design guidelines and moderate numerical means, the former results clearly demonstrate the working principle of the grating assisted rectangular microresonators, at least in terms of numerical simulations. We find the shape of resonances as predicted for high contrast standing wave resonators with finite waveguide segments as cavities, but in the present case with realistic material parameters, at the cost of an increased, but still acceptable length of the devices. Light propagation is oriented along a single axis; hence combination of this concept with an anisotropic electrooptic material for purposes of tuning poses no principal problems.

The design leaves plenty of room for further optimization. Apart from the theoretical limit of equal quarter transmission to all four ports at resonance, this concerns in particular the Bragg reflectors: Modifying the grating with the aim of a narrow, properly positioned bandgap should allow to restrict the spectral response to a single resonance. Alternatively, this could be achieved by means of two slightly different Bragg gratings at both ends of the cavity, adjusted such that their regions of high reflectivity overlap in only a narrow wavelength region. In principle, this should lead to devices with infinite free spectral range and finesse.

The authors would like to thank E. van Groesen, H. J. W. M. Hoekstra, and R. Stoffer for many fruitful discussions on the subject. Financial support by the European Commission (project IST-2000-28018, 'NAIS') and by the Royal Netherlands Academy of Arts and Sciences (KNAW, project 99–WI–44) is gratefully acknowledged.

[1] B. E. Little, S. T. Chu, W. Pan, and Y. Kokubun. Microring resonator arrays for VLSI photonics. *IEEE Photonics Technology Letters*, 12(3):323–325, 2000.

[2] Next-generation active integrated optic subsystems. Information society technologies programme of the European Commission, project IST-2000-28018, http://www.mesaplus.utwente.nl/nais/

[3] S. Follonier, M. Fierz, I. Biaggio, U. Meier, Ch. Bosshard, and P. Günter. Structural, optical, and electrical properties of the organic molecular crystal 4–N,N–dimethylamino–4'–n–methyl stilbazolium tosylate. *Journal of the Optical Society of America B*, 19:1990–1998, 2002.

[4] C. Manolatou, M. J. Khan, S. Fan, P. R. Villeneuve, H. A. Haus, and J. D. Joannopoulos. Coupling of modes analysis of resonant channel add-drop filters. *IEEE J. of Quant. Electr.*, 35(9):1322–1331, 1999.

[5] M. Lohmeyer. Mode expansion modeling of rectangular integrated optical microresonators. *Optical and Quantum Electronics*, 34(5):541–557, 2002.

[6] M. Hammer. Resonant coupling of dielectric optical waveguides via rectangular microcavities: The coupled guided mode perspective. *Optics communications*, 214(1–6):155–170, 2002.

[7] S. Kriswandhi. Simulation of a rectangular optical microresonator using bidirectional eigenmode propagation, 2002. C2V app. note A2002005, http://www.c2v.nl/software/support/appnotes/A2002005.pdf

[8] M. Hammer and E. van Groesen. Total multimode reflection at facets of planar high contrast optical waveguides. *Journal of Lightwave Technology*, 20(8):1549–1555, 2002.

[9] M. Lohmeyer and R. Stoffer. Integrated optical cross strip polarizer concept. *Optical and Quantum Electronics*, 33(4/5):413–431, 2001.

[10] OlympIOs Integrated Optics Software. C2V, P.O. Box 318, 7500 AH Enschede, The Netherlands; http://www.c2v.nl/software/

Papers presented at OWTNM 2003

Oral 11 **H.-C. Chang, C.-P. Yu, and Y.-C. Chiang**
National Taiwan University, Department of Electrical Engineering, Taipei, TAIWAN

Oral 12 **S. Helfert and R. Pregla**
FernUniversitaet in Hagen, Hagen, GERMANY

Oral 13 **E. Bekker, P. Sewell, T. Benson, and L. Melnikov**
Nottingham University, School of Electrical and Electronic Engineering, Nottingham, UK

Oral 14 **E E. Cassan, S. Laval, and L. Vivien**
Université Paris-Sud, Institut d'Electronique Fondamentale, UMR CNRS

Oral 15 **G. Bao and K. Huang**
Michigan State University, Department of Mathematics, East Lansing, MI, USA

Oral 16 **A. Delage and K. Dossou**
National Research Council Canada, Institute for Microstructural Sciences, Ottawa, ON, CANADA

Oral 17 **B.A. Usievich, V.A. Sychugov, D.H. Nurligareev, and O. Parriaux**
Institute of General Physics Moscow, Moscow, RUSSIA
Jean Monnet University, TSI Lab, Saint-Etienne, FRANCE

Oral 18 **P. Fernandez, J. C. Aguado, J. Blas, and R. Duran**
University of Valladolid, Signal Theory, Communications and Telematic Engineering Department, Valladolid, SPAIN

Oral 19 **B. Maes, P. Bienstman, and R. Baets**
Ghent University IMEC, Department of Information Technology, Ghent, BELGIUM

Oral 20 **J. Wykes, J. Bonnyman, P. Sewell, T. Benson, S. Sujecki, E. Larkins, L. Borruel, and I. Esquivias**
The University of Nottingham, School of Electrical and Electronic Engineering, Nottingham, UK

Oral 21 **G. Bellanca, A. Parini, S. Trillo, L. Saccomandi, and P. Bassi**
University of Bologna, Dipartimento di Elettronica Informatica e Sistemistica, Bologna, ITALY

Oral 22 **A. Irman and T. P. Valkering**
University of Twente, Applied Physics, Enschede, THE NETHERLANDS

Oral 23 **M. Hammer**
University of Twente, MESA+ Research Institute, Department of Applied Mathematics, Enschede, THE NETHERLANDS

Oral 24 **S. S. A. Obayya, B. M. A. Rahman, and K. T. V. Grattan**
City University London, School of Engineering and Mathematical Sciences, London, UK

Oral 25 **M.A Luque-Nieto, J.G. Wangüemert-Pérez, and I. Molina-Fernández**
Malaga University, Dpto. Ingeniería de Comunicaciones, Málaga, SPAIN

Oral 26 **S. L. Chui and Y. Y. Lu**
City University of Hong Kong, Department of Mathematics, Kowloon, HONG KONG

Oral 27 **H. P. Uranus, H. J. W. M. Hoekstra, E. van Groesen**
University of Twente, MESA+ Research Institute, Lightwave Devices Group, Enschede, THE NETHERLANDS

Oral 28 **R. Pregla**
FernUniversitaet in Hagen, Hagen, GERMANY

Oral 29 **L. Cahill**
La Trobe University, Department of Electronic Engineering, Bundoora, AUSTRALIA

Oral 30 **C. Styan, A. Vukovic, P. Sewell, and T.M. Benson**
The University of Nottingham, School of Electrical and Electronic Engineering, Nottingham, UK

Oral 31 **A. Stump, J. Kunde, U. Gubler, A. - C. Pliska-LeDuff, and Ch. Bosshard**
CSEM SA, Alpnach, SWITZERLAND

Oral 32 **W. Pascher, J. H. den Besten, D. Caprioli, X. Leijtens, M. Smit, and R. van Dijk**
FernUniversität, Elektromagnetische Feldtheorie, Hagen, GERMANY
Eindhoven University of Technology, Opto-Electronic Devices group, Eindhoven, THE NETHERLANDS
TNO Physics and Electronics Laboratory, The Hague, THE NETHERLANDS

Oral 33 **B. M. A. Rahman, S. S. A. Obayya, N. Somasiri, M. Rajarajan, C. Themistos, and K. T. V. Grattan**
City University London, School of Engineering and Mathematical Sciences, London, UK

Oral 34 **S.V. Boriskina, T. M. Benson, P. Sewell, and A. I. Nosich**
The University of Nottingham, School of Electrical and Electronic Engineering, Nottingham, UK

Oral 35 **A. Melloni, F. Morichetti, and M. Martinelli**
Politecnico di Milano, Dip. Elettronica e Informazione, Milano, ITALY

Oral 36 **V. Mezentsev, S. Turitsyn, S. Yakovenko, S. Kobtsev, S. Kukarin, and N. Fateev**
Aston University, Photonics Research Group, Birmingham, UK

Oral 37 **A. Cachard, E. Bonnet, A. Tishchenko, O. Parriaux, X. Letartre, and D. Gallagher**
Jean Monnet University, TSI Lab, Saint-Etienne, FRANCE Photon Design, Oxford, UK

Oral 38 **H. B. H. Elforai and H. J. W. M. Hoekstra**
University of Twente, MESA+ Research Institute, Lightwave Devices Group, Enschede, THE NETHERLANDS

Applications of the Finite Difference Mode Solution Method to Photonic Crystal Structures

Hung-chun Chang*, Chin-ping Yu, and Yen-Chung Chiang
Department of Electrical Engineering and Graduate Institute of Communication Engineering
National Taiwan University, Taipei, Taiwan 106-17, R.O.C.
hcchang@cc.ee.ntu.edu.tw

**also with the Graduate Institute of Electro-Optical Engineering, National Taiwan University*

A finite difference mode solver is employed with appropriate modifications for studying the modes on photonic crystal fibers and planar waveguides as well as the band gap structures of 2-D photonic crystals.

Keywords: finite difference mode solver, photonic crystals, photonic crystal fibers, photonic crystal waveguides

Electromagnetic mode solvers based on the finite difference method have been one of the popular techniques for analysis of waveguide modes on various optical or dielectric waveguides. Full-vectorial version for such solvers has been well known. In this paper we report on applications of such finite difference method to the study of three photonic crystal related problems: modes on photonic crystal fibers (PCFs), modes on photonic crystal planar waveguides, and band gap structures of two-dimensional photonic crystals.

PCFs are novel photonic structures that represent one successful application of the photonic crystal concept. We demonstrate that the full-vectorial finite difference method can be efficiently used to obtain the propagation characteristics, including the effective indexes and field distributions, of different PCFs. We study various kinds of holey fibers [1] as well as PCFs with a large air core [2]. In the calculation the cross section of the PCF is discretized into many mesh points with the Maxwell differential equations finite differenced to form a set of elementary matrix equations. The effective indexes of the guided modes are obtained by finding out the eigenvalues of the matrix equations, and the field distributions from solving the eigen vectors. Since the guided modes are found well confined, the computational window is not necessarily large and the absorbing boundary condition is utilized at its boundary.

For calculating modes guided on photonic crystal planar waveguides, for which line defects are introduced to form a guiding region, we modify the mode solver for treating the “super cell” that extends one period along the wave propagation direction and several periods in the transverse direction. Periodic boundary conditions are imposed upon the two boundaries separated by one period and absorbing boundaries are considered for the other two. Propagation constants and the mode fields for both TE and TM modes are successfully obtained. Calculation of the relevant photonic band gaps (PBGs) can also be achieved by a similarly modified solver. For the PBG calculation, the periodic boundary condition is used at all of the four boundaries. For treating dielectric interfaces with curvature, we have derived a general relation, considering an interface condition, between a sampled point and its nearby points in the finite difference scheme and highly accurate numerical results have been achieved [3].

References

[1] Knight et al., *Opt. Lett.* **21**, 1547–1549, 1996.
[2] Cregan et al., *Science* **285**, 1537–1539, 1999.
[3] Y. C. Chiang et al., *J. Lightwave Technol.* **20**, 1609–1618, 2002.

Numerical stable determination of Floquet–modes and their application to the computation of band structures

Stefan F. Helfert and Reinhold Pregla
FernUniversität in Hagen, Germany
Stefan.Helfert@FernUni-hagen.de *R.Pregla@FernUni-Hagen.de*

A stable way to determine Floquet–modes is presented. This is done by transforming a reflection coefficient from the output of a periodic segment to its input and then by computing the field in opposite direction. By this, exponential increasing terms are avoided. The formulas are applied to determine the band structures in photonic crystals.

Keywords: Floquet–modes, periodic structures, photonic crystals

Introduction

Periodic structures are important components in optical circuits. Examples are Bragg–gratings, polarization converters or photonic bandgap strucures. The analysis of such devices has been described in [1] where the method of lines has been combined with Floquet's theorem. Doing this e.g. a Bragg–grating with some ten thousand periods was examined without numerical problems and in very fast way.

Developed algorithm and application

Particularly, the determination of the Floquet– (or Bloch–) modes is of importance. Transfer matrix expressions work very well in case of short distances and low losses as in [1]. However, the exponential increasing terms can lead to numerical problems for longer devices. In the presentation we will show the determination of the Floquet–modes in a numerical stable way. This is done by transforming reflection coefficients from the output of one period to its input(see Fig. 1), and by computing the fields in opposite direction. By this only exponential decreasing terms are used for the analysis.

We will then show how band structures of photonic crystals can be determined with the method of lines, where we introduces the derived expressions. Fig. 2 shows the diagram for a square array of dielectric columns in air [2](p. 56). In our computation the circles were approximated by areas with squares or with crosses. A very good agreement is observable.

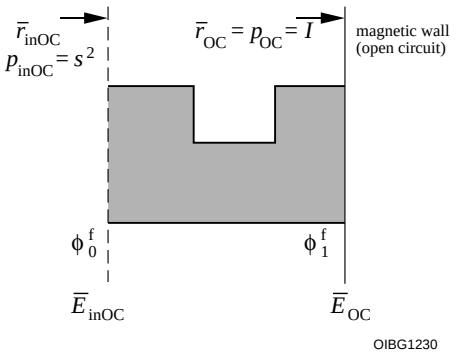

Fig. 1: Transformation of the reflection coefficient to determine Floquet–modes

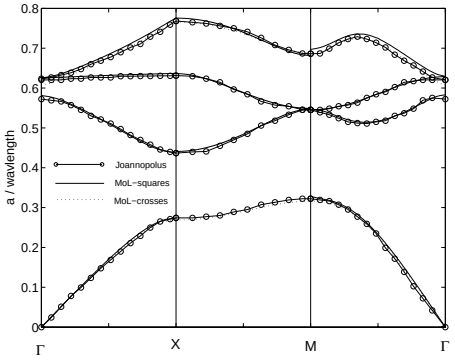

Fig. 2: Computed band structure compared with Joannopoulos [2]

[1] S. F. Helfert and R. Pregla, *J. Lightwave Technol.*, vol. 16, no. 9, pp. 1694–1702, Sep. 1998.

[2] J. D. Joannopoulus, R. D. Meade, and J. N. Winn, *Photonic Crystals - Molding the Flow of Light*, Princton University Press, 1995.

Numerical investigation of holey fibres with polygon shaped holes

Ella Bekker[1], Phillip Sewell[1], Trevor Benson[1], Leonid Melnikov[2]
[1]*School of Electrical and Electronic Engineering, University of Nottingham, UK*
[2]*Physics Department, Saratov State University, Saratov, Russia*

We apply the localized function method to holey fibres with arbitrary polygon shaped holes and demonstrate the applicability and efficacy of the method for modal analysis and investigations of the dispersion characteristics of microstructured fibres with circular, hexagonal and triangular shaped holes.

Keywords: photonic crystal fibre, eigenmode solving, localized function method, dispersion characteristics.

The localized function method [1] is an effective tool for calculating the vector and scalar modes supported by photonic crystal fibres with localized defect. We demonstrate the extension of the method to holey fibre cross-sections with arbitrary polygon shaped holes and general hole shapes that are approximated by linear segments.

The motivation for considering arbitrarily shaped microstructured fibres arises from the need to accurately model the modal characteristics of particular holey fibres [2]. Moreover, although the effects used in photonic crystal fibres are based on the periodical lattice properties, the shape of the holes can also contribute to the holey fibre properties. These shape effects could provide enormous advantages, for example allowing engineering of the bandgap position and shape.

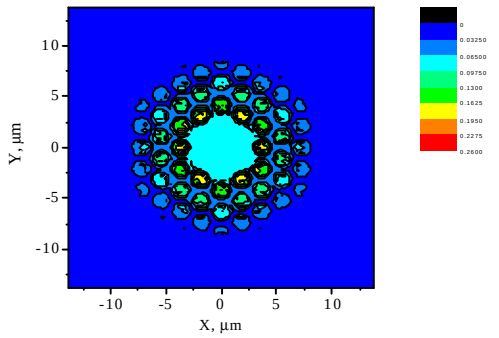

Fig.1. Ey field component in a holey fibre with hexagonal shaped holes (Λ/λ =2., air is fraction 70%.

The basis of the localized function method is to expand the modal field by Hermite-Gaussian functions and to solve the governing wave equations analytically with the aid of a Fourier series representation of the refractive index profile [1]. When solving for the Fourier coefficients we use Green's theorem [3] to take the integrals over the surface of the holes, whose boundaries are described by piecewise linear functions. The method can be considered as an alternative to the finite element method [4]. The principal advantage of the proposed technique is that the Fourier coefficients are found analytically. Once found they can be used directly for calculation at different wavelengths. Furthermore, we will show that the coefficients can be presented in a form that allows different materials and material dispersion to be studied without recalculation of the coefficients. Finally, we note that the Fourier transform coefficients obtained can also be applied within a plane wave expansion method.

As an example the E_y field component of a holey fibre hexagonal holes is shown in Fig. 1. We will demonstrate the flexibility and wide applicability of the method by analysing and comparing the dispersion characteristics of photonic crystal fibres containing circular, hexagonal and triangular holes and combinations of these. We will also show that the use of a rhombic supercell and the related Fourier transform functions are useful for excluding parasitic modes when calculating the guided modes of photonic crystal fibres.

References

[1]D.Mogilevtsev, T.A.Birks, P.St.J.Russell, *J. of Lightwave Techn.*, V.17, N.11, 1999, PP. 2078-2081.
[2]T.M.Monro, D.J.Richardson, N.G,R.Broderick, P.J.Bennett, *J. of Lightwave Techn.*, V.18, N.1, 2000.
[3] W.Kaplan, Advanced Mathematics for Engineers, Addison-Wesley, 1981.
[4] F.Brechet, J.Marcou, D. Pagnoux, and P.Roy, *Optical Fiber Technology* 6, 181-191, 2000.

Modeling of Optical Microcavities in High-contrast index Microwaveguides

Eric Cassan*, Suzanne Laval, and Laurent Vivien
Institut d'Electronique Fondamentale, UMR CNRS 8622, bât. 220, Université Paris-Sud, 91405 Orsay, France
eric.cassan@ief.u-psud.fr

Bragg gratings and optical microcavities are key components to reflect, confine, and filter light in optical integrated circuits [1,2]. In the case of high-contrast index structures, their design needs 3D modeling, although 2D numerical simulations are often performed. In this work, we report a comparison between three-dimensional (3D) modeling, and simplified two-dimensional (2D) and one-dimensional (1D) device modeling of high-index waveguide devices that are obtained from the 3D geometry using the effective index method. They consist of waveguide-based Bragg gratings and optical microcavities, obtained by full etching of narrow slits in strip silicon-on-insulator (SOI) waveguides of different heights and widths.

Results have been obtained using Finite Difference Time Domain simulation (FDTD) [3]. They show that simplified 1D (obtained after top/side or side/top reductions) or 2D (either 2D top-view or 2D side-view) approaches, based on effective-index-reductions, generally fail to give an accurate description of real waveguide device characteristics. In the case of such high-contrast index periodic devices, light propagation is governed by both refractive and diffractive effects in the three dimensions of space. All approaches that try to simplify the problem inherently alter the 3D waveguiding properties, which is both detrimental to the description of multiple-reflected-wave mechanisms, and to the estimate of out-of-waveguide losses. It is found that using simplified approaches, Bragg mirror photonic bandgap is systematically overestimated, and that the whole spectrum is shifted towards higher wavelengths, if compared with results of the full 3D approach. In the case of optical microcavities that have to be designed with a nm-range precision, mistakes in the estimate of the resonance wavelengths up to 50 nm can be obtained between 2D and 3D device modeling, depending on the waveguide geometry.

As a typical example, **Fig. 1** is a plot of power transmittances calculated with all 1D/2D/3D approaches for an optical microcavity formed with a silicon non-etched waveguide region of 0.792 µm length, inserted between two Bragg mirrors with four slits each, to create a defect state in the band gap. Height and width of the considered strip waveguide are 0.2 µm and 0.5 µm, respectively, slit width is 0.1 µm, and the mirror period is 0.288 µm. The mismatch between transmission resonance wavelengths predicted by 2D and 3D FDTD is about 25 nm in the best case.

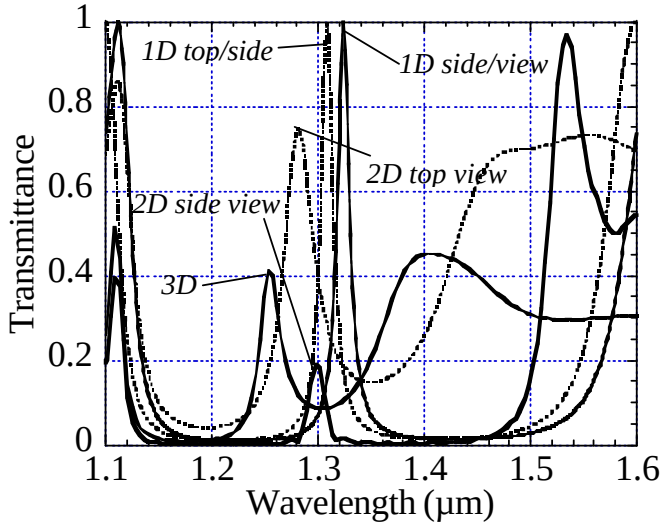

Fig. 1: Power transmittance of an optical microcavity obtained with 8 slits full-etched into a 0.2 µm × 0.5 µm SOI strip waveguide (Λ = 0.288 µm, l_{SiO2} = 0.1 µm, l_{cavity} = 0.792 µm), calculated with several 1D/2D/3D methods.

Acknowledgment

The authors acknowledge Taha Benyattou from the Laboratoire de Physique de la Matière (Lyon, France) for fruitful discussions.

REFERENCES

[1] J. S. Foresi et al., Nature, **390**, pp. 143-145, 1997.

[2] D. J. Ripin et al., Journal of Applied Physics, **87**, n°3, pp. 1578-1580, 2000.

[3] http://www.ise.ch: EMLAB

Optimal Design of Guided Mode Grating Resonance Filters

Gang Bao
Department of Mathematics, Michigan State University, East Lansing, MI 48824,USA

Kai Huang
Department of Mathematics, UC Irvine, Irvine, CA 92697, USA

A novel approach is presented for optimal design of waveguide-grating resonances. Our approach is based a combination of spectral theory and local optimization methods.

Keywords: guided-wave optics, gratings, optimal design

The anomalies of optical diffraction gratings have been of interest since they were originally discovered by Wood in 1902. They manifest themselves as rapid variation in the intensity of the various diffracted spectral orders within certain narrow frequency bands. There are two principal types of anomalous effects: the Rayleigh type which is the classical Wood's anomaly, and the less known resonance type. The Rayleigh type is due to one of the spectral orders appearing (or disappearing) at the grazing angle (propagating along the surface); while the resonance type anomaly is due to possible guided modes supportable by the waveguide grating. We focus on the design of guided mode grating resonance filters (GMGRF).

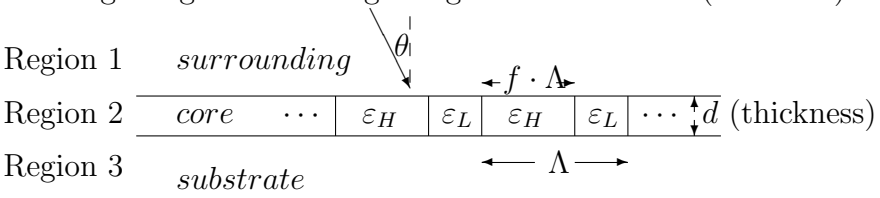

Fig. 1. Waveguide (Single layer)

A conceptual structure representing a GMGRF is illustrated in Figure 1: Region 2 consists of a planar thin film that separates two homogeneous half-spaces. The upper half-space, Region 1, is the "surrounding", while Region 3 is the lower half-space or the "substrate". In addition, Region 2 is required to have a periodically modulated dielectric function and have an average refractive index greater than the refractive indices of both half-spaces.

The basic idea of GMGRF is clear. For a given incident plane wave of wavelength λ, incident angle, and polarization, it is possible to find a grating period Λ such that a diffractive order of the grating couples to a guided mode of the waveguide. By arranging the grating to support only the zero propagating order, energy of the guided mode diffracted out of the core can only lie along the direction of the incident wave, and through this coupling a resonance is established which can lead in principle to 100% reflectance in a very narrow spectral bandwidth. Moreover, the resonant wavelength is determined primarily by the grating period (and the polarization).

With such extraordinary potential performance, these "resonant reflectors" have attracted attention for many significant applications, such as lossless spectral filters with arbitrarily narrow, controllable line width, efficient and low-power optical switch elements, polarization control, and laser technology.

We propose to formulate the resonance problem as an eigenvalue problem or a dissipative problem for determining the scattering frequency, and develop a Newton like method for solving the optimal design problem. Based on useful engineering intuition, a reasonably good initial guess can be chosen which partially explains the rapid convergence of our design method. A numerical example is also given to validate the design approach.

PDL calculation for a Metalised Echelle Grating

André Delâge
National Research Council, Institute for Microstructural Sciences, Ottawa, ON, Canada, K1A 0R6
andre.delage@nrc-cnrc.gc.ca

Kokou Dossou
Département de mathématiques et de statistiques,Université Laval, Québec, Qc, Canada, G1K 7P4

We describe an efficient numerical method to establish the reflectivity of an integrated echelle grating. The modeling is based on a combination of the Finite Element Method and the Rayleigh field expansion. Results show a net polarisation dependence loss (PDL) as a function of the wavelength, due to two factors: a lower reflectivity for the TM field and a shift in its spectral response.

Keywords: optical waveguide theory, numerical modelling, guided-wave optics, echelle gratings, periodic structures, diffraction theory, PDL

Introduction

Echelle grating is considered as a serious candidate for dense wavelength division multiplexers with a large number of channels. The obvious disadvantage of an Echelle grating multiplexer made of glass resides in the fact that the reflectivity of the facets is intrinsically of only few percents. An easy choice for increasing this reflectivity in term of fabrication is the addition of a metallic layer; but the metal on the non-reflecting facets introduces polarisation dependant effects, since the TM and TE polarised light reacts very differently in the presence of metal in its surrounding.

Modeling

We have adapted the method proposed by Petit[1] to the echelle grating using the Finite Element Method inside the grating teeth ($y \le a$) matched to a Rayleigh expansion outside ($y \ge a$). The periodicity of the grating limits our computational window to only one tooth; cyclic boundary conditions assure that field in this region represents the field of an infinite grating. Other boundary conditions impose zero field on the reflecting facet and respectively zero field and zero field derivative on the non-reflecting facet for the TM and TE polarisation. The boundary condition at $y=a$ is not physical and has to be absolutely transparent. This boundary is critical, since it is the matching of the field on its both sides that unambiguously determines the set of Rayleigh coefficients, *i.e.* the coupling of the diffracted field into each possible order.

Results

Fig 1 shows the coupling efficiency into adjacent orders for a grating of order 20 illuminated at normal incidence on the reflecting facet. The perfectly conductive non-reflective facet cannot tolerate a E_y field parallel to it and greatly perturbs the TM polarised light in its vicinity.

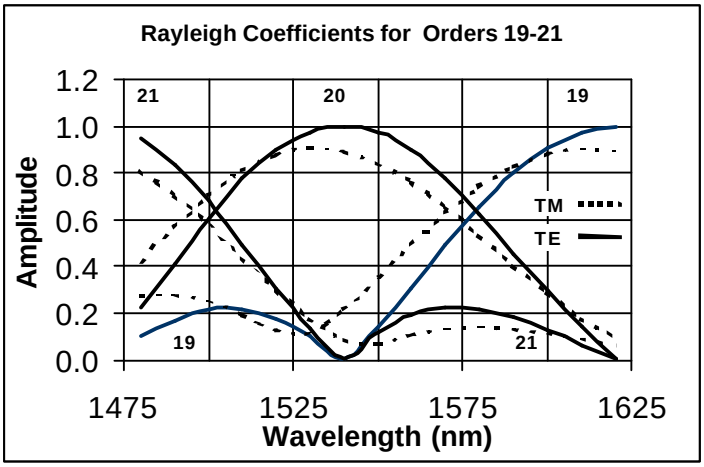

References

[1] R. Petit, "Electromagnetic theory of gratings" ed. by R. Petit, **Springer-Verlag, 1980, Berlin ; New York, Chapter 1**

Grating waveguide resonance makes multilayer resonances sharper

B.A. Usievich, V.A. Sychugov, D.H. Nurligareev, O. Parriaux(*)
Institute of General Physics Moscow, borisu@kapella.gpi.ru
(*) TSI Laboratory, Jean Monnet University, France

Pass band filters are important elements in spectroscopy, in spectrum analysis and WDM communications. The technology of multilayer filters was a few years ago the only one ready to fit the needs and specifications of optical communications. It became soon clear however that multilayer filters would find it increasingly difficult to meet the trend to denser WDM systems with narrower and narrower channel spacing, one of the difficulties being the needed sharpness of the transmission peak.

In its simplest form a pass band filter is a 1st order Fabry-Pérot with two multilayer mirrors. One solution for narrowing the transmission peak without irreasonably increasing the number of layers is to replace one of the multilayers by a resonant mirror comprising a slab waveguide and a coupling grating. It is known that such grating waveguide can exhibit a sharp and close to 100% abnormal reflection when properly designed[(1)]. Such structure appears therefore as a good candidate to act as one of the mirrors of a Fabry-Pérot filter giving rise to a sharp and close to 100% transmission peak. One of the advantages of such structure is that it exhibits a single transmission peak instead of the usual comb of peaks given by a standard Fabry-Pérot filter. Such combination between a multilayer and a grating in one of the layers is not new and such sharp transmission peak was found numerically and reported[(2)].

A purely numerical modelling doesn't however give much insight in the behaviour of this not so simple structure which is actually a combination of two resonators: the grating waveguide and the Fabry-Pérot. We will show that a phenomenological understanding of the combined structure gives much design power. In particular, the quality factor of both resonators must be somehow related for the best performance of the combined filter; this translates into simple rules governing the few phenomenological parameters of the structure. Also, the two coupled resonators must be suitably coupled. We will show that the key parameter responsible for the final filter sharpness is not the amplitude of the reflection peak of the grating waveguide: it is the phase change in the resonance domain. Having realised and prooved this, the design of the structure becomes an easier task where the ultimate performance can be achieved explicitely with a range of dimensional parameters which remains reasonable for manufacturing objectives.

The contribution will describe the rationale of the two resonator structure modelling and give some relevant examples of fabricable structures having filter features matching the demands of DWDM optical communications as well as a new type of laser resonator.

References

1. G.A. Golubenko, A.S. Svakhin, V.A. Sychugov, A.V. Tishchenko, Sov. J. Quantum Electronics, Vol.5, N7, pp. 886-887 (1985)
2. S. Tibuleac, R. Magnusson, Photonics Tech. Lett., Vol. 9, N4, pp. 464-466

Apodisation strength optimisation for linearly chirped Bragg gratings in dispersion compensation applications

Patricia Fernández, Juan Carlos Aguado, Juan Blas, Ramón Durán, Javier Durán, Ignacio de Miguel, Rubén Lorenzo, Evaristo Abril

Department of Signal Theory, Communications and Telematic Engineering, University of Valladolid, Campus Miguel Delibes, 47011 Valladolid, Spain

patfer@tel.uva.es

We present an improved design of linearly chirped gratings for dispersion compensation applications showing the optimum apodisation strength that optimises spectral behaviour parameters as group delay ripple impact, dispersion level and 3 dB bandwidth.

Keywords: numerical modelling, guided-wave optics, periodic structures, Bragg gratings, component design and optimisation

Introduction

Apodised and linearly chirped fibre Bragg gratings are proving to be an effective solution to compensate the chromatic dispersion of dense high bit-rate WDM optical communication systems [1]. In this paper, a series of Bragg grating based dispersion compensators for a typical standard optical link will be modelled and simulated and it will be demonstrated that an apodization factor range between 0.75 and 0.8, for standard optical links between 70 km and 120 km, results in optimum behaviour since it ensures minimum group delay ripple impact [2], minimum dispersion deviation from the required level and maximum bandwidth. As an example, it can be observed in Fig. 1 that the group delay ripple amplitude is minimum inside the optimum range and in Fig. 2 that the dispersion level equals the required value for the same apodisation factors. The influence of the optical link length in the optical behaviour of these devices will be also discussed and taken into account, in order to refine the general rule, given that for shorter distances the optimum strength becomes closer to ~0.75 whilst for longer ones is preferable to choose a_{eff}~0.8.

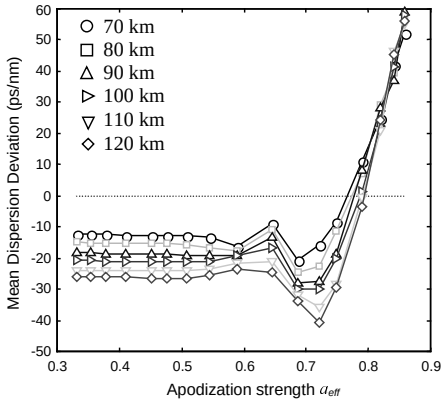

Fig. 1. Deviation of the mean dispersion from the ideal value $D_f \times L_f$ (ps/nm) versus apodisation strength for each DCG.

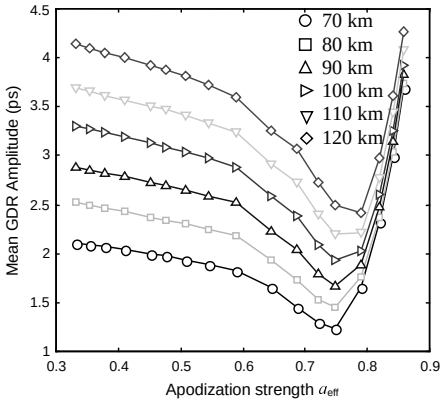

Fig. 2. Mean group delay ripple amplitude versus apodisation strength for each DCG

References

[1] L.D. Garret, A.H. Gnauck, *et al*., *IEEE Photonics Technol. Lett.,* **12**, 356-358, 2000 .

[2] B.J. Eggleton, A. Ahuja, P.S. Westbrook *et al*., *J.Lightwave Tech*., **18**, 1418-1432, 2000

Rigorous modelling of non-linear wavelength-scale structures with mode expansion and spatial index discretisation

Björn Maes, Peter Bienstman, Roel Baets
Department of Information Technology, Ghent University-IMEC, St.-Pietersnieuwstraat 41, 9000 Ghent, Belgium
bjorn.maes@intec.rug.ac.be

We describe a numerical method to accurately simulate the third order Kerr effect in wavelength scale dielectric structures, expanding upon the linear mode expansion method by computing the non-linear refractive index on a spatial grid.

Keywords: numerical modelling, non-linear photonics, Kerr effect

Introduction

The interest in all-optical functions and the high confinement in structures such as photonic crystals or photonic wires, fuels the need for rigorous and efficient field simulations of non-linear effects in integrated components. A lot of attention is paid to the almost instantaneous Kerr effect, giving rise to an intensity dependent index change, allowing very fast processing. In linear materials the mode expansion method for modelling is well established. In such models one divides the structure in longitudinally invariant sections, wherein the field can be described by a superposition of eigenmodes of the local transversal index profile in the section. We expanded this technique, building upon the advanced mode expansion tool CAMFR, developed at our department [1].

Method and results

To incorporate the Kerr effect and thus a spatially dependent index, we divide the nonlinear parts of the structure in small rectangles, wherein we consider a constant index during each iteration. Starting from a certain index distribution, e.g. the linear index, we perform a linear CAMFR calculation, which gives us an intensity distribution. With these intensities and the Kerr index equation, we derive a new index distribution. If this new index distribution equals the previous one, within a certain accuracy, we converged to a solution. If not, we repeat the above procedure.
We confirmed that results are independent from the specific choice of the spatial discretisation grid, if the grid is fine enough. Then we performed simulations on feedback devices which can exhibit bistability above certain input thresholds, such as a Fabry-Perot cavity and a Bragg grating. Our results compare quantitatively with the literature [2,3]. The method is thus capable of calculating the stable solution curves, characteristic of bistability. Convergence to a solution is reached fairly smoothly, though extreme non-linearities have to be handled more carefully.
The main advantage of this method, apart from its rigorous character, is that only the non-linear parts of the device need to be discretised. The linear parts need to be calculated only once, without any additional discretisation. Moreover, we only need to use an index or intensity grid, in contrast with e.g. FDTD, which works with all field components on all points of the grid. With our tool it is thus possible to study generic Kerr-like non-linear structures accurately and efficiently.

References

[1] P. Bienstman, R. Baets, *Opt. Quantum Electron.* **33**(4-5), 327-341, 2001. (CAMFR is freely available at http://camfr.sourceforge.net)

[2] K. Ogusu, *IEICE. Trans. Electron.* **E76-C**(6), 1000-1006, 1993.

[3] W. Chen, D.L. Mills, *Phys. Rev. B* **36**(12), 6269-6278, 1987.

Utilisation of Parallel Processing Techniques to Maximise the Computational Efficiency of an Advanced High-Power Semiconductor Laser Model

James Wykes, James Bonnyman, Phillip Sewell, Trevor Benson, Slawomir Sujecki, Eric Larkins
School of Electrical & Electronic Engineering, University Of Nottingham, Nottingham NG7 2RD, UK
eezjw@gwmail.nottingham.ac.uk

Luis Borruel, Ignacio Esquivias
Dept. Tecnología Fotónica, Univ. Politécnica de Madrid, Ciudad Universitaria s/n., Madrid 28040, Spain

Abstract: To effectively simulate a high-power tapered laser diode, the coupled non-linear optical, electrical and thermal processes that take place in the cavity must be modelled. Modelling each of these processes is computationally intensive; hence parallelisation is implemented to reduce the simulation times.

Keywords: semiconductor lasers, numerical modelling, beam propagation method, parallel processing

Optical fields in a laser cavity are simulated by a full 3D Beam Propagation method (3D-BPM). This is coupled with an electrical-thermal model which calculates the carrier density at transverse 2D slices along the cavity using the drift-diffusion, Poisson, quantum well capture escape, heat generation and thermal conduction equations. The models are coupled via the photon density, refractive index perturbation and gain distributions. An iterative approach is adopted to calculate the photon and carrier density distributions in the cavity on successive round-trips until the optical field at the back facet converges.

If the longitudinal carrier and thermal spreading is ignored, the electrical-thermal slices along the propagation axis are decoupled from each other. Therefore parallel computation of multiple slices is possible, resulting in a drastic reduction of the calculation time for the electrical-thermal parts of the model. It is noted that the coupling method had to be reorganised for optimised use of the parallel facility, since the single processor implementation used a Coupled Solution Method (CSM) [1], whereby the optical and thermal-electrical models are coupled at each slice as the optical propagation proceeds. This was found to offer superior stability and rate of convergence, but does not allow for parallelisation. Hence the parallelised version is restricted to a Separate Solution Method (SSM), whereby the optical and electrical-thermal slices are coupled after a number of optical steps (usually after each optical sweep along the cavity).

Results will be presented to demonstrate the reduction in computation time provided by various parallelisation strategies. Discussion will also be made about issues of stability and rate of convergence brought about by the use of the SSM.

References

1. J G Wykes, S Sujecki, P Sewell, T M Benson, E C Larkins, I Esquivias, L Borruel, *IEE 4th Int. Conference on Computation in Electromagnetics, CEM 2002 (Ref. 02/063)*, 2002.

The authors thank EPSRC and the European Commission for their support under grant references GR/R05741 and IST project no. 1999-10356 respectively.

Transfer matrix and full Maxwell time-domain analysis of nonlinear gratings

Gaetano Bellanca, Alberto Parini, Stefano Trillo
Dipartimento di Ingegneria, Via Saragat 1, University of Ferrara, Italy (strillo@ing.unife.it)

Luca Saccomandi, Paolo Bassi
Dip. di Elettronica Informatica e Sistemistica, Viale Risorgimento 2, University of Bologna, Italy

The transfer matrix approach and the direct integration of full time-dependent Maxwell equations are shown to improve nonlinear distributed feedback structure description and capture new features.

Keywords: nonlinear guided-wave optics, periodic structures, characterization methods

One-dimensional nonlinear periodic structures give rise to a number of intriguing phenomena such as bistability, limiting, self-transparency mediated by gap and forward-resonance soliton propagation. All these phenomena have been demonstrated in optical fibers or planar waveguides [1]. So far nonlinear gratings have been studied using consolidated methods based on the coupled-mode theory (CMT) and its extension using Bloch functions. Here we demonstrate the effectiveness of two different methods such as the transfer matrix method (TMM) [2] or the direct integration of Maxwell equations in time-domain via the finite-difference (FD-TD) technique [3] emphasizing that they have much wider range of applicability than CMT.

The TMM uses proper transfer matrices guaranteing field continuity between homogeneous sections of a stratified medium [2]. TMM is well suited to study the CW grating response and is exact for arbitrary large index changes. Its extension to the nonlinear regime simply requires to change the wavevectors to account for the intensity-dependent refractive index change $n_{2I}I$, being I the field intensity. Though it is often taken for granted that $I \propto |E^+|^2 + |E^-|^2$ (see, e.g., [4]), the correct expression for the total intensity $I \propto |E|^2$ contains a beating term which, being resonant with the period Λ, cannot be dropped. This is also at the origin of discrepancies between CMTs derived from first principles and by continuation of TMM techniques [4, 5]. A correct implementation of the nonlinear TMM technique requires then the calculation of the matrices on a scale much shorter than the grating period Λ. Comparing CMT and TMM results in the stationary limit for the in-out characteristics of a nonlinear grating we found that differences increase abruptly beyond a threshold value for the relative linear index change $\Delta n/n \sim 0.02$, above which the TMM must be taken as the only accurate method.

The FD-TD technique solves numerically the Maxwell equations directly in the time domain with no simplifying hypothesis. FD-TD is intrinsecally suited to investigate the transient behavior and the stability of the field configuration inside the excited structures. We used it to study the following aspects of the grating behavior: (i) bistability; (ii) spontaneous self-pulsing under continuous wave excitation; (iii) impact of third-harmonic generation (or second-harmonic in media with quadratic response); (iv) importantly, trapping of non-propagating (zero velocity in the lab frame) light inside the grating from external pulsed illumination.

In conclusion we have assessed that nonlinear gratings can be effectively studied beyond the simplifying assumptions implicit in the CMT approach, by means of TMM or FD-TD.

[1] M. de Sterke et al. *Spatial Solitons*, S. Trillo and W.E. Torruellas eds., Springer, Berlin, 2001.

[2] A. Yariv and P. Yeh, *Optical waves in Crystals* J. Wiley & Sons, 1984.

[3] A. Taflove, *Computational Electrodynamics: the FD-TD method for Electromagnetics*, Artech House, 1985.

[4] D.E. Pelinovsky, L. Brzozowski, and E. H. Sargent, Phys. Rev. E **62**, R4536-R4539 (2000).

[5] D.E. Pelinovsky, J. Sears, L. Brzozowski, and E. H. Sargent, J. Opt. Soc. Am. B **19**, 43-52 (2002).

Validity bounds of the Coupled Mode equations in a Kerr grating

Arie Irman, Theo P Valkering
MESA+ Research Institute, University of Twente,
PO Box 217, 7500AE Enschede, The Netherlands
t.p.valkering@tn.utwente.nl

Solutions of the Coupled Mode equations for monochromatic waves in the band gap of a Kerr grating are compared with numerically obtained solutions of the Helmholtz equations. Validity bounds of the former equations are obtained in terms of the index contrast of the grating.

Keywords: grating, band gap, coupled mode equations, chaos

Introduction

Monochromatic waves near the first band gap in a 1-dimensional Kerr grating are usually described by the Coupled Mode equations [1] for the slowly varying mode amplitudes A_+ and A_- of two counter-propagating modes $\exp(\pm ik_B z)$. Here $k_B = \pi / d$ is the Bragg wavenumber of a grating with period *d* and *z* is the direction of propagation.

We consider a specific case: standing waves in a multilayer with index contrast ε, and frequency in the band gap (mid-gap). One conclusion is that waves with wavelength (of the envelope) longer than (the order of) $d \times \varepsilon^{-2}$ show irregular features both in phase and in wavelength, that are not covered by the CM equations. A second conclusion is that for values $\varepsilon \gtrsim 0.2$ the CM equations do not apply at all.

These results are interpreted as follows: the Helmholtz equations can be transformed exactly to a set of coupled differential equations of the first order for the amplitudes A_+ and A_-. The resulting equations depend explicitly and periodically on the propagation direction *z*. They consist of two parts, a *z*-independent part and a part that depends on *z* and that has zero average. The CM equations are obtained if one neglects the latter part. The use of these approximate equations can be justified for a shallow grating by the Averaging Theorem, which provides a estimate of the error in terms of the small parameters in the problem [2].

Since the CM equations are autonomous, the resulting trajectories are equilibria, periodic or localized (the gap soliton). The trajectories of the full equations however show irregular, 'chaotic' behavior. Consequences of this property will be explored.

References

[1] C.M. de Sterke, J.E. Sipe, '*Gap Solitons*', in *Prog in Opt XXXIII, E.Wolf (ed),* Elsevier 1994.
[2] J.A. Sanders, F. Verhulst, *Averaging Methods in Nonlinear Dynamical Systems,* Springer, 1985.
[3] R.C. Hilborn, '*Chaos and Nonlinear Dynamics*', Oxford University Press 1994.

Quadridirectional eigenmode expansion scheme for 2-D modeling of wave propagation in integrated optics

Manfred Hammer
MESA$^+$ Research Institute, University of Twente, P.O. Box 217, 7500 AE Enschede, The Netherlands.
m.hammer@math.utwente.nl

Superpositions of two perpendicularly oriented bidirectional eigenmode propagation (BEP) fields, composed of basis modes that satisfy Dirichlet boundary conditions, can establish rigorous semianalytical solutions for problems of 2-D fixed-frequency wave propagation on unbounded, cross-shaped domains.

Keywords: Waveguide optics, numerical modeling, omnidirectional beam propagation, Helmholtz problems.

Intended for devices that consist of sequences of piecewise homogeneous waveguide segments, bidirectional eigenmode propagation (BEP) methods are established as standard tools for 2-D simulations in integrated optics. While the BEP techniques can adequately capture effects like wide angle propagation and backscattering, a common starting point is that one identifies one major axis of light propagation, along which also the interesting input and output waves evolve. The electromagnetic field is expanded into the sets of local eigenmodes, defined by suitable boundary conditions at the ends of a lateral computational window.

While this procedure appears to be adequate for a variety of guided wave problems, in particular for the presently discussed high contrast structures like photonic crystals or microresonator devices the viewpoint of a dominant axis of propagation seems unnatural. In a simulation of e.g. a waveguide crossing as in the figure below, one would expect the propagation along the two coordinate axes to be treated completely identically, with direct access to the four waveguide ports. The presentation will show how this can indeed be realized on a semianalytical level, if one combines two BEP expansions, where for one the horizontal axis is the dominant one, while the other is set up along the vertical axis. Dirichlet boundary conditions (hence real mode profiles and effective mode permittivities) are sufficient to establish solutions of the relevant Helmholtz wave equation on a rectangular computational domain, formed by the overlap of the lateral windows of the two BEP sets, with fully transparent boundaries (exception: the corner points). Modeling simultaneous influx and outflux over all four boundaries is straightforward; the computational effort remains moderate. Since modes propagating in the positive and negative directions along the horizontal and vertical axes play a role, this approach could be called a "quadridirectional eigenmode propagation" (QUEP) method.

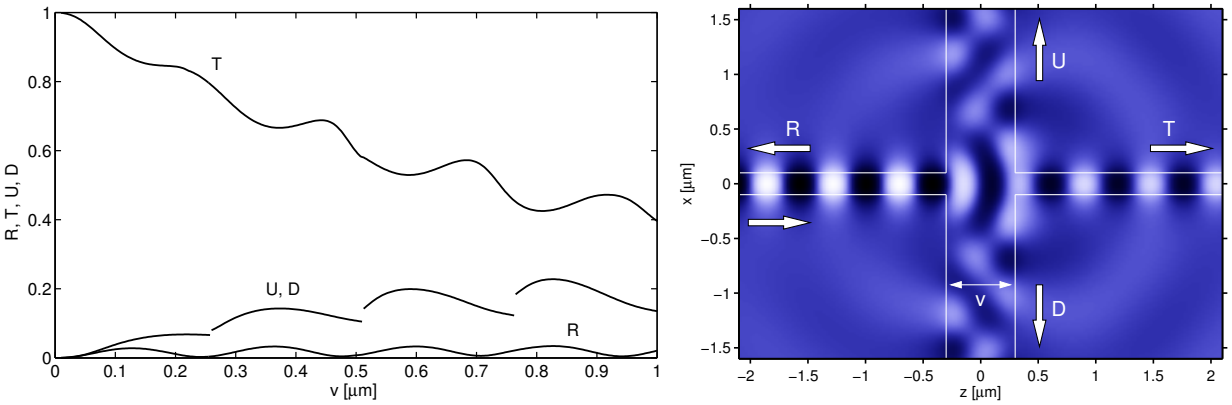

QUEP simulations of waveguide crossings; 100×100 *expansion terms on a* $6\,\mu m \times 6\,\mu m$ *computational window. A horizontal guide (thickness* $0.2\,\mu m$*, refractive indices* 1.45 *and* 3.40*) is intersected by a vertical core of variable width* v*. TE polarized light with wavelength* $1.55\,\mu m$ *is inserted via the fundamental mode of the horizontal waveguide. Left: Dependence of the relative guided power fractions* R, T, U, D *(see annotations) on* v*. Right: Snapshot of the single optical electric field component* E_y*, for* $v = 0.6\,\mu m$*.*

Accurate Finite Element Computation of Full Vectorial Modes in General Optical Waveguides

S S A Obayya, B M A Rahman and K T V Grattan
School of Engineering and Mathematical Sciences
City University London
Northampton Square, London EC1V 0HB, UK
Tel: +44 207 040 8123 Fax: +44 207 477 8568 Email: B.M.A.Rahman@city.ac.uk

Since most photonic devices are designed around optical waveguides, it is a basic and indispensable approach accurately to solve for the modes of these optical waveguides. Thus, there is a particular need for modelling techniques capable of performing accurately the modal analysis of a wide range of both lossless and lossy (or with gain), linear and nonlinear optical dielectric waveguides and also to provide the general complex propagation constants and the full vectorial fields of different modes of such waveguides. On the other hand, the analysis of light propagation in longitudinally varying optical devices has been successfully performed using one of the most common techniques: the beam propagation method (BPM). Since the pioneering work of Feit and Fleck on which the first BPM algorithm, based on the fast Fourier transform (FFT-BPM), was reported, many alternative BPM algorithms have been reported, based on the finite difference (FD-BPM) and the finite element (FE-BPM) approaches. However, most of these BPM formulations are thus far, scalar or semivectorial, these being numerically efficient as they deal with one single field component. However, due to the hybrid nature of the optical waveguide modes, the use of a full vectorial approach is more accurate. In our recent work [1], the authors presented a numerically very efficient, and yet accurate, full vectorial finite element-based beam propagation method (VFEBPM). The formulation is based on the use of the two transverse magnetic field components and the polarisation effects and conversion terms are accurately accounted for by using line integral terms around the part of the element boundary which lies between two different materials. Also, the robust perfectly matched layer (PML) boundary condition is incorporated into the formulation to absorb effectively the radiation waves out of the computational window.

Although the BPM has been seen to be useful to study the wave evolution along longitudinally varying structures, recently, the imaginary distance beam propagation method (IDBPM) also has shown its usefulness as a mode solver of optical waveguides. By propagating an arbitrary starting field along, in general, a complex axis, and with the appropriate selection of the step size, different modes can be sequentially extracted from that starting field. The main advantages of using the IDBPM are that the matrices of the BPM are in general complex, so, lossy (or with gain) waveguides can be treated as conventionally as those that are lossless, without any additional computational effort. Also, the incorporation of an absorbing boundary condition into the BPM algorithm makes it capable of dealing not only with guided modes but also with leaky modes as well. In this paper, the combination of the VFEBPM with the IDBPM is employed for the accurate calculation of the complex modes in general lossless and lossy optical waveguides. Examples presented will include the full vectorial modal analysis results of standard rib waveguide for comparison with results from literature, semiconductor laser waveguide with gain, leaky mode optical waveguide, curved waveguides and nonlinear optical waveguide with and without bistabilities.

[1] S S A Obayya, B M A Rahman, and H A El-Mikati, "New full-vectorial numerically efficient propagation algorithm based on the finite element method", IEEE J. Lightwave Technol., vol. 18, pp. 409-415, March 2000.

A Novel Fourier Based 3D-Full Vectorial Beam Propagation Method

Luque-Nieto, M.A.; Wangüemert-Pérez, J.G.; Molina-Fernández, I.

Dpto.Ingeniería de Comunicaciones, Universidad de Málaga, Campus de Teatinos s/n, 29071 Málaga, Spain
maluque@ic.uma.es, gonzalo@ic.uma.es, imf@ic.uma.es

In this paper a Fourier based Vectorial-BPM with PML absorbing boundary conditions is presented. To test and quantify its performance, the propagation through a strongly-guiding step-index optical fiber is simulated for different initial x and y-excitations.

Keywords: beam propagation method, absorbing boundary conditions, perfectly matched layer, Fourier series.

Introduction

The global numerical methods based on expanding the electric field profile in a finite series of complete and orthogonal basis functions (Fourier [1], Hermite-Gauss [2]) have been successfully applied to the modal analysis of dielectric waveguides. Global methods based on the Fourier series expansion were also originally used to study light propagation by means of the Beam Propagation Method (FFT–BPM), but they have been pushed into the background by other discretisation techniques, such as Finite Element and Finite Differences, which offer a superior performance when dealing with outstanding radiation (first with the use of Transparent Boundary Conditions and later on with the Perfectly Matched Layer absorbing boundary conditions). Even though new works have been recently published to improve the efficiency of this family of methods [3], the fact is that none of them make use of the PML-type boundary conditions or solve the full vectorial propagation problem. In this work a Fourier based full vectorial-BPM method is presented for the first time. This technique makes use of a novel formulation of the vectorial-BPM including PML boundary conditions of coordinate stretching type, followed by a Fourier discretisation of the equations in the transversal direction based on the 'matrix operator' concept [1]. Results obtained for light propagation in a single-mode strongly-guiding optical fibre, under Gaussian x-polarized excitation, are shown in the Figs. 1-3. It can be seen that: i) the vector nature of light is taken into account, ii) an acceptable accuracy is obtained with a reduced number of harmonics, and iii) complete absorption of outstanding radiation is attained by the PML region before reaching the edge of the computational window.

References

[1] J.G. Wangüemert-Pérez, I. Molina-Fernández, *IEEE J.Lightwave Tech.* **JLT-10, Vol.19,** 1614-1627, 2001.
[2] A. Ortega Moñux, J.G. Wangüemert-Pérez, I. Molina-Fernández, *J. Opt. Soc. Am–A*. **JOSA-A**, 557-568, 2003.
[3] M.A. Forastiere, G.C. Righini, *Opt. And Quantum Elect.* **OQE-34,** 559-575, 2002.

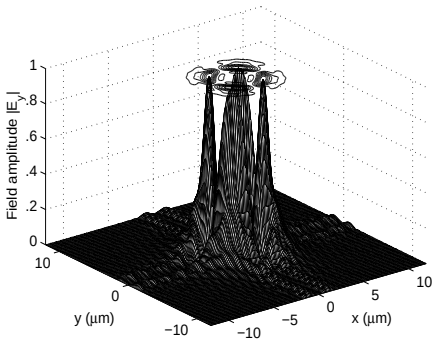

Figure 1. Propagated $|E_y|$ field after z=2000 μm in a high-contrast single-mode step-index optical fiber (n_{film}=1'5, n_{cover}=1). A x-polarized Gaussian profile (spotsize of 1 μm) was used at z=0 as initial field. 32 harmonics have been used in each direction.

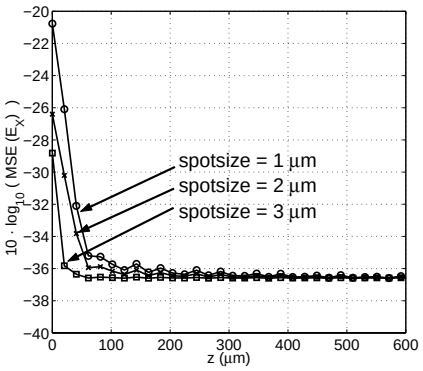

Figure 2. Convergence of the Mean Square Error between the propagated E_x field and the fundamental exact mode (HE_{11}^x) for different x-polarized Gaussian excitations (spotsizes 1-3 μm). Notice that only 16 harmonics has been used in each direction.

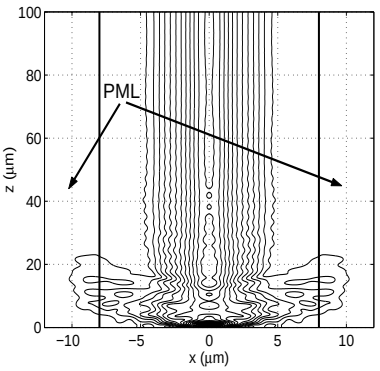

Figure 3. Contour map of the propagated $|E_x|$ field using a 4 μm wide PML for a x-Gaussian excitation (spotsize of 1 μm). The initial radiation is correctly absorbed with 16 harmonics in each direction.

A Wide-Angle Full-Vector Beam Propagation Method Based on ADI Preconditioner

Siu Lit Chui, Ya Yan Lu
Department of Mathematics, City University of Hong Kong, Kowloon, Hong Kong,
mayylu@math.cityu.edu.hk

The beam propagation method (BPM) is a widely used technique for simulation of wave propagation in guided-wave and fiber-optic devices. While the simplest BPM is derived from the slowly varying envelop approximation (SVEA), the more advanced variants are based on rational approximants of the square root operator or the exponential of the square root operator. For three dimensional guided-wave structures, the scalar and semi-vectorial formulations of the BPM are often not sufficient. A full-vector formulation is necessary for polarization-dependent and coupling devices. Most full-vector BPMs developed in the literature are based on the SVEA. In particular, the finite difference SVEA-based BPMs use the ADI (alternating direction implicit) method for efficient marching of the wave fields in the propagating direction.

The limitation of SVEA is well known: it is only accurate for waves propagating in a small angle around the waveguide axis. Wide-angle full-vector BPM can be easily formulated. Let z be the propagation direction, x and y be the transverse variables, the full-vector BPM in terms of the transverse magnetic field $u = [H_y, -H_x]^T$ can be regarded as further approximations of the following ideal one-way equation:

$$\frac{\partial u}{\partial z} = ik_0 n_* \sqrt{1 + X}\, u, \tag{1}$$

where k_0 is the free space wavenumber, n_* is a reference refractive index, X is a 2×2 transverse operator matrix and the time dependence is $e^{-i\omega t}$ for an angular frequency ω. For a step from z_j to $z_{j+1} = z_j + \Delta z$, (1) can be discretized and approximated by

$$u_{j+1} = e^{is\sqrt{1+X}}\, u_j \approx \sum_{k=1}^{p} \frac{a_k}{1 + b_k X}\, u_j = \sum_{k=1}^{p} a_k w_k$$

where $s = k_0 n_* \Delta z$, X is evaluated at $z_j + \Delta z/2$, the propagator $P = e^{is\sqrt{1+X}}$ is approximated by its $[(p-1)/p]$ Padé approximant for an integer p [1] and w_k satisfies

$$(1 + b_k X)\, w_k = u_j. \tag{2}$$

In this paper, we develop an efficient solver for (2). When the x and y variables are discretized by M and N points respectively, X is approximated by a sparse $2MN \times 2MN$ matrix. A direct solver based on Gaussian elimination for banded matrices is very expensive. Modern Krylov iterative methods can certainly be applied to (2), but a good preconditioner is essential. We develop a preconditioner based on the ADI method. In particular, we calculate the optimal parameters used in the ADI iterations. The full-vector BPM based on the efficient algorithm of (2) is then used to calculate the field propagating through a three dimensional Y-branch.

[1] Y. Y. Lu and P. L. Ho, "Beam propagation method using a $[(p-1)/p]$ Padé approximant of the propagator", *Optics Letters*, vol. 27, No. 9, pp. 683-685, May 2002.

Simple High-order Galerkin Finite Element Scheme for the Investigation of Both Guided and Leaky Modes in Axially Anisotropic Planar Waveguides

H.P. Uranus, H.J.W.M. Hoekstra, E. van Groesen
Lightwave Devices Group and Applied Analysis and Mathematical Physics Group,
MESA+ Research Institute, University of Twente, P.O. Box 217, 7500 AE, Enschede, The Netherlands.
h.p.uranus@el.utwente.nl

A simple high-order Galerkin finite element scheme is formulated to compute both the guided and leaky modes of anisotropic planar waveguides with diagonal permitivity tensor. Schemes up to 8^{th}-order of accuracy in the effective index are demonstrated.

Keywords: finite element method, high-order scheme, transparent boundary conditions, leaky modes, guided modes, anisotropic waveguides, arbitrary index profile.

Introduction

Optical waveguides that are made on a high index substrate are particularly interesting. This class of waveguides includes structures made on a semiconductor wafer. Structures that are composed of silicon compounds (silicon oxynitride, silicon nitride, silica, etc.) grown on the top of silicon substrate do not only take benefits from the low cost of silicon wafer, but also share the well developed technologies used by the microelectronics industries, and enable better integration between the optical and electronic circuits. It has been shown that structures made by these materials have a wide range of available refractive indices. Besides, arbitrary refractive index profiles can be made by precise computer control of the fabrication parameters as has been demonstrated by the realization of a rugate filter[1]. This feature gives more degree of freedom in refractive index profile engineering, i.e. tailoring of the refractive index profiles to meet certain desired properties of the waveguide, like bandwidth, mode profiles, phase matching of modes of different wavelengths, etc. Hence, the numerical investigations of this class of structure become important.

The Scheme

In this work, we proposed a simple high-order 1-D Galerkin FEM scheme. By using transparent boundary conditions derived from the Sommerfeld radiation condition and allowing the transverse wave vector to have a complex value, it can allow light to leak into high index substrate/cladding, but decay into low index substrate/cladding, hence able to compute both the guided and leaky modes. The inclusion of Richardson extrapolation and simple mesh-adjustment scheme enable a high order of accuracy to be achieved by using only first-order-polynomial basis functions. The sparse non-linear matrix eigenvalue equation produced by the scheme can be solved using a simple iteration scheme. Hence, it turns out to be very simple, easy to implement, but highly accurate scheme. The method is suitable for leaky planar waveguides of arbitrary index profile with a diagonal permitivity tensor. Schemes up to 8^{th}-order of accuracy in the effective index are demonstrated. Some applications examples including investigations of ARROW structures and buffer-layer optimization of silicon-compounds-based leaky waveguides are demonstrated.

References

[1] S. Lim, S. Shih, J.F. Wager, *Thin Solid Films*, **Vol. 277**, 144-146, 1996.

Modeling of Optical Waveguide Structures with General Anisotropy in Arbitrary Coordinate Systems

Reinhold Pregla

FernUniversität, 58084 Hagen, Germany

Abstract

The algorithm for the analysis of optical waveguide structures is extended to the general case of structures which can be described in arbitrary orthogonal coordinate systems. The materials can have an arbitrary anisotropy. The generalized transmission line equations are extended adequately. Impedance/admittance transfomation formulas are developed. The fulfilment of boundary conditions is described. The proposed algorithm is verified by numerical results.

SUMMARY

Only in special cases optical waveguide devices like integrated circuits have a simple form. An example of a complex planar circuit is shown in Fig. 1. The cross-sections may be multilayered as shown in Fig. 2. The

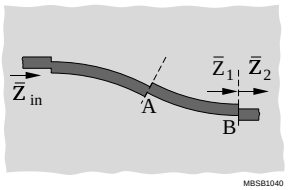

Fig. 1. Optical S-bend: Sections of various curvature are concatenated

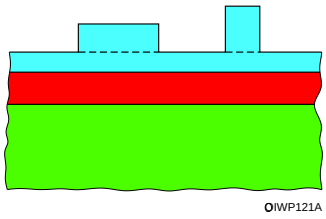

Fig. 2. Cross-section of multilayered optical waveguide

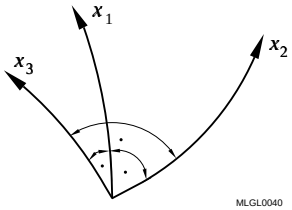

Fig. 3. General orthogonal coordinate system

material of the layers may have a general anisotropic behavior. Generally, such structures can be understood as concatenation of waveguide sections and waveguide junctions. Consequently, the analysis should take into account the propagation through the sections and the scattering at the junctions. A suitable analysis procedure is required to model such devices. Among other methods the Method of Lines (MoL) can be used. In the past efficient and powerful algorithm were developed based on generalized transmission line (GTL) equations and impedance/admittance transfomation for e.g. planar straight and curved optical devices [1][2], fibers [3]. In this contribution the algorithms will be generalized to structures in arbitrary orthogonal coordinate systems and for arbitrary anisotropic materials. It will be shown that the GTL-equations in general orthogonal coordinates (see Fig. 3) with arbitrary anisotropy can be obtained from the equations in Cartesian coordinates by a simple transformation. Furthermore, the difficult problem of boundary conditions in case of anisotropic materials is solved. The results are not only important for the MoL, but also for other eigenmode algorithms and other finite difference algorithms. The proposed algorithm is verified by numerical results.

REFERENCES

[1] R. Pregla, "The impedance/admittance transformation - an efficient concept for the analysis of optical waveguide structures", *Integrated Photonics Research Topical Meeting*, July 1999, Santa Barbara, USA, pp. 40–42.

[2] R. Pregla, "Analysis of Planar Microwave and Millimeterwave Circuits with Anisotropic Layers on Generalized Transmission Line Equations and on the Method of Lines", *2001 URSI International Symposium on Electromagnetic Theory*, Victoria, Canada, May 13-17 2001, paper MN-T06.25.

[3] R. Pregla, "Novel algorithms for the analysis of optical fiber structures with anisotropic materials", *International Conference on Transparent Optical Networks*, June 1999, Kielce, Poland, pp. 49–52.

The Modelling of Generalized Mach-Zehnder Optical Switches and Power Splitters

Laurence Cahill
Department of Electronic Engineering, La Trobe University, Victoria, Australia 3086
l.cahill@latrobe.edu.au

A new matrix model to describe the performance of generalised Mach-Zehnder devices is presented. It is shown that this model leads to useful design formulae for optical switches and variable -ratio power splitters.

Keywords: optical switches, optical power splitters, numerical modelling, guided wave theory

Introduction

Integrated photonic devices that can provide power splitting and switching functions are important components for optical fibre communication systems and integrated optics circuits. Generalized Mach-Zehnder (GMZ) structures [1] can provide these functions.

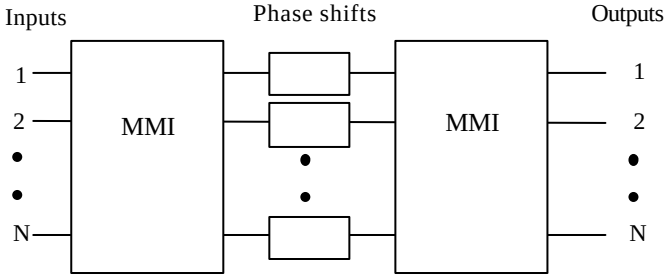

Figure 1. Layout of an NxN GMZ device

New Matrix Model

The overall transfer matrix T relating the output field vector E^{out} to the input field vector E^{in} for the GMZ structure is given ideally by $T = S\Lambda S$, where S is the NxN transfer matrix of each MMI coupler, $\Lambda = diag\ \{p\}$ is the transfer matrix of the phase shifters, with phase factors p.

The essence of this new approach is to expand the overall transfer matrix T so that the output field can be expressed in the form

$$E^{out} = \frac{1}{N}\sum_{n=1}^{N} e_n^{in} A_n p,$$

where e_n^{in} is the *n'th* component of E^{in} and A_n is an NxN matrix.

The unambiguous determination of the phase factor vector p to achieve a variety of optical processing functions becomes a straightforward process once this new matrix formulation is employed. For example, the phase shifts required to establish a switch connection between input port *i* and output port *j* can be found simply from

$$p = N e_i^{in} A_i^{-1} E^{out}, \text{ given } E^{out} = \left[0,0,....e_j^{out}...,0\right]^t.$$

The same process can be used also in the design of variable-ratio power splitters.

Reference

[1] N.S. Lagali, M.R. Paiam, R.I. MacDonald, K. Worhoff, and A. Driessen, IEEE *Lightwave Technol.* **17,** 2542-2550, 1999.

Adaptive Synthesis for Optical Waveguides: CAD or fad ?

C. Styan, A. Vukovic, P. Sewell, T.M. Benson
School of Electrical and Electronic Engineering, University of Nottingham, University Park, Nottingham, NG7 2RD, UK. eexcjs@nottingham.ac.uk

Effective use of multi-dimensional optimisation tools in a general wave guiding problem is investigated. Designs are obtained quickly and efficiently by using multiple robust routines and accuracy variation.

Keywords: Synthesis, Optimisation, Spectral Index, Fibre Coupling, Rib Waveguide, CAD

Introduction

The increasing complexity of optoelectronic components and systems has lead designers to utilise multi-dimensional optimisation tools in product design synthesis. Using global methods such as Evolutionary Algorithms or Simulated Annealing a user defined figure of merit can be minimised over a large problem space, automatically obtaining a structure with desired operating characteristics. We have shown such methods capable of generating useful counter intuitive solutions to practical problems [1]. Modern applications demand highly accurate numerical simulations, which in turn require long simulation times. These simulations are also often prone to instabilities. Both of these factors limit the applicability of standard large heuristic optimisation methods. We will show that adaptive synthesis can be successfully applied in optoelectronic design. However a number of issues, not least accuracy management must be addressed to enable widespread adoption across the field.

Adaptive Synthesis

In this work we exploit the advantages of two simulation routines to produce a novel efficient method of generating rib waveguide designs. Using a semi-analytical method allows a trade off of solution accuracy for runtime. By adaptively altering the accuracy demand as the optimisation progresses the time taken to obtain solutions to user defined accuracy is greatly reduced. The method employed would prove very useful as part of an optoelectronic CAD suite. The Effective Index (EI) method allows initial fast interrogation of the search space giving approximate solutions. Once a minimum is identified the simulation switches to the more accurate semi-analytical Spectral Index (SI) method. Initially though the accuracy demanded is low. As the solutions begin to converge the accuracy management scheme should adaptively alter for optimal performance, using the highest precision in the final stages. This way we investigate the search space quickly, only calculating solutions with high numerical accuracy when they are known to be near a global minimum.

We demonstrate the method applied to the minimisation of coupling losses when coupling to a single mode fibre from a Silicon-on-Insulator (SOI) rib waveguide. This relatively simple example enables us to obtain accurate designs quickly and efficiently. We describe how the principle could be extended further for use with alternative hierarchical simulation schemes and how solutions may be used to seed structures investigated with numerical techniques, resulting in novel, highly effective designs.

[1] P. Sewell, A. Vukovic, and T. M. Benson, "Component Synthesis in Optoelectronics Modelling," *Microwave and Optical Tech. Letters*, vol. 33, 2002.

A Microring Structure for Practical Devices

Andrin Stump, Jens Kunde, Ulrich Gubler, Anne-Claire Pliska-LeDuff, Christian Bosshard
CSEM SA., Untere Gründlistrasse 1, 6055 Alpnach, Switzerland
andrin.stump@csem.ch

We report on simulations of a microring structure that is based on the combination of a low-refractive-index contrast bus-waveguide and a high-index contrast ring-waveguide. The structure provides a better coupling efficiency with an external fiber and relaxes restrictions on the precision in the fabrication process.

Keywords: microring, fiber coupling, fabrication tolerances, optical filter

Introduction

Microrings have been suggested for different kinds of wavelength selective elements, where the small size and the capability for large-scale integration are needed. Waveguides with a large refractive index contrast have to be used for realizing rings with small diameters. However, this approach leads to high coupling losses for butt-coupling to an external standard single-mode fiber and to a very critical coupling between the bus- and the ring-waveguide. These two problems that are due to the small dimensions of the used waveguides are addressed with our proposed structure.

Design and Simulation Results

The most important aspects in the design of the bus- and the ring-waveguide are the phase mismatch in the coupling region as well as the coupling efficiency between the bus and an optical fiber. For efficient coupling with single-mode fibers the bus-waveguide is maximized while still fulfilling the single mode condition. With the chosen materials (see fig.1) a coupling efficiency of 70% is achieved, which is an improvement of ~10dB compared to high index contrast waveguides [1]. The phase mismatch is minimized by raising the effective index in the bus choosing maximized dimensions as well as by lowering the effective index in the ring choosing small waveguide dimensions.

We modelled the structure with a coupled mode theory adapted for non-identical waveguides [2]. This theory shows that the coupling becomes asymmetric between two non-identical waveguides. Although the coupling efficiency is certainly reduced by the asymmetry, it is still strong enough for various applications such as e.g. optical frequency filtering. Additionally, our design is suitable for applications that require large intensities in the ring.

As the coupling coefficient depends exponentially on the separation of the two waveguides, the exact positioning of the ring relative to the bus is very important. In Figure 1 the change of the coupling coefficient as a function of the position is shown. For positioning the ring on top of the bus-waveguides wafer bonding is most often used, where fabrication tolerances of 1 μm can be assumed. Within these tolerances the change of the coupling strength is only 7% in the proposed structure whereas it is more than 55% when using a small bus-waveguide.

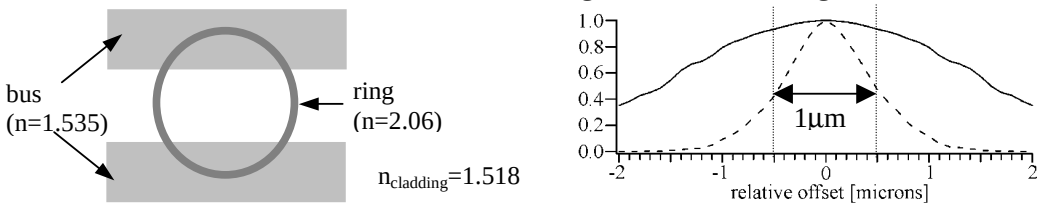

Figure 1 Microring structure with nonidentical waveguides and relative change of the coupling coefficient as a function of the relative position of the ring- and the bus-waveguide (0 = waveguides centered on each other).

[1] W.E. Svendsen, H.T. Philipp, M. Svalgaard, H. Mertens, K.N. Andersen, *Proceedings of ECOC 2002*

[2] S.-L. Chuang, *J. of Lightwave Technology*, LT-5 (1), 5-15, 1987

Design and Optimization of a Velocity-Matched Travelling-Wave Electro-Optic Modulator on InP

Wilfrid Pascher
Elektromagnetische Feldtheorie, FernUniversität, 58084 Hagen, Germany
Wilfrid.Pascher@FernUni-Hagen.de

Jan Hendrik den Besten, Davide Caprioli, Xaveer Leijtens, Meint Smit
Opto-Electronic Devices group, Eindhoven University of Technology
Eindhoven, The Netherlands

Raymond van Dijk
TNO Physics and Electronics Laboratory, The Hague, The Netherlands

An InP Mach-Zehnder modulator is optimized for velocity match between optical wave and microwave and for low loss. Various aspects of the device design are investigated in the modelling using the method of lines.

Keywords: electro-optical devices, method of lines

High-speed modulators are of great interest for 40 Gb/s transmission systems and beyond. In order to enhance the bandwidth and the modulation efficiency in Mach-Zehnder based modulators, a good velocity match between optical wave and microwave must be achieved besides a low microwave loss. This requires both optical and microwave design considerations.

Mach-Zehnder modulators on InP make use of a p-i-n double hetero structure, in which the doping profile ensures an efficient overlap of the optical and electrical field. From a microwave point of view, the p-doped cladding of the optical ridge waveguide should be as narrow and highly doped as possible. This minimizes the microwave attenuation, because the microwaves encounter less damping oscillations in the resistive semiconductor.

However, from an optical point of view, a lower doped and wider waveguide structure is preferred to avoid absorption of the optical carrier. In a previously presented design [1], we favoured a low optical insertion loss over a low microwave loss. Therefore and because of technological limitations at the time, we chose a shallowly etched waveguide. This limited the intrinsic modulation bandwidth to 20 GHz, due to an imperfect velocity match besides a higher microwave attenuation.

In this presentation we investigate a deeply-etched modulator, which is now feasible with our recently enhanced technological capabilities. In a travelling-wave design, a proper velocity-match is of utmost importance, to fully exploit the potential for a wide-band modulator. The use of a deeply etched waveguide eases a velocity match, since the microwave index is reduced and the optical group index is slightly increased. Furthermore, since the capacitance of the modulator transmission line is reduced, its characteristic impedance is increased and accomplishes a better impedance match with a 50 Ω driver. In combination with the above mentioned reduced microwave attenuation, a bandwidth of over 40 GHz is expected for a Mach-Zehnder modulator with deeply-etched arms.

The model structure is analyzed by the method of lines (MoL), which has been efficiently used for the simulation of various planar waveguides in both integrated optics and microwave circuits. A sensitivity analysis is performed in order to evaluate the influence of material parameters, e.g., doping levels, and layer dimensions on the performance of the device.

[1] Wilfrid Pascher, Jan Hendrik den Besten, and Meint Smit, "Modelling and design of a travelling-wave electro-optic modulator on InP," in *Proc. 10th International Workshop on Optical Waveguide Theory and Numerical Modelling*. Apr. 2002, Nottingham, UK.

Polarization Issues in Optical Waveguides and Optoelectronic Systems

B M A Rahman, S S A Obayya, N Somasiri, M Rajarajan, C Themistos, and K T V Grattan

City University
School of Engineering and Mathematical Sciences
Northampton Square, London EC1V 0HB
Tel: +44-20-7040-8123 Fax: +44-20-7040-8568
Email: B.M.A.Rahman@city.ac.uk

Many integrated optical subsystems incorporate guided-wave photonic devices and connecting optical waveguides with two-dimensional confinement and a high index contrast. The modes present in such waveguides and devices are not purely of the TE or TM type but are hybrid in nature, with all the six components of the electric and magnetic fields being present. Polarization issues in silica-based systems, are not negligible, and often create significant problem for optical networks, such as through the polarization mode dispersion (PMD). However, in optoelectronic components and subsystems fabricated in semiconductors, the polarization issue is dominant.

Over the last three decades, may semi-analytical and numerical approaches have been developed to study the modes present in optical waveguide structures: however, to characterize the polarization properties of such systems a fully vectorial approach is necessary. In that respect the fully vectorial **H**-field based finite element method (FEM) is one of the most rigorous and versatile of the approaches that may be considered. The main advantage of the FEM over the many other methods available is it enables a more accurate representation of the waveguide cross-section, using triangles of irregular shapes and sizes. This particular advantage is more significant when waveguides have curved or slanted side walls, or have arbitrary shapes or index distributions. The **H**-field based FEM [1] may be used to obtain both the modes and supermodes of the various types of guided-wave devices.

In an optoelectronic system, when the modes are hybrid in nature, polarization conversion can take place in the optical system, either unintentionally or deliberately at different waveguide junctions. Hence, it is also necessary to obtain the scattering parameters at the butt-coupled junctions between the uniform sections. Often the overlap integral method is used to find the transmission coefficients and a simpler impedance-based approach may be employed to find the reflection coefficients at the junction interfaces. However, it has been shown that the least squares boundary residual method [2], which is fully vectorial and rigorously convergent, can be used to obtain both the transmission and the reflection coefficients of all the polarized modes by considering both the guided and discretized radiation modes of the structures. The beam propagation method (BPM) is field evolutionary in its approach and represents a versatile approach for the characterization of a guided-wave structure, which is continuously or arbitrarily changing its cross-section. A numerically efficient full-vectorial FEM-based BPM approach [3] has been developed to characterize z-dependent photonic devices and optoelectronic subsystems.

Results for the polarization cross-talk in such systems will be presented, along with various approaches to its minimization. Results will also be described for the design optimization of various compact polarization rotators using cascaded sections, with or without a slanted side wall and also with curved waveguide sections. The design of compact polarization splitters using metal clad directional couplers, and using single and double section MMI sections will also be presented, along with the design of the AlGaAs waveguide using a layered core, which supports only a single polarized wave.

REFERENCES

[1] B M A Rahman and J B Davies, 'Finite-element solution of integrated optical waveguides,' *J. Lightwave Tech*., 2, pp.682-688, 1984.

[2] B M A Rahman and J B Davies, 'Analysis of optical waveguide discontinuities, *J. Lightwave Tech*., 6, pp.52-57, 1988.

[3] S S A Obayya, B M A Rahman, and H A El-Mikati, 'New full vectorial numerically efficient propagation algorithm based on the finite element method,' *J. Lightwave Tech*., 18, pp.409-415, 2000.

Integral equation method for studying the resonant spectra of isolated and waveguide-coupled optical microcavities

Svetlana V. Boriskina, Trevor M. Benson, Phillip Sewell
School of Electrical and Electronic Engineering, University of Nottingham, University Park, Nottingham NG7 2RD, UK
eezsb@gwmail.nottingham.ac.uk

Alexander I. Nosich
Institute of Radio Physics and Electronics, National Academy of Sciences of Ukraine, Ul. Proskury. 12, Kharkov, 61085, Ukraine

A boundary integral equation method based on the Green's function technique is developed to compute resonances in arbitrary-shape dielectric cavities. Several 1-5 μm-sized high-confinement optical microcavities are investigated for possible applications as filters and laser resonators for dense wavelength-division multiplexing. TE- and TM- resonance spectra together with Q-factors and FSR are calculated in the 1.55 μm wavelength band.

Keywords: integral equations (IE), Green's functions, optical microcavities, wavelength division multiplexing (WDM), laser resonators, optical waveguide filters

Dielectric microcavities are versatile elements for dense WDM optical systems. They are characterized by a single-mode operation and large free spectral range (FSR). High-Q modes of such microcavities are confined by the nearly-total reflection mechanism. Therefore, their evanescent side-coupling to optical waveguides can be easily achieved. Numerous passive and active photonic devices using microcavities of various cross-section shapes have been demonstrated. They include add/drop filters, demultiplexers, modulators, and microcavity semiconductor lasers.

We present an efficient numerical analysis of the TE- and TM- resonant modes of several practical high-Q high-contrast microresonators in the 1.55-μm telecommunications band. A fast and robust algorithm is developed based on the boundary integral equation formulation of the full wave equations. A set of coupled IEs is derived by applying the Green's theorem and discretized by the Galerkin method with angular exponents as global test and trial functions. The resulting fully discrete scheme has a very high convergence rate, thus enabling fast, accurate and versatile codes to be realised for CAD and optimization purposes. The method developed generates scattering characteristics, complex natural frequencies, and resonance field distributions, such as those of Fig. 1, with higher accuracy than standard mode-matching, FD or MoM procedures.

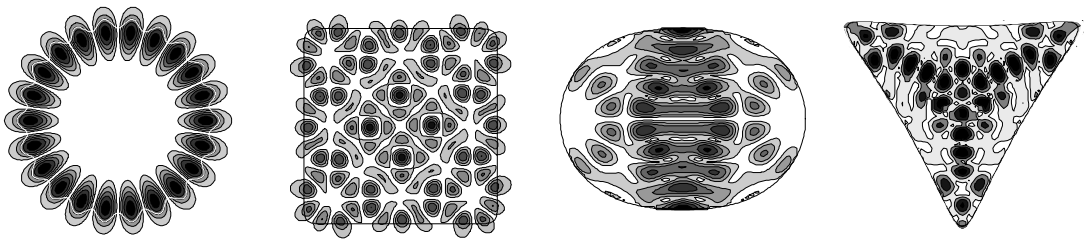

a) b) c) d)

Fig. 1. Near-field intensity patterns of optical microcavities. a) whispering-gallery mode in a microgear cavity; b) volume resonance in a square; c) bow-tie resonance in a quadrupole; d) first-order transverse mode in an equilateral triangle.

An Equivalent Circuit of Partial Reflectors for Circuit Synthesis

Andrea Melloni
*Dip. Elettronica e Informazione, Politecnico di Milano, Via Ponzio 34/5, 20133 Milano (Italy)
melloni@elet.polimi.it

Francesco Morichetti and Mario Martinelli*
CoreCom, COnsortium for Researches in Optical Processing and Switching,
Via G. Colombo 81, 20133 Milano (Italy)

An equivalent circuit of a partial reflector such as a bulk, fiber or waveguide Bragg grating or a defect in PBG waveguide is proposed. The equivalent circuit is of great aid for the synthesis of devices and circuits.

Keywords: circuit synthesis, numerical modelling, photonic crystals, Bragg reflectors

Fiber and waveguide Bragg gratings (Fig. 1a), bulk multilayer and partial reflector in photonic band gap waveguides (Fig. 1b) are usually analysed by means of numerical electromagnetic methods. A great aid in both analysis and circuit synthesis is achieved by transforming the electromagnetic environment into a circuit abstraction described by port-based parameters. For partial reflectors we propose the equivalent circuit shown in Fig. 1c), composed by an ideal partially reflecting mirror (t, r) placed between two sections of propagating regions (L_e, n_B). The equivalent circuit contains only two parameters, r and L_e that can be determined analytically, numerically with classical electromagnetic technique or even experimentally. The parameters are generally wavelength dependent. An important feature of the proposed equivalent circuit is that it is circuit-oriented and permits to access to advanced synthesis techniques of components containing several reflectors. Bandpass filters and dispersion compensating devices based on cascaded gratings can be successfully and easily designed with the aid of the proposed equivalent circuit, without recurring to time and memory expensive optimization procedures. Finally, it is easily combined with port-based models of other components in computer aid design software in order to analyse, design and optimise complex devices, either passive or active and also non-linear, such as slow-wave structures. Examples of the design of a single cavity and multiple cavities circuits that exploit the chromatic dispersion and the reflector dimensions to fulfil the requirements on both the Free Spectral Range (FSR) and the resonant frequency will be given.

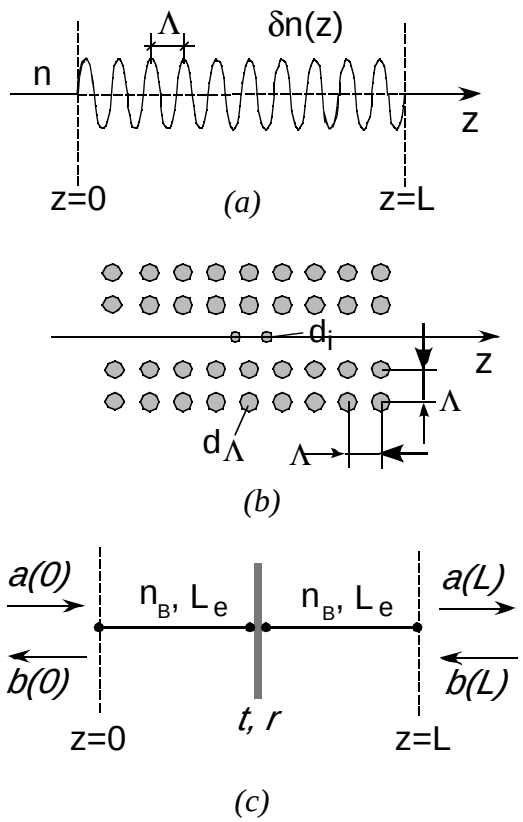

Fig. 1: a) Bragg grating; b) Reflector in PBG waveguide; c) the equivalent circuit

References

[1] A. Melloni, M. Floridi, F. Morichetti and M. Martinelli, "Equivalent circuit of Bragg gratings and its application to Fabry-Perot cavities", *J. Opt. Soc. Am. A, Vol. 20, No. 2, 273-281,* 2003.

[2] R. Costa, A. Melloni and M. Martinelli, "Bandpass resonant filters in photonic crystal waveguides", *IEEE Photon. Technol. Lett*. March 2003.

Numerical Modal Analysis of Silica/Air-Clad Dual-Core Fibres

Vladimir Mezentsev, Sergei Turitsyn
Photonics Research Group, Aston University, Birmingham B4 7ET United Kingdom

Stepan Yakovenko, Sergei Kobtsev, Sergei Kukarin, Nikolai Fateev
Laser Systems Laboratory, Novosibirsk State University, Pirogova 2, Novosibirsk 630090, Russia

A numerical modal analysis is performed of the specially fabricated dual-core tapered fibre.

Keywords: guided-wave optics, dual-core fibre, mode analysis, fibre coupler

Silica/air-clad fibres are promising photonic devices due to extraordinary dispersion and nonlinearity. Supercontinuum SC generation is one of many stunning examples [1]. The properties of the generated SC, as well as its occurrence, are rather sensitive to the interplay between nonlinearity and dispersion. In a recently developed dual-core tapered fibre [2], a new geometry and a new degree of freedom (the core separation) are introduced that can be used to design fibres with optimal characteristics. A dual-core fibre configuration is characterized by the core

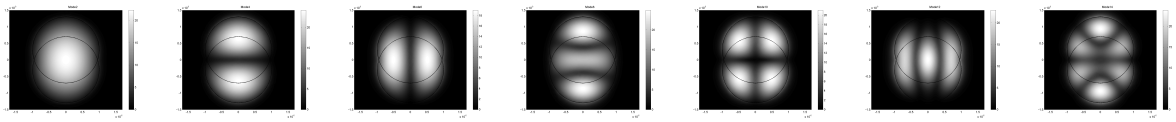

Fig. 1. Mode gallery of the silica/air dual-core fibre

diameter b and distance between the core centres a or aspect ratio b/a. Lowest modes for each configuration have been computed using full vectorial mode simulations. Fig.1 shows examples of the mode profiles.

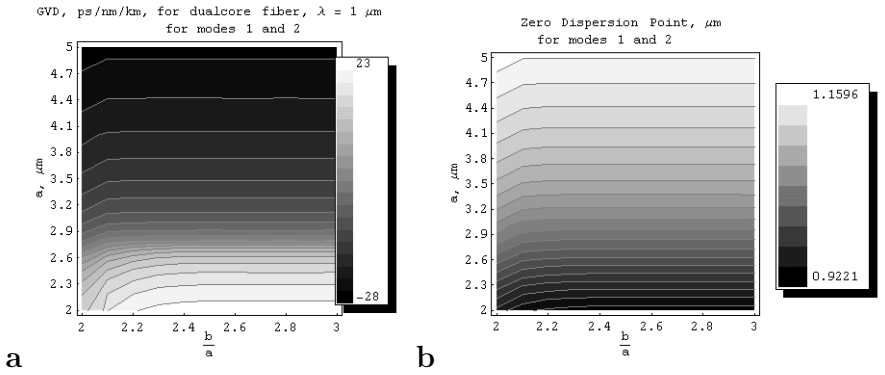

Fig. 2. Group velocity dispersion (a) Zero dispersion point (b) vs aspect ratio and core diameter

Dispersion of the dual-core fibre has also been investigated numerically Several general features can be observed. Smaller core diameter and larger distance between the cores correspond to higher dispersion. Another distinctive property is a noticeable shift of zero dispersion wavelength with variations of the core diameter.

[1] T.A. Birks et al. OECC'2000, PD2-3, pp. 20-21.

[2] S. Kobtsev et al. Quant. Electr., 32 (2002), 11.; S. Kobtsev et al. OFC'2003

Anomalously large reflection of a focused free space beam from a high contrast segmented waveguide under normal incidence

A. Cachard, E. Bonnet, A. Tishchenko, O. Parriaux, X. Letartre(*)
TSI Lab, Jean Monnet University, F-42023 Saint-Etienne, parriaux@univ-st-etienne.fr
(*) LEOM, Ecole Centrale Lyon, F-69031 Ecully
D. Gallagher, Photon Design, Oxford OX4 1TW, UK, dfgg@photond.com

At the Nottingham Workshop in 2002 it was shown that the known effect of abnormal reflection of a plane wave from a grating waveguide[1] also exists for a cylindrically focused incident beam under normal incidence on a high index contrast segmented waveguide. The numerical modelling was performed by means of a FDTD method and the understanding of the coupling mechanism involved was undertaken by resorting to a coupled mode formalism; this showed that the amplitude and sharpness of the resonant reflection increase with the intra-guide coupling coefficient between counterpropagating modes of the segmented waveguide, the latter being obtained by a virtual prism coupling experiment[2].

After some doubts have been raised at the reviewing stage concerning the very existence of this effect for a confined incident beam, a systematic check has been made by means of an eigenmode expansion method which confirmed independently the existence and the properties of this resonance effect. Meanwhile we have also shown that the intra-guide coupled mode interpretation of the reflection mechanism is of limited usefulness as the concerned waveguide modes have a dominant standing wave character. In an attempt to bring more intelligibility in this interesting effect, we have deepened the interpretation drafted at the Nottingham workshop of an interference representation between the three non-evanescent eigenmodes propagating through the grating segments orthogonally to the segmented waveguide plane.

The results of this modelling, their comparison with those given by the eigenmode expansion method will be submitted to the attendance of the next workshop, and examples of applications of the effect will be given and discussed.

Exact Analytical Solution for the local density of Modes in Planar Structures

Hala B. H. Elrofai, H.J.W.M. Hoekstra
Lightwave Devices Group, Faculty of EWI, University of Twenty
H.B.H.Elrofai@el.utwente.nl, H.J.W.M.Hoekstra@el.utwente.nl

Keywords: optical waveguide theory, modeling, guided-wave optics, radiationmodes, spontaneous emission, density of modes.

Summary:
The local density of modes plays a dominant role in spontaneous emission of excited atoms and molecules. Over the years, various papers have been published on spontaneous emission in planar structures [1,2,3], to best of our knowledge no full treatment has been presented so far. In principle exact analytical expressions could be obtained by using Green functions techniques, but these are normally quite cumbersome to evaluate and usually not very transparent. Therefore, it is interesting to look for simple, complete and exact expressions.
Expressions for the local density of modes can obtained by considering the energy flow into radiation and guided modes from a classical dipole positioned in one of the layers. For layered structure the problem corresponds to a inhomogeneous Helmholtz equation with a localized source term. In the presentation it is shown that simple and transparent expressions can be obtained by solving the problem in the Fourier domain.

A presentation of the theory behind the expressions as well as its applications to some interesting structures will be given during the workshop.

References
[1] Martijn Wubs, A. Lagendijk, Phys Rev E. vol. 65, 046612, 1-12.
[2] Danae Delbeke, Ph.D thesis, university of Gent, 2002.
[3] W. Lukosz , phys. Rev. B, vol. 22, 3030-3038, 1980.

Posters

Poster 1 **M. Montecchi, E. Nichelatti, R. M. Montereali, M. Piccinini, and F. Somma**
ENEA, Advanced Physical Technologies Department, Rome, ITALY
INFN-LNF, Rome, ITALY
University of Rome, Department of Physics, Rome, ITALY

Poster 2 **L. Kotačka, H. J. W. M. Hoekstra, and J. Čtyroký**
Optiwave Corporation, Ottawa, ON, CANADA
University of Twente, MESA+ Research Institute, Department of Applied Physics, Enschede, THE NETHERLANDS
Institute of Radio Engineering and Electronics, Academy of Sciences of the Czech Republic, Prague, CZECH REPUBLIC

Poster 3 **N. Sakhnenko and A. Nerukh**
Kharkov National University of Radio Electronics, Kharkov, UKRAINE

Poster 4 **L. N. Illyashenko, A. I. Nosich, T. M. Benson, and P. Sewell**
Institute of Radio-Physics and Electronics NASU, Department of Computational Electromagnetics, Kharkov, UKRAINE
The University of Nottingham, School of Electrical and Electronic Engineering, Nottingham, UK

Poster 5 **J. Kašpar, I. Richter, and P. Fiala**
Czech Technical University in Prague, FNSPE, Prague, CZECH REPUBLIC

Poster 6 **W. C. L. Hopman, R. M. de Ridder, P. Pottier, and R. M. de la Rue**
University of Twente, MESA+ Research Institute, Lightwave Devices Group, Enschede, THE NETHERLANDS
University of Glasgow, School of Electrical and Electronic Engineering, Glasgow, UK

Poster 7 **A. G. Nerukh, F.V. Fedotov, T. M. Benson, and P. Sewell**
University of Nottingham, School of Electrical and Electronic Engineering, Nottingham, UK

Poster 8 **N. Ruzhytska, A. G. Nerukh, and D. Nerukh**
Kharkiv National University of Radio Electronics, Kharkov, UKRAINE
University of Cambridge, Department of Chemistry, Cambridge, UK

Poster 9 **A. V. Tishchenko, O. Parriaux, and D. Neuschäfer**

Jean Monnet University, TSI Lab, Saint-Etienne, FRANCE
Novartis Pharma AG, Basel, SWITZERLAND

Poster 10 **P. Peterka, B. Faure, W. Blanc, M. Karasek, and B. Dussardier**
Université de Nice - Sophia Antipolis, Laboratoire de Physique de la Matičre Condensée CNRS, Nice, FRANCE
Institute of Radio Engineering and Electronics, Academy of Sciences of the Czech Republic, Prague, CZECH REPUBLIC

Poster 11 **A. V. Tishchenko**
Jean Monnet University, TSI Lab, Saint-Etienne, FRANCE

Poster 12 **E. Romanova and S. Gaal**
Saratov State University, Department of Physics, Saratov, RUSSIA

Poster 13 **N. E. Nikolaev and V.V. Shevchenko**
Peoples' Friendship University of Russia, Department of Radiophysics, Moscow, RUSSIA

Poster 14 **V. Němeček, I. Richter, P. Fiala, and J. Kratochvil**
Czech Technical University in Prague, FNSPE, Prague, CZECH REPUBLIC

Poster 15 **M. Novák, I. Richter, and P. Fiala**
Czech Technical University in Prague, FNSPE, Prague, CZECH REPUBLIC

Poster 16 **L. Prkna, J. Čtyroký, and M. Hubálek**
Institute of Radio Engineering and Electronics, Academy of Sciences of the Czech Republic, Prague, CZECH REPUBLIC

Poster 17 **N. P. Yeung, E. Y. B. Pun, and P. S. Chung**
City University of Hong Kong, Department of Electronic Engineering, Hong Kong, HONG KONG

Poster 18 **E. I. Smotrova, A. I. Nosich**
Institute of Radio-Phisics and Electronics NANU, Kharkov, UKRAINE

Poster 19 **H. V. Baghdasaryan, T. M. Knyazyan, and A. A. Mankulov**
State Engineering University of Armenia, Fiber Optics Communication Laboratory, Yerevan, ARMENIA

Poster 20 **H. Alatas, A. A. Iskandar, M. O. Tjia**
Institut Teknologi Bandung, Dept. of Physics, Bandung, INDONESIA
University of Twente, Faculty of Applied Physics, Enschede, THE NETHERLANDS

Poster 21 **J. Prawiharjo, A. A. Iskandar, M. O. Tjia, and E. van Groesen**
Institut Teknologi Bandung, Dept. of Physics, Bandung, INDONESIA
University of Twente, MESA+ Research Institute, Enschede, THE NETHERLANDS

Poster 22 **A. Bertolani, A. Cucinotta, M. Fuochi, F. Poli, S. Selleri, and M. Zobo**
University of Parma, Dipartimento di Ingegneria dell'Informazione, Parma, ITALY
University of Modena and Reggio Emilia, Dipartimento di Ingegneria dell'Informazione, Modena, ITALY

Increase of refractive index induced by absorbing centres: homogeneous and inhomogeneous line-broadening cases

Marco Montecchi, Enrico Nichelatti
ENEA – C.R. Casaccia, Advanced Physical Technologies Dept.
Via Anguillarese, 301 – 00060 Rome, Italy
nichelatti@casaccia.enea.it

Rosa Maria Montereali
ENEA – C.R. Frascati, Advanced Physical Technologies Dept.
P.O. Box 65 – 00044 Frascati (Rome), Italy

Massimo Piccinini
INFN-LNF, Via E. Fermi, 40 – 00044 Frascati (Rome), Italy

Fabrizia Somma
Physics Dept. and UdR INFM, Roma Tre University
Via della Vasca Navale, 84 – 00146 Rome, Italy

Besides extinction coefficient, refractive index of a dielectric medium is modified by presence of absorbing centres. Analytical expressions of the overall complex refractive index dispersions are derived for homogeneous and inhomogeneous mechanisms of absorption-line broadening.

Keywords: refractive index, dispersion, absorption, optical waveguides

Absorbing centres in a dielectric medium contribute to the overall dielectric permeability with an additive dielectric-susceptibility term [1]. Under the assumptions that the centres can be considered as elementary two-level quantum systems and that all the centres are identical, this additive term is [1]

$$\varepsilon_0\chi(E) = \varepsilon_0 \frac{\chi_0\,\Delta E_0}{E_0 - E + \mathrm{i}\,\Delta E_0}\,, \tag{1}$$

where ε_0 is the dielectric constant of vacuum, $\chi(E)$ is the dielectric susceptibility of the centres, E is the photon energy, χ_0 is the amplitude at the peak absorption energy, E_0, and ΔE_0 is the half width at half maximum (HWHM) of the imaginary part of $-\chi(E)$, which has a Lorentzian lineshape. This case corresponds to the homogeneous broadening mechanism of the absorption line. The additive term displayed in Eq. (1) increases the overall refractive index of the medium volume containing the centres at photon energies $E < E_0$ [1]; in the case of four-level systems, this increase of refractive index can be exploited to confine the Stokes-shifted radiation emitted by the centres, so that active waveguiding applications can be foreseen [2].

In this contribution, the *analytical* expression of $\chi(E)$ is derived also for the case of inhomogeneous broadening of the absorption line (Gaussian lineshape). The derivation starts from elementary considerations regarding the statistical distribution of the peak absorption energy for a collection of centres that are not identical. This approach permits also to derive *analytical* expressions of $\chi(E)$ for intermediate cases (Voigtian lineshape), which are usually tackled with integral or approximate expressions, between the limiting cases of homogeneous and inhomogeneous broadening. It is shown that the refractive index is increased at energies $E < E_0$ even for Gaussian and Voigtian lineshapes, therefore confirming the possibility of waveguiding applications. The Kramers-Kronig relations are discussed in this framework, too.

Examples involving colour centres in lithium fluoride (LiF) are reported.

[1] M. Montecchi, E. Nichelatti, A. Mancini, R.M. Montereali, *J. Appl. Phys.* **86**, 3745-50, 1999.

[2] R.A. Nunes, H.J. Kalinowski, S. Paciornik, A.M. De Souza, L.C. Scavarda do Carmo, *Nucl. Instr. Meth. Phys. Res. B* **32**, 222-224, 1988.

Length Dependence of the ČSHG in Planar Waveguides: Critical Assessment

Libor Kotačka,
*Optiwave Corp., 7 Capella Court, K2E 7X1 Ottawa, ON, Canada (also with *)*
libor.kotacka@optiwave.com

Hugo J. W. M. Hoekstra,
Light Devices Group, Department of Applied Physics, MESA+ Research Institute, University of Twente, Box 217, 7500 AE Enschede, The Netherlands.

Jiří Čtyroký
**Institute of Radio Engineering and Electronics AS CR, Chaberská 57, 182 51 Praha 8, Czech Republic*

The behaviour of the Čerenkov regime SHG (ČSHG) conversion efficiency in planar waveguides is numerically investigated with a respect to the propagation length. The variations of the propagation length exponent from a value close to zero to a quadratic dependence is analysed for three-layer planar waveguides as the function of the guide thickness and the pump wavelength.

Keywords: second harmonic generation, Čerenkov regime, optical planar waveguides, length dependence, SHG conversion efficiency

This contribution is based on our recent theoretical observations [1-3] reporting variations in dependence of the ČSHG on the interaction length. It was thought [4] that the ČSHG conversion grows *just* proportionally with the interaction length everywhere inside the so-called Čerenkov region [1, 2, 5]. We have however shown [2, 3] that the $L^{3/2}$ dependence occurs only under very specific circumstances of the sharply peaked ČSHG conversion efficiency [5]. The study [3] generalised the length dependence behaviour for a "bulk" Gaussian beam SHG interactions and took this even further predicting *continuous* transition from linear to quadratic dependence of the interaction length on the Čerenkov angle. The most recent study [1] presented comprehensive treatment of this phenomenon. Using Fourier domain analysis [1] the conversion efficiency approximately obeys the following formula (terms not neglecting on L omitted for the brevity)

$$P_{2\omega}(L) \approx CL^2 \int_0^K Sinc^2\left[\left(\sqrt{K^2 - k_{x,3}^2} - \beta_s\right)L/2\right] dk_{x,3} \,,$$

with C being a constant and L is the interaction length. $K = 4\pi n/\lambda$, where λ is the wavelength of the pump radiation, n is the nonlinear substrate refractive index for the SH frequency. β_s is the SH field propagation constant, $k_{x,3} = \sqrt{K^2 - k_z^2}$ with $k_z \in \langle 0, K \rangle$. Few realistic waveguide arrangements are investigated similarly to [1] and [5] including four SHG regime categories demarcation (e.g. pure ČSHG regime etc.). When analysing $P_{2\omega}$ behaviour with respect to the interaction length, a role of several structural parameters as the pump wavelength, the guide thickness, and refractive indices values (and their desired accuracy) on the L-dependence is depicted. The origin of the limiting cases, e.g. the (quasi)quadratic dependence for short devices and the linear dependence inside the classical ČSHG region is explained.

References

[1] H.J.W.M.Hoekstra, J.Čtyroký, L.Kotačka, *J.Lightwave Technol.* (accepted Sept. 2002).

[2] J.Čtyroký, L.Kotačka, *Opt.Quant. Electron.* **32**, 799-818, 2000.

[3] L.Kotačka *et al.*, *Proc. ECIO'01*, April 4-6, 2001, Paderborn 325-328, 2001.

[4] H.Tamada, *IEEE J. Quantum Electron.* **27**, 502-508, 1991.

Dielectric Resonator with Time-Varying Parameters

N. Sakhnenko, A. Nerukh
Kharkov National University of Radio Electronics14 Lenin Ave., Kharkov, 61166, Ukraine
E-mail: nataliya_sakhnenko@rambler.ru

A model of a dielectric resonator which material properties change in time is investigated by the Volterra integral equation method allowing to combine analytical and numerical approaches. The resonator has a form of a circular cylinder and the electromagnetic field is represented in a polar system of coordinates. The resonance properties are investigated and the expressions for the field inside the resonator as well as outside of it are obtained.

Keywords: dielectric resonator, time-varying medium, integral methods in time domain.

The main goal of our research is the study of electromagnetic field propagation through nonstationary media in rigorous mathematical manner on basis of Volterra integral equation approach. In this paper we consider what happens with a plane wave with harmonic time dependence propagating through a dielectric with time varying permittivity. Variation of time varying properties is modeled by changing in time the dielectric permittivity inside a cylinder of finite radius. The cylinder is restricted by two perfectly conducting plates that simulates semiconductor layers of very high conductivity. Analytical solution is obtained for the case when the dielectric permittivity changes abruptly.

Corresponding integral equation [1] in cylindrical system of coordinates originates from the formulation of the problem via Maxwell's equations by virtue of the Green's function [2]. Evolutionary method for handling transient electromagnetic problems is used. According to this approach the solution procedure is separated into two stages: solution of the initial (unbounded) problem, i.e. that permittivity changes in the whole space; then construction of the resolvent operator that corresponds to the influence of the cylinder boundary using an already found solution of the unbounded problem.

The solution is obtained in the form of Laplace representation whose isolated singularities define the wave form. Residue in one of them gives well known solution of plane wave scattering problem on dielectric cylinder, others describes the new features connected with transients.

Exact solution for abruptly changing of permittivity allows numerical evaluating for arbitrary time dependence of dielectric permittivity inside the cylinder.

References

[1] A.G. Nerukh, I. V. Scherbatko, M. Marciniak. *Electromagnetics of Modulated Media with Applications to Photonics.* Warsaw 2001.

[2] N. Sakhnenko, A. Nerukh, "Transient Axially Symmetric Radiation of Source in a Plane Waveguide", *Kharkov National University Digest*, special issue on Radio-Physics & Electronics, KNU Press, ¹ 467, 2000, pp. 144-147 (in Russian)

Modeling of 2D Photonic Crystals by Using the Method of Integral Equations

Lyudmila N. Illyashenko, Alexander I. Nosich
Institute of Radio-Physics and Electronics NASU, 12, Proskury Str., Kharkov, Ukraine
lyusi@vil.com.ua

Trevor M. Benson, Phillip Sewell
School of Electrical and Electronic Engineering, University of Nottingham, United Kingdom

2D photonic crystals with arbitrarily shaped rods are considered. An Integral Equation method is used for the numerical modeling of both crystal waveguides and coupled defect resonant cavity filters formed in these photonic crystals. Results indicate a strong dependence of filter characteristics on rod shape.

Keywords: Photonic Crystals, Photonic Bandgap structures, Numerical Modeling, Boundary Integral Equations, Analytical Regularization, arbitrary polygonal cross-section.

Introduction

Photonic Crystals are very important for modern technology. These structures can be devised to have a photonic bandgap, i.e. a band of frequencies that cannot propagate through it and are mainly used for suppression of radiation of light source into unwanted directions, where it is blocked by forbidden band of the surrounding photonic crystal. Much current interest is in quasi-2D optical systems formed by etching arrays of cylinders filled with air or another low-index material into a semiconductor slab waveguide [1]. The Method of Lines was considered in [2] for modeling the inverse problem, i.e. 2D photonic crystals consisting of square dielectric rods in air. In this paper we use the Method of Integral Equations [3] combined with the Method of Analytical regularization [4] to develop highly accurate models of 2D photonic crystals comprised of dielectric rods of arbitrary polygonal cross-section.

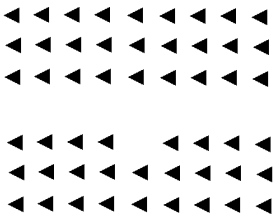

Fig.1: Geometry of the problem

Method of solution

We formulate the problem in terms of boundary integral equations by presenting the field inside the rods and the field outside as single layer potentials. By satisfying the boundary conditions the problem is reduced to a system of integral-differential equations. A Galerkin Method of Moments is used to obtain a system of linear algebraic equations, which is solved numerically with arbitrary pre-established accuracy. The equations and the method of solution of the key scattering problem for a single dielectric polygonal cylinder are considered in [5]. Single pillars or whole rows of pillars can be removed from the photonic crystal structure without affecting the solution algorithm. In this way, the field distribution in channel (line defect) waveguides can be calculated and the properties of resonant cavity coupled to these straight waveguides investigated. The method considered does not have any restriction on angles of wave incidence, refractive index of materials, shape and position of rods. The set of obtained results indicate that there is a dependency of all the basic properties of 2D PCs on the rod shape and configuration of the structure.

[1] H. Benisty, C. Weisbuch, *at al.,* Optical and confinement properties of two-dimensional photonic crystal, *J. Lightwave Technol.,* vol.17, pp. 2063-2077, 1999.
[2] A. Barcz, S. F. Helferd, R. Pregla, Modeling of 2D Photonic Crystals by Using the method of Lines, Proc. International conference ICTON 2002, pp. 45-48.
[3] D. Colton, P. Kress. *Integral Equation Methods in Scattering Theory*, Wiley, NY, 1983.
[4] A. I. Nosich, Method of an analytical regularization in wave scattering and eigenvalue problems, IEEE Antennas & Propagation, Vol. 41, No. 3, pp. 34-45, 1999.
[5] L.N. Illyashenko, A.I. Nosich and T.M. Benson, Integral equation analysis of a polygonal semiconductor microcavity, *Proc. Int. Conf. NUSOD 02,* Zurich, 2002, pp. 72-73.

Modeling special properties of subwavelength structures with effective medium theory

Jan Kašpar, Ivan Richter, and Pavel Fiala

Czech Technical University in Prague, Faculty of Nuclear Sciences and Physical Engineering, department of Physical Electronics, Břehová 7, 115 19 Praha 1, Czech Republic

A software tool for modeling special properties of subwavelength structures with use of approach based on effective medium theory is presented. Polarization-selective and color-selective characteristics of several high space frequency gratings (HSFG) and an optical multilayer with embedded HSFG are also studied.

Keywords: high-spatial frequency grating, effective medium theory, form birefringence, artificial anisotropy, numerical modeling, diffraction grating analysis, thin films, photonic crystals

High spatial frequency gratings (HSFG) and other optical devices composed of subwavelength structures (SWS) form an important part of diffractive optics. They are also of large interest throughout the field diffractive and waveguide optics. SWS are characterized by a very small period with respect to wavelength ratio, i.e. in such a case only zero diffraction orders are diffracted (reflected / transmitted), and thus such structures exhibit characteristic properties. These special properties of HSFG and other SWS can be simulated with our modeling tool based on the effective medium theory (EMT) which we developed in MATLAB environment within the diploma project [1]. Difficult and time consuming computations of this problem by rigorous methods are effectively compensated with effective medium theory. EMT is an approximate approach based on electromagnetic formulation of diffraction problem in HSFG. Within EMT assumptions, a grating profile / modulation is shown to have properties of a homogenous thin film with form birefringent characteristics. The diffraction problem is thus converted to interference problem of electromagnetic waves on an optical thin layer or multilayer system to obtain the final solution for reflection / transmission. We have implemented two modifications of EMT; noted EMT-R (originally developed by Rytov [2]) and EMT-L (a general profile modification of classical EMT using the Fourier series according to Lalanne [3]). Both of them employ multilayer approach, implemented into 2x2 matrix method [4]. As an example, simulations of color-selective properties of several HSFG are presented, using our programs developed with GUI (EMT 1D ANALYZER, EMT 2D ANALYZER). Also, numerical properties of our implementations have been tested. Moreover, combination of EMT with 2x2 matrix method offers new possibilities in modeling optical multilayer structures with embedded HSFG. Polarization-selective effect of such structures has been simulated using our MULTILAYER ANALYZER. Application of the EMT and the 2x2 method to the photonic band gap structure simulations can also be highlighted. Under some restrictions, EMT can thus provide approximate numerical modeling tool for band gap structure properties.

References

[1] J. Kašpar, Analysis of high spatial frequency gratings with effective medium theory, *Diploma thesis* (in Czech), CTU Prague, 2003.
[2] M. Rytov, Electromagnetic properties of a finely stratified medium, *Soviet Physics JETP* **2**, 466-475, 1956.
[3] P. Lalanne, D. Lemercier-Lalanne, On the effective medium theory of subwavelength periodic structures, *Journal of Modern Optics* **43**, 2063-2085, 1996.
[4] P. Yeh, *Optical waves in layered media*, A Wiley-Interscience, USA, New York, 1988.

Experimental Verification of Modelling Results of Deeply Etched Bragg Gratings

Wico C.L. Hopman, René M. de Ridder
Lightwave Devices Group, MESA+ Research Institute, University of Twente, P.O Box 217, 7500 AE Enschede, The Netherlands, phone +31 534894440, W.Hopman@uwtente.nl, R.M.deRidder@utwente.nl

Pierre Pottier, Richard M. de la Rue
Optoelectronics Research Group, Dept of Electronics and Electrical engineering, University of Glasgow, G12 8QQ, Scotland,UK, R.delaRue@elec.gla.ac.uk, Pottier@elec.gla.ac.uk

Deeply etched Bragg gratings having 20 or 150 periods have been fabricated and characterized using both a white light source and a tuneable laser in the visible. The results have been compared with COST268 [1] and additional modelling results.

Keywords: guided-wave optics, photonic crystals, periodic structures, characterization, gratings

A photonic crystal (PhC) slab is a thin high-index dielectric slab waveguide patterned with a periodic structure of holes. A PhC slab waveguide is a quasi 2-dimensional (2D) structure: the slab acts as a dielectric waveguide confining the light in the third dimension by total internal reflection. Light propagating through a PhC slab may be diffracted out of the plane of periodicity. Full modelling of these losses would require 3D calculations, requiring often prohibitive amounts of computing power. However, it is expected that a quasi 1D structure (in this case a grating, deeply etched into a slab waveguide) can serve as a model for calculating the out of plane diffraction losses [1]. In order to check the validity of such models, we have fabricated and characterised such gratings, having periods down to 190 nm using direct e-beam writing and reactive ion etching.

Both fabricated gratings (20 and 150 periods long), have been characterised using two light sources: a broad spectrum light source (fig.2) and a tuneable dye laser (fig.3) for measuring the transmission (note the different horizontal scales). The simulation results (FDTD) for two different etch depths of the groove are shown in figure 1. The results confirm the expected stop band, and the oscillatory behaviour in the transmission bands. There are however discrepancies that might be attributed to fabrication imperfections, additional modelling or fabrication improvements are required to verify this. More modelling (BEP) and experimental results will be presented in the poster presentation.

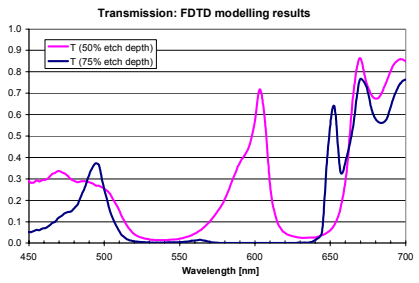

Fig.1 FDTD calculation: Λ=0.19µm, 20 periods d_{core}=0.21µm, n_{subs}=1.46, n_{core}=2.01, n_{clad}=1.

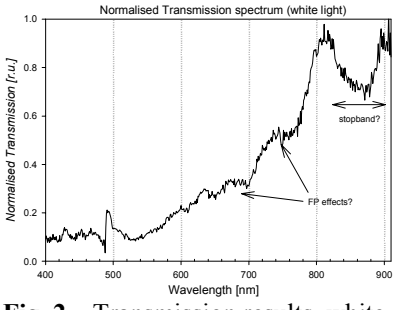

Fig. 2 Transmission results, white light; Λ=0.27µm; groove depth about 75% 20 periods.

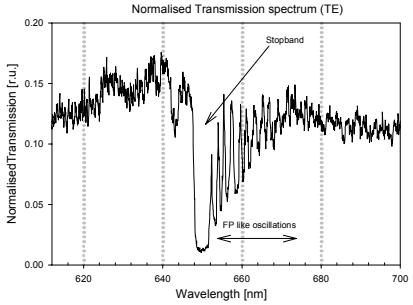

Fig.3 Transmission results, tuneable laser; Λ=0.19µm; groove depth about 75%,150 periods.

[1] J. Čtyroký, S. Helfert, R. Pregla, P. Bienstman, R. Baets, R.M. de Ridder, R. Stoffer, G. Klaasse, J. Petráček, P. Lalanne, J.-P. Hugonin, R. M. De La Rue, *Optical and Quantum Electronics*, vol. 34, pp. 455-470, 2002.

Analytic-Numerical Approach to Nonlinear Problems in Dielectric Waveguides

A. G. Nerukh, F.V. Fedotov, T. M. Benson, P. Sewell
School of Electrical & Electronic Engineering, University of Nottingham, University Park, Nottingham, NG7 2RD, UK, eezagn@gwmail.nottingham.ac.uk

A combined analytic-numerical approach, based on the resolvent method for the Volterra integral equation, is presented for investigations of electromagnetic signal propagation in waveguides containing a nonlinear medium.

Keywords: dielectric waveguide, nonlinear medium, integral methods in time domain.

According to the approach described in [1] the behaviour of an electromagnetic field in a dielectric waveguide is given by the resolvent operator

$$\mathbf{E}(t,\mathbf{r}) = \mathbf{F}(t,\mathbf{r}) + \int_{t_n}^{\infty} dt' \int d\mathbf{r}' \hat{R}_n(t-t',\mathbf{r},\mathbf{r}')\mathbf{F}(t',\mathbf{r}') \qquad (1)$$

where t_n is the initial moment and the term $\mathbf{F}(t,\mathbf{r})$ is determined by the prehistory of the field prior to t_n. The resolvent operator can be found exactly in the case when the medium properties jump in time. This renders the non-linear problem solvable by approximating the time-varying properties of the non-linear medium by a set of time step functions. This means that the permittivity is equated to $\varepsilon_n = \varepsilon_d + \chi_{NL}^{(3)} E_{n-1}^2 = const$ over the n-th time interval, which starts at time t_n. Here, ε_d is the linear permittivity inside the waveguide, $\chi_{NL}^{(3)}$ is the non-linear susceptibility and E_{n-1} is the field magnitude at the end of the previous interval $[t_{n-1}, t_n]$.

In the context of the approximation adopted, the formula (1) gives the exact solution to the problem of the transformation of an electromagnetic field in the waveguide with a non-linear material in the core. Such an approach explicitly takes into account the influence of the waveguide walls as well as the changes in the medium properties. Replacing the continuously changing non-linear medium parameters by jump changes is the only approximation in this algorithm.

The expressions for the resolvent for a planar dielectric waveguide were obtained in [2] where it was shown that there are time-spatial zones that are not influenced by the waveguide boundaries and near-boundary zones where the influence of the waveguide boundaries is taken into account exactly by the additive terms in the resolvent. The condition on the duration of time interval $[t_{n-1}, t_n]$ when these zones are separated is obtained.

Illustrative results will be presented by calculation of a short pulse transformation in a plane non-linear waveguide when there is no restriction on the pulse width, the parameters of the waveguide, nor the magnitude of the non-linearity.

References

[1] Nerukh A.G. and Khizhnyak N.A, *Modern problems of transient macroscopic electrodynamics* (in Russian), Test-Radio Publ., Kharkov, 1991.
[2] A. Nerukh, T. Benson, in *Proc. of 2002 4th Int. Conf. on "Transparent optical networks",* April 21-25, 2002, Warsaw, Poland, Vol. 1.

Dependence of Electromagnetic Signal Complexity on Medium Disturbances

N. Ruzhytska, A. Nerukh
Kharkiv National University of RadioElectronics,14 Lenin Avenue, Kharkov, 61166, UKRAINE: E-mail: rzhtsk@ums.kharkov.ua
D. Nerukh
Unilever Centre for Molecular Informatics, Department of Chemistry, University of Cambridge, Lensfield Road, Cambridge, CB2 1EW, UK

The influence of the medium disturbances on the complexity of electromagnetic signal is considered. The disturbances have the form of rectangular pulses, the magnitudes and durations of which do not have any restrictions.

Keywords: Electromagnetic transients, integral equations in time domain, time-varying medium.

The influence of a single sharp disturbance of a medium on a signal is known [1]. Subsequent changes of the medium make the picture very complex the details of which depend strongly on the number of the modulation disturbances, their intensity, and duration.

The following model is considered. A primary electromagnetic signal in the form of a Gaussian pulse $E_0 = \exp(-(t - x/v)^2 / 4\eta^2)$ exists before zero moment of time. Starting at zero moment the medium permittivity changes under the action of the external forces in the form of finite packet of repeating cycles. Transformation of the primary signal is investigated and the complexity of the transformed signal is calculated. The complexity calculation is done in the framework of Crutchfield's 'computational mechanics' approach [2] by the procedure described in [3]. The signal shape and its complexity after two cycles of medium modulation for the case of $a = \sqrt{\varepsilon / \varepsilon_1} = 0.75$, where ε and ε_1 are the undisturbed and the disturbed permittivity respectively, is shown in Fig. 1. The complexity of the transformed signal reaches high magnitudes in the wide range of the durations of the modulation cycles.

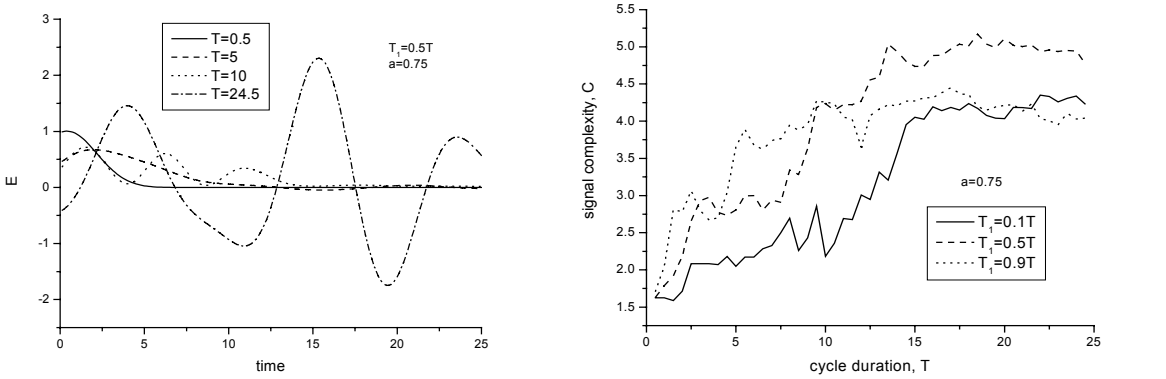

1) 2)

Fig.1. Signal shape after two cycles of the medium modulation (1), and dependence of the signal complexity on the cycle duration T for various durations T_1 of the disturbance interval (2).

References

[1] F. R. Morgenthaler, *IRE Transactions* **MTT-6**, 167, 1958.
[2] J. P. Crutchfield, K. Young, *Phys. Rev. Lett.*, **63,** 105-108,. 1989.
[3] D. Nerukh, G. Karvounis, R. C. Glen, *J. Chem. Phys.*, **117**(21), 9611-9617 (2002).

Waveguide grating coupling of a 2D focused beam under normal incidence : a phenomenological approach

A. V. Tishchenko, O. Parriaux, D. Neuschäfer*
University Jean Monnet, TSI Laboratory, 23 rue Paul Michelon, F-42023 Saint-Etienne
e-mail : tishchen@univ-st-etienne.fr
* Novartis Pharma AG, CH-4004 Basel
e-mail: dieter.neuschaefer@pharma.novartis.com

The coupling of a 2D focuced beam under oblique incidence into a grating waveguide was solved by means of a coupled wave formalism where the phenomenological parameters are given by a simple plane wave diffraction analysis [1]. This approach was shown to give correct results even in the presence of a strong grating on a high index contrast waveguide. This work was intended to be the first step towards the solution of the practically more interesting but more intricate coupling problem of a narrowly focused free space beam under normal incidence.

The proposed contribution will similarly describe a coupled wave representation where the phenomenological parameters are determined by a plane wave diffraction analysis. It will be shown that under the same hypotheses of large grating strength and high index contrast the usual formalism of coupled propagating modes does not provide a correct electromagnetic representation of the coupling event. It will be shown that the guided modes which must be considered in the situation of normal incidence are coupled waves exhibiting features of standing wave as well as a propagating character. The plane wave diffraction analysis of the poles corresponding to these modes reveals their interesting properties and helps to establish the suitable phenomenological representation of the coupling event.

The aim of this approach was to find out the conditions for maximum light confinement in a grating waveguide in the perspective of the high efficiency excitation of a high density pixellated array of biosensor sites.

Reference

1. A. V. Tishchenko, M. Hamdoun, and O. Parriaux “Two-dimensional coupled mode equation for grating waveguide excitation by a focused beam”, Opt. Quantum Electron. Special Issue on Workshop WTNM, Nottingham, April 2001.

Theoretical Modelling of S-band Thulium-Doped Fibre Amplifiers

Pavel Peterka[1,2], Basile Faure[1], Wilfried Blanc[1], Miroslav Karasek[2], Bernard Dussardier[1]
peterka@ure.cas.cz

[1]*Laboratoire de Physique de la Matière Condensée CNRS - Université de Nice - Sophia Antipolis, Parc Valrose, 06108 Nice, France*
[2]*Institute of Radio Engineering and Electronics AS CR, Chaberská 57, 182 51 Praha 8, Czech Republic*

A comprehensive numerical model of a Tm-doped silica fibre is presented. The model is used for predicting the S-band amplifier performance under different pumping schemes.

Keywords: fibre amplifiers, fibre lasers, numerical modelling, optical fibres

The thulium-doped fibre amplifiers, TDFA's, are promising candidates for the telecommunication S-band (1460-1530 nm), the next logical frontier for optical amplification following the C- and L-band (1530-1565 nm and 1570-1610 nm, respectively) already covered by the erbium-doped fibre amplifiers, EDFA's. A majority of the TDFA modules is based on fluoride Tm-doped fibres, which results in difficulties with fabrication and robustness of the host material. Furthermore, the fusion splicing to standard telecommunication fibre is impossible. This necessitates the use of butt mechanical splices that are comparatively lossy and prone to damage under high power pumping. These limitations have spurred the development of alternative host materials [1]. Recently, gain of 12 dB [2] and more than 20 dB [1] was reported for a silicate glass host.

In spite of an extensive experimental effort in the field of TDFA's within the last ten years, there is a lack in detailed theoretical analysis of the amplifier performance by means of comprehensive numerical models that were successfully adopted in EDFA optimisation. To the author's knowledge, only in Ref. [3] such a model was presented.

In this paper we present a comprehensive, spectrally and spatially resolved numerical model of the TDFA. In contrary to the referenced model [3], the energy transfer between neighboring atoms, the silica fibre host and various pumping schemes are considered. The longitudinal evolution of the signal and pump radiation is obtained by an iterative solution of propagation equations and laser rate equations. Since many radiative and nonradiative transitions are involved, a set of laser rate equations is more complex than that of erbium. In transversal direction, the interaction of the optical radiation field with the Tm ions is modeled using spectrally dependent overlap factors that take into account the real refractive index profile of the fiber and the distribution of dopants. The spectroscopic and waveguide parameters used in the model were measured in the Tm-doped preforms and fibres made in LPMC Nice. Some of the spectroscopic parameters were also carefully selected from the literature or calculated using Judd-Ofelt analysis. The model is used for predicting the S-band amplifier performance under different pumping schemes and for optimisation of the pump wavelengths.

References

[1] J. Minelly and A. Ellison, "Applications of antimony-silicate glasses for fiber optic amplifiers," *Optical Fiber Technology*, 8(2): 123-138, 2002
[2] B. Cole and M. L. Dennis, "S-band amplification in a thulium doped silicate fiber," *OFC'01*, Anaheim, Los Angeles, USA, TuQ3, 2001
[3] W. J. Lee *et al.*, "Study on the pumping wavelength dependency of S^+ band fluoride based thulium doped fiber amplifiers," *OFC'01*, Anaheim, Los Angeles, USA, TuQ5-1-4, 2001

The Generalized Source Method: a fast numerical method for the analysis of 2D waveguide gratings

A. V. Tishchenko
University Jean Monnet, TSI Laboratory, 23 rue Paul Michelon, F-42023 Saint-Etienne
e-mail : tishchen@univ-st-etienne.fr

2D layered structures are of great interest for the in-situ monitoring of processes in the future developments of microelectronic technologies. The operating conditions are such that the direct problem must be solved very quickly for the optimising algorithm aimed at solving the inverse problem to retrieve the profile of 2D diffractive structure in real time.
It will be shown that the Generalized Source Method [1] is a good candidate for meeting the demands on computing speed and accuracy because

- unlike more popular techniques it tackles 2D structures with the same algorithm as 1D structures;
- in a "S-matrix" formalism, the exact calculation of each S-matrix takes no longer than to compound this S-matrix with other S-matrices.

The proposed contribution will describe the method and give comparative results with a known reference method.

1. A. V. Tishchenko, "Generalized source method: New possibilities for waveguide and grating problems", Opt. and Quantum Electron. **32**(6/8) 971-980 (2000).

Feasibility of the Slowly Varying Envelope Approximation in simulations of light scattering on step-like discontinuities of dielectric waveguides

Elena Romanova
Saratov State University, Astrakhanskaya 83, 410026 Saratov, Russia
romanova@optics.sgu.ru

Scabolcs Gaal
Essent Energy Trading B.V., Hertogenbosch, the Netherlands

Modal field scattering on step-like discontinuities of planar waveguides is simulated comparatively by the Finite-Difference Beam Propagation Method and the Green's Function Method.

Keywords: light scattering, dielectric waveguides, numerical simulations

Recently, due to the progress in non-linear glass materials, it became possible to design all-optical guiding devices consisting of segments exhibiting different non-linear properties [1,2]. Transmittance of such structures is intensity dependent and can be controlled by an appropriate adjustment of their geometry. Accurate simulation of spatial transient process resulting from light scattering on discontinuities is a critical point here. The Finite-Difference Beam Propagation Method (FD-BPM) is commonly used now to model light propagation in non-linear guiding structures. The Slowly-Varying Envelope Approximation (SVEA) reduces the problem to the one-way propagation and numerical solution of relatively simple paraxial wave equation.

The purpose of this work is to estimate validity of the SVEA in modelling of linear mode scattering on a step-like discontinuity of dielectric planar waveguide. For comparative simulations we use the Green's Function Method (GFM) based on the total field approach (as well as the FD-BPM) however free of the SVEA. Rigorous implementation of the GFM is relatively complicated and require solution of an infinite set of equations. However, if just the forward propagating field is taking into account, the problem can be simplified to evaluation of just one-dimensional integrals. Physical reason for such one-way treatment is that the refractive index contrast of an optical waveguide is usually small so that the reflected field can be neglected.

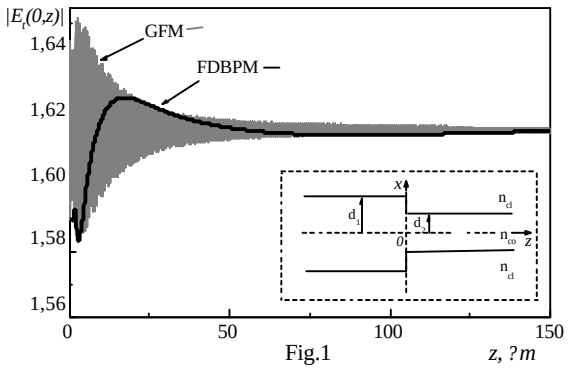

Fig.1

In our numerical experiments, single-single and single-bimodal transformations of the input TE modal field have been considered. For comparison, transverse and longitudinal distributions of the total field $E_t(x,z)$ and the radiation field $E_{rad}(x,z)= E_t(x,z)-E_{mod}(x,z)$ have been calculated, as well as power flow and signal spectrum. Our results show that, $E_{rad}(x,z)$ can be simulated quite accurately by the FD-BPM if the field divergence is small. However the FD-BPM provides rough approximation to the GFM solution for $E_t(x,z)$ (Fig.1) because interference of the guided mode field $E_{mod}(x,z)$ and non-paraxial components of $E_{rad}(x,z)$ is not accounted for in the paraxial model. This doesn't influence linear transmittance of the structure, however accurate evaluation of the non-linear transmittance which is determined, for example, by the values of $n_K|E_t(x,z)^2|$ for a Kerr medium, becomes questionable if the SVEA is applied.

[1] L. Brzozowski, E.H Sargent: *IEEE Journ. of Quant.Electron*. **36**, 5-8, 2000.
[2] E.V.Bekker,E.A.Romanova,L.A.Melnikov,T.M.Benson,P.Sewell, *Appl. Physics B*, **B73**, 531-534, 2001.

On Capability and Accuracy of Shift Formula Method as Applied to the Problem of Synthesis of Graded-Index Planar Waveguides

N.E. Nikolaev
Radiophysics Dept.
Peoples' Friendship University of Russia,
Mikluho-Maklaya str., 6, Moscow, 117198, Russia
nnikolaev@sci.pfu.edu.ru

V.V. Shevchenko
Institute of Radioengineering and Electronics
Russian Academy of Sciences
Build. 7, Mokhovaya str. 11, Moscow, 101999, Russia
sto@cplire.ru , fax: (7-095) 2038414

The paper consider the capabilities and accuracy of Shift Formula Method as applied to the synthesis of graded-index planar waveguides. The advantage of Shift Formula Method is shown, compared with other methods.

Keywords: gradient index optics, planar waveguides, optical waveguides, refractive index, shift formula method

It is of great importance to determine the refractive-index profile of a planar waveguide. The accuracy of profile reconstruction and the number of initial data needed depend on the form of the profile. Besides the method used for this purpose is also important. The well-known WKB-method [1] gives good results for refractive-index profiling of multi-mode waveguides and fails when applied to single-mode waveguides.

We use the Shift Formula Method (SFM) [2] which can be applied to single-mode waveguides, and besides has some advantages over the other methods. It uses very convenient mathematical model [3–6] to describe a refractive-index profile. This model is suitable for representation of smooth profiles such as gaussian profile, complementary-error function profile and many others. As far as profile is characterized by its peak index, depth, and shape at least three effective indexes are required for the profile reconstruction. To obtain these values of effective indexes for single-mode waveguide it is possible to measure effective indexes for the waveguide with different external refractive indexes. We show that this technique allows to find the exact refractive-index profile.

Compared with similar technique used with other methods [7], the Shift Formula Method allows to reconstruct the waveguide profile using less external effective indexes, and besides with more accuracy.

[1] J.M. White and P.F. Heidrich, *Appl. Opt.*, **15**, 151–155, 1976.

[2] V.V. Shevchenko, *Sov. J. of Commun. Technology and Electronics.*, **31**, 28, 1986

[3] N.E. Nikolaev and V.V. Shevchenko, *J. of Commun. Technology and Electronics.* **42**, 837, 1997,

[4] N.E. Nikolaev and V.V. Shevchenko, *J. of Commun. Technology and Electronics.* **43**, 651, 1998.

[5] N.E. Nikolaev and V.V. Shevchenko, *Proc. 9th Intern. Workshop on Optical Waveguide Theory and Numerical Modelling, April 6–7, 2001, Paderborn, Germany.*

[6] N.E. Nikolaev and V.V. Shevchenko, *Proc. 10th Intern. Workshop on Optical Waveguide Theory and Numerical Modelling, April 5–6, 2001, Nottingham, UK*

[7] K.S. Chiang, C.L. Wong, S.Y. Cheng, and H.P. Chan, *J. Lightwave Technol.*, **18**, 1412–1417.

Analysis and design of waveguide grating couplers

Václav Němeček, Ivan Richter, Pavel Fiala, and Jan Kratochvíl

Czech Technical University in Prague, Faculty of Nuclear Sciences and Physical Engineering, department of Physical Electronics, Břehová 7, 115 19 Praha 1, Czech Republic

Keywords: waveguide grating coupler, numerical modelling, perturbation method, iterative method, grating theory,

Our scope of work concentrates on the analysis and design of waveguide grating couplers. By analyzing a waveguide grating coupler we mainly mean to determine the attenuation factor □ which dictates how much the incident guided wave is attenuated. So far we have implemented two effective simulation methods: the perturbation method and the iterative method. The perturbation method is the one having the least accuracy yet gaining practically usable results for many cases of practical interest. The iterative method is, in fact, an extension to the perturbation method since it uses its results to solve the wave equation more precisely. We present a software tool WGC (WAVEGUIDE GRATING COUPLER) developed for analysing and designing such grating couplers based on these methods. The methods have been put together inside a complex design system with graphical user interface (Matlab environment) that enables to observe parametric dependencies. Moreover, for comparison purposes, the design system calculates theoretical values of diffraction efficiencies of thin gratings. Finally, we plan to use this computer design system to create waveguide grating couplers with gratings recorded in a thin film of photoresist on a glass plate.

PBS Solver – a software tool for calculating photonic band structures of 2D dielectric photonic crystals based on plane-wave method

Miroslav Novák, Ivan Richter, and Pavel Fiala

Czech Technical University in Prague, Faculty of Nuclear Sciences and Physical Engineering, department of Physical Electronics, Břehová 7, 115 19 Praha 1, Czech Republic

Keywords: plane-wave method, two-dimensional photonic crystals, dielectric photonic crystals, photonic band gap, numerical modelling

We present a software tool developed for calculating photonic band structures of two-dimensional dielectric photonic crystals (2D-PhC). Program is based on standard plane-wave method (PWM) and can be applied to various 2D-PhC structures (various definitions of lattice as well as objects, including their combinations). Two approaches are used for the calculation, analytical method for simpler structures and numerical FFT method for general and more complex structures. Defining new structures (structure editor, k-points editor), setting computational parameters and data management is very easy by using powerful Matlab®'s graphical user interface. Program allows computing of one-dimensional parametric dependencies and thus offers optimisation of the structure for various parameters. The validity of computation was verified using the MPB code [1]. Several interesting examples of calculated spectra will be shown and discussed.

References

[1] S. Johnson and J. D. Joannopoulos, "Block-iterative frequency-domain methods for Maxwell's equations in a planewave basis," *Optics Express* **8**, 173-190, 2001.

Microresonator As a Photonic Structure with Complex Eigenfrequency

Ladislav Prkna, Jiří Čtyroký, Milan Hubálek
Institute of Radio Engineering and Electronics AS CR, Chaberská 57, 182 51 Praha 8, Czech Republic
prkna@ure.cas.cz

Analysis of microresonators is usually based on inherently leaky bent waveguides. More straightforward approach is to characterize microresonator as a lossy resonant structure with complex eigenfrequencies. Propagation of waves with complex frequency in optical waveguides is analyzed. Using this approach it is clearly seen that microresonator radiates not only in radial but also axial direction.

Keywords: microresonator, optical waveguides, leaky modes, complex frequency

Introduction

The analysis of a rotationally symmetric microresonator in the form of a rib waveguide or a disk is usually based on eigenmodes of a bent waveguide. Rotational symmetry of the structure implies that the mode field distribution in a radial direction is generally described in terms of Bessel functions with both complex order ν and argument ρ. The longitudinal phase factor $\exp(ik_0 n_{eff} z)$ for the case of straight waveguide is substituted with the azimuthal dependence $\exp(i\nu\varphi) = \exp(ik_0 n_{eff} R\varphi)$. Leaky character of the eigenmode due to radiation leads to complex n_{eff} and thus to complex ν. Moreover, the argument of the cylindrical functions ($\rho = k_0 nr$) is approximately equal to order in the so-called transition region, where $r \approx R$. The lack of a reliable, accurate and fast code for evaluation of Bessel functions of both complex order and argument in the transtition region makes this approach difficult.

Microresonator as a structure with complex eigenfrequencies

1-D problem

Another, perhaps more appropriate approach is to search complex plane for eigenfrequencies of a microresonator as a rotationally symmetric structure. From symmetry considerations, ν must be an integer, but the eigenfrequencies are complex due to energy radiation leakage out of the microresonator. We shall present results of a rigorous complex solution of a 1-D model (resonator as a circularly bent planar waveguide) for both microring and microdisk resonators.

2-D problem

A more important but also more complicated 2-D microresonator problem can be solved using the "film mode matching" method in cylindrical coordinates. Applying Hertz vectors with only axial component allows us to express mode field in each radially uniform segment ("slice") as a superposition of modes of a multilayer planar waveguide. As the eigenfrequency of a microresonator is complex, we have to find the propagation constants of these modes that correspond to complex frequency. It is easy to show that eigenmodes of a lossless planar waveguide with complex frequency have complex propagation constants that describe field distribution *growing* along the direction of propagation, with non-zero power flow in the direction perpendicular to the propagation direction. As a consequence, 2-D microresonator radiates not only in the radial direction but also along its axis of symmetry. For accurate calculation of eigenmodes using the film mode matching technique, suitable absorbing or transparent boundary conditions (e.g., perfectly matched layers) above and below the microresonator are to be applied.

[1] C. Vassallo, *Optical waveguide concepts*, Elsevier, Amsterdam, 1991

Analysis of a novel broadband Ti: $LiNbO_3$ Mach-Zehnder optical modulator using an extended point-matching method

N.P. Yeung, E.Y.B. Pun, and P.S. Chung
Department of Electronic Engineering, City University of Hong Kong,
Tat Chee Avenue, Kowloon, Hong Kong
Phone:852-2788 7750, Fax: 852-2788 7791, E-Mail: eeapsc@cityu.edu.hk

An extended point-matching method is used to analyze a guided wave optical modulator. A novel design of velocity-matched Ti: $LiNbO_3$ Mach-Zehnder optical modulator with coplanar waveguide structure is proposed.

Keywords: guided-wave optics, optical modulator, extended point-matching method

Titanium indiffused lithium niobate (Ti:$LiNbO_3$) electro-optic (EO) modulator is promising for high-speed optical transmission in long-haul telecommunication network, because it has low chirping parameter, low propagation loss, and wide bandwidth.

To extend the bandwidth and lower the driving voltage, optimization of the modulator design is necessary. In this work we propose a novel modulator structure which is shown in Fig. 1. Variations in electrode and buffer layer thicknesses can be used to achieve both velocity and impedance matching. The structure with dimensions a =4 μm, b = 20μm, c = 28 μm, d = 100 μm, d_s = 1.3 μm, and t = 22.5μm has a microwave effective index of 2.136 and a characteristic impedance of 50.2 Ω, thus both velocity and impedance matching can be obtained. Furthermore, chirping can be reduced without affecting the driving voltage by increasing the distance between the signal electrode and the outer ground electrodes, and both low driving voltage and small chirping (improved by 78%) can be achieved by optimizing the MZ modulator design.

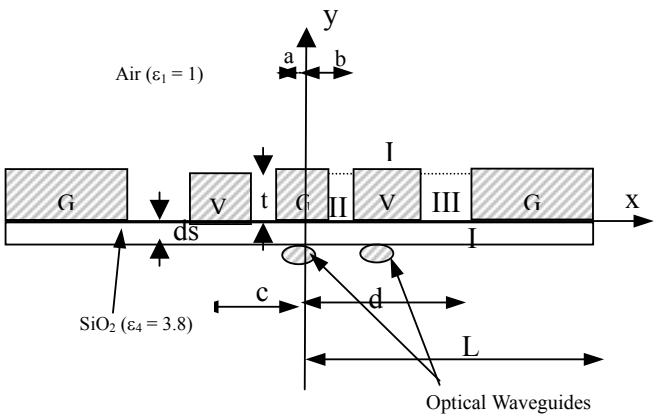

Fig. 1. Schematic of the proposed modulator

MATHEMATICAL STUDY OF THE LASING PROBLEM FOR THE WHISPERING-GALLERY MODES IN A 2-D CIRCULAR DIELECTRIC MICROCAVITY

Elena I. Smotrova, Alexander I. Nosich

Institute of Radio-Physics and Electronics NASU, Kharkov 61085, Ukraine
E-mail: smotrova@ire.kharkov.ua, alex@emt.kharkov.ua

In this paper we consider the lasing eigenvalue problem (LEP) for the 2-D Helmholtz equation where the field $\sim e^{-ikct}$, k=Rek>0. Time-harmonic electromagnetic field is sought in and out of the dielectric circular cylinder of radius a and satisfies tangential-component continuity conditions across its boundary. Refraction index of cylinder is assumed to be $\nu = \alpha - i\gamma, \gamma > 0$. In view of the real value of the wavenumber k, we impose the Sommerfeld radiation condition at infinity ($r\to\infty$). The eigenvalues are the pairs of parameters (κ_j, γ_j). The first of them is the normalized frequency of lasing, $\kappa=ka$, while then second is the threshold gain.

This formulation is different from the "classical" formulation of eigenvalue problem for an open cavity, when the complex-valued frequency k is eigenvalue parameter [1], [2]. Then, the long-living natural oscillations with high Q-factor (i.e., small Imk) are of the main interest; then the condition at infinity should be modified to permit the field growing up. In the case of our formulation, there is no need of such admission of non-physical behavior [3]. Besides, threshold gain appears to be a more adequate parameter characterizing laser operation.

In 2-D, LEPs split into two alternative polarizations. For the circular dielectric resonator, they further split into independent families of transcendental equations with respect to the azimuthal index, n. The roots of each are numbered with the aid of index m, so that $j=n,m$. The field of every WGE_{nm} or WGM_{nm} natural oscillation is characterized by the function

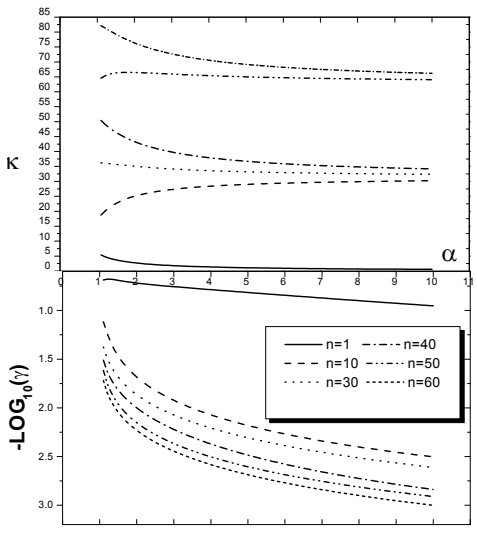

$$U_{nm}(r,\phi) = \frac{H_n^{(1)}(\kappa_{nm})}{J_n(\kappa_{nm}\nu_{nm})} J_n(\kappa_{nm}\nu_{nm}\rho)\cos n\phi,\ \rho<1,\ \text{or}$$

$$H_n^{(1)}(\kappa_{nm}\rho)\cos n\phi,\ \rho>1,\ \rho = r/a, \nu_{nm} = \alpha - i\gamma_{nm}$$

2-D Newton's method was used for the numerical solution of a set of two transcendental equations. Some of the results are presented in the Figure. As expected, it is seen that the higher the azimuthal index n of the lasing mode, the smaller the threshold gain. This is explained by the quasi-total reflection mechanism of the whispering-gallery mode (WGM) field behavior. Besides, the threshold gain of each WGM gets smaller with greater values of refraction index α, while the lasing frequency tends to a limit value. It is also possible to distinguish between the WGMs having the field concentrated near to the boundary and other natural oscillations (with greater thresholds) having significant fields inside the circular cavity. We plan to study, in the similar formulation of LEP, other models of the semiconductor laser microcavities with non-uniform gain and more complicated geometries.

1. S.V. Boriskina, A.I. Nosich, Effect of a layered environment on the complex natural frequencies of 2-D WGM dielectric ring resonator, *IEEE J. Lightwave Technology*, vol. 20, no 8, pp. 1563-1572, 2002.
2. J. Wiersig, Boundary element method for resonances in dielectric microcavities, //arXiv:physics/0206018v2 10Dec2002.
3. A.I. Nosich, Mathematical aspects of eigenvalue problems in optoelectronic simulations of open resonators and open waveguides, *Abstracts of OWTNM-02*, Nottingham, p. 20, 2002.

Numerical Modelling of Absorbing and Amplifying Reflective Microinterferometer Fabry – Perot via the Method of Single Expression

Hovik V. Baghdasaryan, Tamara M. Knyazyan, and Albert A. Mankulov
Fiber Optics Communication Laboratory, State Engineering University of Armenia
105, Terian str., Yerevan 375009, Armenia
hovik@seua.am

To model reflective microinterferometer Fabry-Perot the novel method of single expression (MSE) is used. The-metal-dielectric-metal structure consisting of a high reflective mirror and absorbing (or amplifying) layer sandwiched between dielectric layers is considered. Electric field amplitude and power flow density distributions across single metallic layer, as well as Hagen-Rubens relation are obtained. For an absorbing (and amplifying) microinterferometer reflection spectrum, field and power flow density distributions along the structure at the minimum and maximum reflection are obtained. A real model of amplifying semiconductor microresonator is considered.

Keywords: Gires-Tournois microinterferometer, metallic mirrors, resonant absorbtion and amplification, method of single expression, numerical modelling

The correct numerical modelling of reflective microinterferometer Fabry – Perot (Gires-Tournouis resonator) is carried out by the non-traditional method of single expression (MSE) [1-3]. An absorbing microinterferometer with a bismuth semitransparent layer, as well as a model of amplifying microinterferometer corresponding to the real semiconductor transmitter (metallic substrate / p(or n)layer / active transient layer / n(or p) layer) are considered.
As a mirror a silver layer is chosen. The normalized thickness of silver is chosen to be close to the saturated value of the reflectivity of the infinitely thick metallic layer. The execution of the Hagen-Rubens relation, corresponding to the saturated value of the loss in the metallic half-space is shown.
As a result of numerical modelling by the MSE, reflection coefficient and energy loss dependences from the relative thickness of both silver and bismuth layers are obtained. Penetrated electric field and power flow distributions across the metallic layers are presented. The value of bismuth layer relative thickness corresponding to the deepest minima of the microinterferometer's reflection is found. This value corresponds to the optimal relation between the thickness and permittivity of metal, given analytically in [4] for an idealized model. Spectral dependences of microinterferometer's reflectivity are obtained for different values of dielectric layer permittivities. Electric field amplitude and power flow density distributions along the reflective microinterferometer are obtained at the points of minimum and maximum reflection, forming travelling and standing waves from the illuminated side of the microinterferometer. An amplifying Gires-Tournouis microresonator, corresponding to the real semiconductor transmitter at localization of standing wave in the active p-n transition is considered.

References

[1] H.V. Baghdasaryan, "Method of backward calculation", in *Photonic Devices for Telecommunications: how to model and measure*, G.Guekos, Ed. Springer-Verlag, 56-65,1999.
[2] H.V. Baghdasaryan and T.M. Knyazyan, *Opt. and Quantum. Electron.*, **31**, 1059-1072, 1999.
[3] H. V. Baghdasaryan and T. M. Knyazyan, *in Proc. 4th International Conference on Transparent Optical Networks –ICTON 2002*, Poland, 157 – 162, 2002.
[4] L.M. Brekhovskikh, *Waves in Layered Media, New-York, Academic Press*, 1960.

In-Gap Dark and Antidark Soliton in Deep Nonlinear Bragg Grating

H. Alatas, A. A. Iskandar, M. O. Tjia

Dept. of Physics, Institut Teknologi Bandung, Jl. Ganesa 10, 40132, Bandung, Indonesia
alatas@hfi.fisika.net

T. P. Valkering
Faculty of Applied Physics,University of Twente, Enschede, The Netherlands

A study of nonlinear Bragg grating has been carried out using a modified scheme of approximation originally proposed by Iizuka and de Sterke. A complete classification of the solitonic solutions in the system was given. We further demonstrated in this work the existence of in-gap dark and antidark soliton, in addition to the out-gap solutions reported previously. We found that the existence of either dark or antidark profile controlled by the input field envelopes, $E = f \exp(i\phi)$.

Keywords: gap soliton, deep nonlinear Bragg grating

Introduction

The subject of nonlinear Bragg grating has been studied analytically using the coupled mode theory of forward and backward envelope fields of linearly polarized electromagnetic wave. Recently, Iizuka and de Sterke [1] have considered a model for deep nonlinear Bragg grating using a formalism based on the work of Sipe et. al. [2] to derive the govern equations for deep nonlinear Bragg garting. In this formalism the properties of the system were treated by an asymptotic series. The field was expanded by a superposition of all the harmonics of plane waves, in conjunction with expansions of the linear and nonlinear susceptibilities in Fourier series. Two of the harmonic fields were assumed to be the dominant forward and backward fields, while the others were considered to be of minor roles. The resulted governing coupled equations are dependent on the depth of the grating. Differing from the formalism employed in ref. [1] where the average of nonlinearity effect was put on equal order of approximation with the gentleness of the modulation, we have instead introduced a different and more flexible scheme for the formulation of the smallness parameters.

Results

While this modified scheme results in the same characterization of the “finite” and “narrow” gaps, this model admits the additional solutions of stationary in-gap dark and antidark soliton solutions as depicted by the following phase portraits in the Cartesian coordinates $(x = f\cos\phi, y = f\sin\phi)$ and the corresponding pulse profiles, f, in the direction of propagation, z.

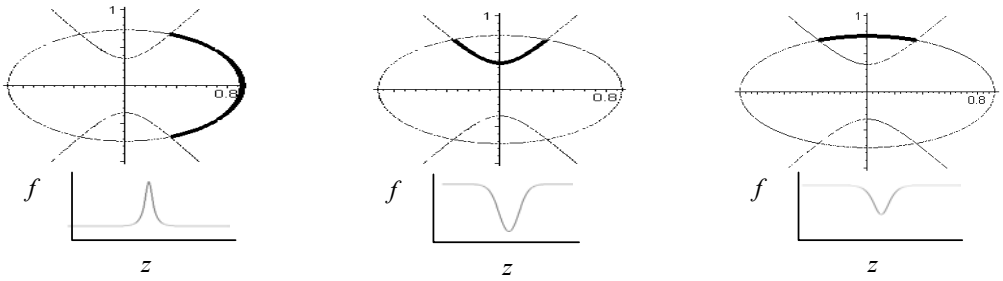

References

[1] T. Iizuka, C. M. de Sterke, Phys. Rev. E **61**, 4491 (2000)
[2] J.E. Sipe, L. Poladian, C.M. de Sterke, J. Opt. Soc. Am. A **11**, 1307 (1994)

Band Gap Characterization of One Dimensional Dielectric Omnidirectional Reflector

J. Prawiharjo, A. A. Iskandar, M. O. Tjia
Department of Physics, Institut Teknologi Bandung, Jalan Ganesha 10, Bandung 40132, Indonesia
jep@orc.soton.ac.uk, iskandar@fi.itb.ac.id, fismots@fi.itb.ac.id

E. van Groesen
MESA$^+$ Research Institute, University of Twente, PO Box 217, 7500 AE Enschede, The Netherlands
groesen@math.utwente.nl

A derivation of approximate analytical expressions for band edges $\omega^{\pm}$ of the first band gap of a multilayer periodic structure is presented for both TE and TM waves at arbitrary angle of incidence. It is found that the approximate expressions give an excellent agreement with the numerical results as verified by the band edge variations with respect to the filling fraction $\nu = \frac{d_2}{d}$ and refractive index contrast Δn. The analytical expressions for the band edges are further employed to derive a semi numerical optimization of the relative gap width $\xi = \frac{\Delta\omega}{\langle\omega\rangle}$ with respect to the filling fraction ν. This result is also shown to be in good agreement with the numerical result.

Keywords: photonic band gaps, periodic structures, omnidirectional reflectance

Introduction

Recent theoretical and experimental investigations have shown that one-dimensional photonic crystals are capable of exhibiting a complete photonic band gaps associated with one-dimensional omnidirectional reflector (ODR). This is achieved by a structure made of a finite number of dielectric slabs of alternating refractive indices n_1 and n_2 embedded in a background medium with refractive index n_0 satisfying $n_0 < n_1 < n_2$.

Being the boundaries of a photonic band gap, the band edges constitute an important set of design parameters of an ODR. Due to complexity of the dispersion relation defining the band edges, only an approximate analytical expression for these band edges has been proposed. Examination of this result shows that the proposed expression does not yield a correct behavior and values of the band edges as compared with the exact numerical results for certain 1D multilayer structures. An improved scheme leading to quadratic approximation is presented.

Band Gap Characterization

The dispersion relation of a 1D which can be written as $\sin\phi^{\pm} = A\cos\left[B\left(\frac{\pi}{2} \pm \phi^{\pm}\right)\right]$, where the factors A and B contain information of the material and structure parameters as well as the incidence angle. Taking advantage of the well known smallness of $\phi^{\pm}$, and employing the Taylor series expansion leads to a quadratic equation for $\phi^{\pm}$. The band edge frequencies $\omega^{\pm}$ are obtained from $\phi^{\pm}$.

A minimum refractive indices required by the ODR operation in both TE and TM modes was established. Further, a semi numerical scheme has been developed on the basis of our approximate band edge formulation for the optimization of the relative bandwidth with respect to the filling fraction, allowing the determination of the maximum band gap by a proper choice of system parameters.

[1] J.N. Winn and Y. Fink and S. Fan and J.D. Joannopoulos, *Opt. Lett.* **20**, 1573 (1998).

[2] J. Lekner, *J. Opt. A-Pure Appl. Op.* **2**, 349 (2000).

[3] D.N. Chigrin and A.V. Lavrinenko and D.A. Yarotsky and S.V. Gaponenko, *J. Lightwave Technol.* **17**, 2018 (1999).

Numerical Analysis of Lithium-Niobate Electro-Optical Modulators through a Full-Vectorial Three-Dimensional Finite Element based Beam Propagation Method

A. Bertolani, A. Cucinotta, M. Fuochi, F. Poli, S. Selleri
Dipartimento di Ingegneria dell'Informazione. University of Parma
Parco Area delle Scienze 181/A, 43100 Parma, Italy
stefano.selleri@unipr.it

L. Vincetti, M. Zoboli
Dipartimento di Ingegneria dell'Informazione. University of Modena and Reggio Emilia
Via Vignolese 905B, 41100 Modena, Italy

A full-vectorial three-dimensional Beam Propagation Method is applied to investigate the electromagnetic field propagation within integrated electro-optic modulators. A directional coupler modulator and a Mach-Zender modulator are analyzed. Field and power distribution, modulation speed and half-wavelength voltage are given for both devices.

Keywords: Electro-optical modulators, Finite Element Method, Beam Propagation Method

Introduction

The increased demand of wide-band services, observed all over the world in the last years, has led optical communication society to continuously improve the characteristics of transmitted signals. Therefore optical modulation has become a critical matter, also due to the interaction with electric phenomena, that in general represent a constraint for the overall performances of an optical system.

Many solutions are known to impress information on optical carriers, starting with direct modulation of laser sources, passing through optical-plasma modulation and ending to the attractive technique of acousto-optic modulation. Nevertheless, nowadays, the attention of research in integrated-optics seems to concentrate on lithium niobate electro-optical modulators, which represent a good compromise between performances and physical dimensions [1].

In order to aid the design of lithium niobate electro-optical modulators, many authors developed numerical techniques which could investigate the modal solutions of the devices. For example a z-invariant structure has been studied with a modal formulation of the Finite Element Method (FEM) [2] while, still using the FEM, the problem of the controlling electrodes is addressed in [3]. An integral equation-based hybrid-mode analysis of an optical modulator with a ridge structure is performed in [4] also obtaining important information on field distribution and electrodes characteristics. Such studies take into account the vectorial nature of the field carried by modulators. However, all of them are applied to the transversal cross-section which is supposed to be invariant along the propagation direction.

The numerical tool here presented implements a full-vector Beam Propagation Method (BPM) for the analysis of three-dimensional devices whose structure may vary along the direction of propagation. The method is able to monitor all of the distributions of the electromagnetic field components, on the transverse cross-section of the device, while they propagate along the modulator. The information that can be deduced are very useful for the design and the analysis process, in particular to investigate the effect of structure variations.

The full vector BPM is based on the FEM, which seems to have very high performances in the discretization of any geometrical structure and refractive index distribution [5].

After presenting the analytical formulation, the diffusion model adopted to represent the guiding structures in lithium-niobate substrate is described. The presentation of the numerical

results and the computed figures of merit of the studied modulators conclude the paper.

Finite Element based Beam Propagation Method

The formulation used for the present study is exhaustively described in [5] and here briefly recalled. The curl-curl equation in term of the magnetic field in frequency domain reads:

$$\bar{\nabla} \times \left(\varepsilon_r^{-1} \bar{\nabla} \times \bar{\mathcal{H}}\right) - k_0^2 \bar{\mathcal{H}} = 0, \tag{1}$$

where k_0 and ε_r are the wavenumber in the vacuum and the relative permittivity, respectively. By expressing the magnetic field as the product of an envelope and a fast varying factor along the direction of propagation z, $\bar{\mathcal{H}}(x,y,z) = \bar{H}(x,y,z)e^{-j\beta z}$, being β the phase constant, under the slowly varying envelope approximation for the transverse component, $\partial^2 \bar{H}_t/\partial z^2 << 2j\beta\partial\bar{H}_t/\partial z$, equation (1) yields a three coupled equation system in the three unknowns H_x, H_y and H_z, that represent the formulation assumed as starting point of the finite element approach. By applying the standard Galerkin method to this system and a classical θ parameter step-by-step scheme, it yields:

$$[L(\theta)]\{H\}_n = [L(1-\theta)]\{H\}_{n-1}, \tag{2}$$

$$[L(\theta)] = ([J] - \Delta z\theta[K]), \quad [L(1-\theta)] = (\Delta z(1-\theta)[K] + [J])$$

$$\{H\} = \{H\}(z) = \begin{pmatrix} \{H_x\}(z) \\ \{H_y\}(z) \\ \{H_z\}(z) \end{pmatrix}$$

which relates the magnetic field values at step n in $z + \Delta z$ to those at step $n-1$ in z. $[J]$ and $[K]$ are "$3N \times 3N$" sparse matrices given in [6], with N the total number of points of the whole cross-section. The stability analysis provides the method is unconditionally stable for $0.5 < \theta \leq 1$ [6].

When the method is applied to z-varying structures, the elements of (2) must be updated whenever the optical properties change. This can be accomplished in two main ways. By using an adaptive mesh with constant optical properties over its nodes [5], or by fixing the position of nodes and varying the permittivity related to the nodes themselves. The first method has the advantage of reducing the number of points needed for the discretization of the cross-section, as nodes move following the optical properties variations. Nevertheless, due to the computational complexity of the code that performs this operation, the second method has been chosen to analyze the Mach-Zender Interferometer (MZI) modulator considered in this work and it has revealed to be faster without loosing precision.

Diffusion Model

To obtain guiding regions in lithium-niobate substrate, the technique of titanium diffusion is commonly used. It induces a quite well controllable variation in both ordinary and extraordinary refractive indices of the material. The model adopted in the present study is obtained by [2],[3],[7], and summarized by these values of the refractive indices:

$$\begin{aligned} n_o(x,y) &= n_{os} + \Delta n_o [h(x)g(y)]^\gamma \\ n_e(x,y) &= n_{es} + \Delta n_e [h(x)g(y)], \end{aligned}$$

where o and e means respectively ordinary and extraordinary, s indicates the substrate, $\Delta n_i, i = o, e$ represent the maximum refractive index variations, $\gamma = 0.55$, $h(x)$ is a difference of two erf functions and $g(y)$ is gaussian distribution along y.

Results and Discussion

The first device analyzed is a Directional Coupler (DC) modulator implemented on a lithium niobate substrate, in which two parallel guiding regions are obtained with titanium diffusion as in [2]. Applying a voltage signal to the guiding regions in a push-pull technique, an opposite refraction index variation is induced by means of linear (Pockels) electro-optical effect. When no voltage is applied, at the end of the device chosen equal to coupling length $L_{c0} = \pi/\Delta\beta = 7.33\,mm$, the signal exits on the cross waveguide. On the contrary, the coupling length halves when the voltage is applied, so that the signal exits in the bar guide at the end of the modulator.

The transverse cross-section has been discretized with a 9969-node mesh, the input field has been computed, through a FEM modal solver, at $\lambda = 1550nm$. The BPM has been applied with a propagation step $\Delta z = 0.2\mu m$ and $\theta = 0.7$. The simulation lasted about 300 minutes using an "Athlon" with a $550MHz$ processor and $768MByte$ of RAM. Figure 1 represents the evolution of the main component of the magnetic field, on the transverse section, along the device.

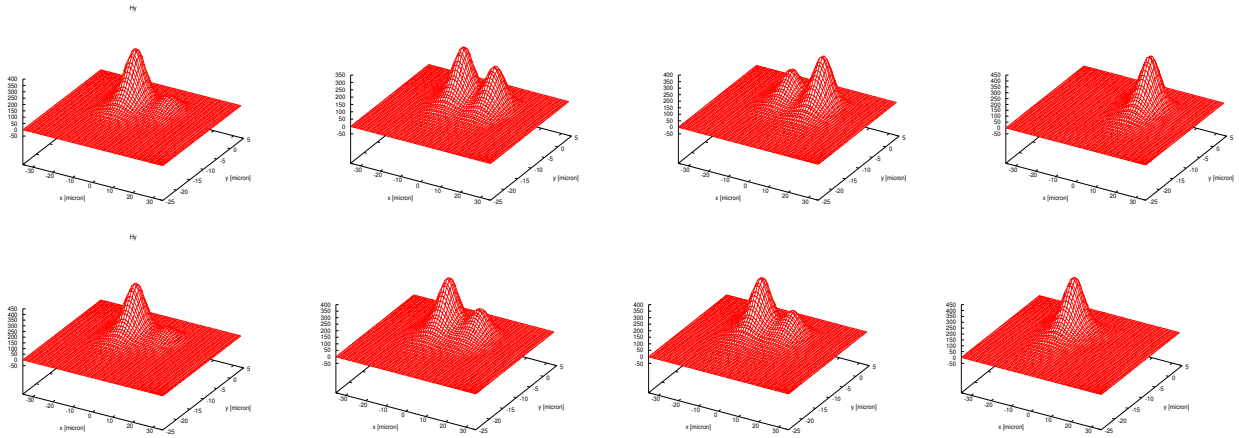

Fig. 1. *Magnetic field main component at $z = 1mm$, $3mm$, $5mm$, $7.3mm$, without (upper) and with (lower) applied voltage in the DC modulator.*

The second device is a MZI modulator, implemented on a lithium niobate substrate diffused with titanium to create the waveguiding regions. If no voltage is applied to the arms of the interferometer, light travels with the same phase delay, interfering constructively at the output of the modulator. A "high" level signal is obtained. This behavior is reported in figure 2. When the voltage is applied, the field in the two arms accumulates an opposite phase delay. By a proper design of the length of the device, destructive interference can be induced at the output, obtaining a "low" signal. The normalized power distribution along the direction of propagation is reported in figure 3. It clearly shows how the input power splits in the two branches at the input and it results in a "high" or "low" level at the output, after a total length $L = 2.82\,mm$, according to the applied voltage. Losses of about $3\,dB$ have been observed, mainly due to the input and output "Y" junctions.

Also in this case the modal solution of the input waveguide at $\lambda = 1550nm$ is used as launching condition. A FEM mesh with 14200 nodes, a propagation step $\Delta z = 0.2\mu m$ and $\theta = 0.7$ have been used. Simulation took about 270 minutes, most due to system matrices updating when the structure changes along z.

A comparison of the performances of the two devices indicates that the MZI modulator can provide much better performances and smaller dimensions than the DC one. In fact the switching voltages V_π are equal $9.18\,V$ and $5\,V$ for the DC and the MZI modulator respectively,

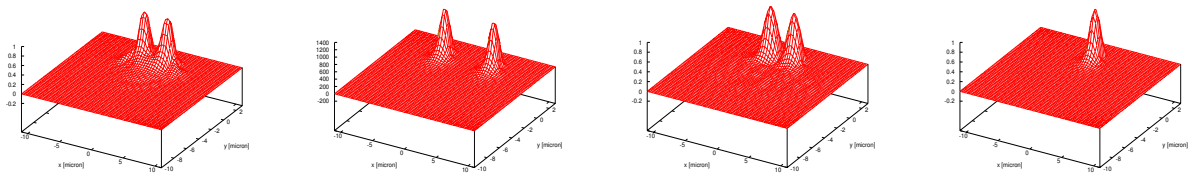

Fig. 2. *Magnetic field main component at* $z = 80\mu m,\ 1mm,\ 2mm,\ 3mm$, *without voltage application in the MZI modulator. When voltage is applied the output field slowly fades to zero.*

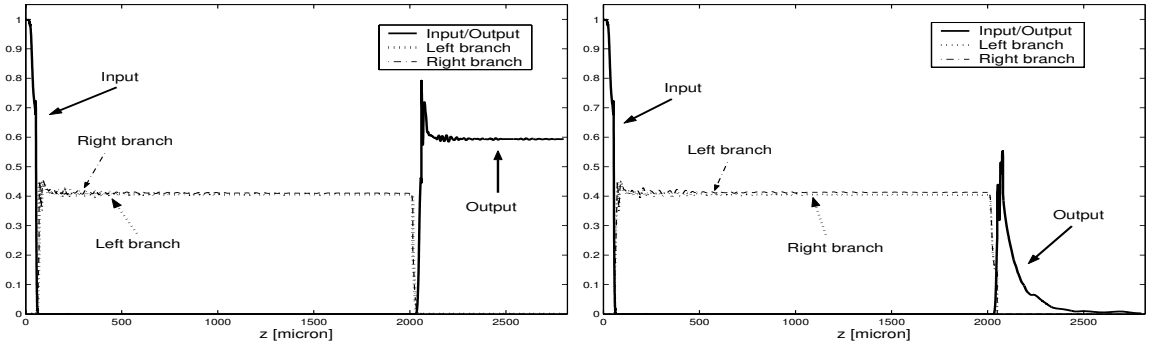

Fig. 3. *Normalized power distribution in input-output waveguide, left and right arms of the modulator, without (left) and with (right) applied voltage.*

which correspond, in the two cases, to $V_\pi \cdot L = 67.29\, V \cdot mm$ and $V_\pi \cdot L = 14.1\, V \cdot mm$. Moreover the modulation speeds, obtained only by accounting for the transit time of the light through the device, are $18.5 GHz$ and $46 GHz$.

In conclusion, the application of the FE-VBPM has provided useful information on fields and power distribution inside electro-optic modulators and can be successfully used to investigate their performances and figures of merit.

[1] E.L. Wooten, K.M. Kissa, A. Yi-ian, E.. Murphy, D.A. Lafaw, P.F. Hallemeier, D. Maack, D.V. Attanasio, D.J. Fritz, G.J. McBrien and D.E. Bossi, "A Review of Lithium Niobate Modulators for Fiber-Optic Comunications Systems", *IEEE J. Selec. Topics Quantum Electron.*, **6**, 69-82, 2000.

[2] N. Anwar, C. Themistos, B.M.A. Rahman and K.T.V. Grattan, "Design Considerations for an Electrooptic Directional Coupler Modulator", *J. Lightwave Technology*, **17**, 598-605, 1999.

[3] M. Koshiba, Y. Tsuji and M. Nisho, "Finite-Element Modeling of Broad-Band Traveling-Wave Optical Modulators", *IEEE Trans. Microwave Theory and Techn.*, **47**, 1627-1633, 1999.

[4] K. Noguchi, O. Mitomi, H. Miyazawa and S. Seki , "A Broad-Band $Ti : LiNbO_3$ Optical Modulator With a Ridge Structure" *IEEE J. Lightwave Technology*, **13**, 1164-1168, 1995.

[5] E. Montanari, S. Selleri, L. Vincetti and M. Zoboli, "Finite-Element Full-Vectorial Propagation Analysis for Three-Dimensional z-Varying Optical Waveguides", *IEEE J. Lightwave Technology*, **16**, 703-714, 1998.

[6] S. Selleri L. Vincetti and M. Zoboli, "Full-Vector Finite-Element Beam Propagation Method for Anisotropic Optical Device Analysis", *IEEE J. Quantum Electr.*, **36**, 1392-1401, 2000.

[7] S. K. Korotky and R. C. Alferness, "Integrated optical circuits and components: design and applications", *Edmond J. Murphy. - New York, Basel, Dekker*, 1999.

Notes